GEAR TECHNOLOGY

The Journal of Gear Manufacturing

JULY/AUGUST 1985

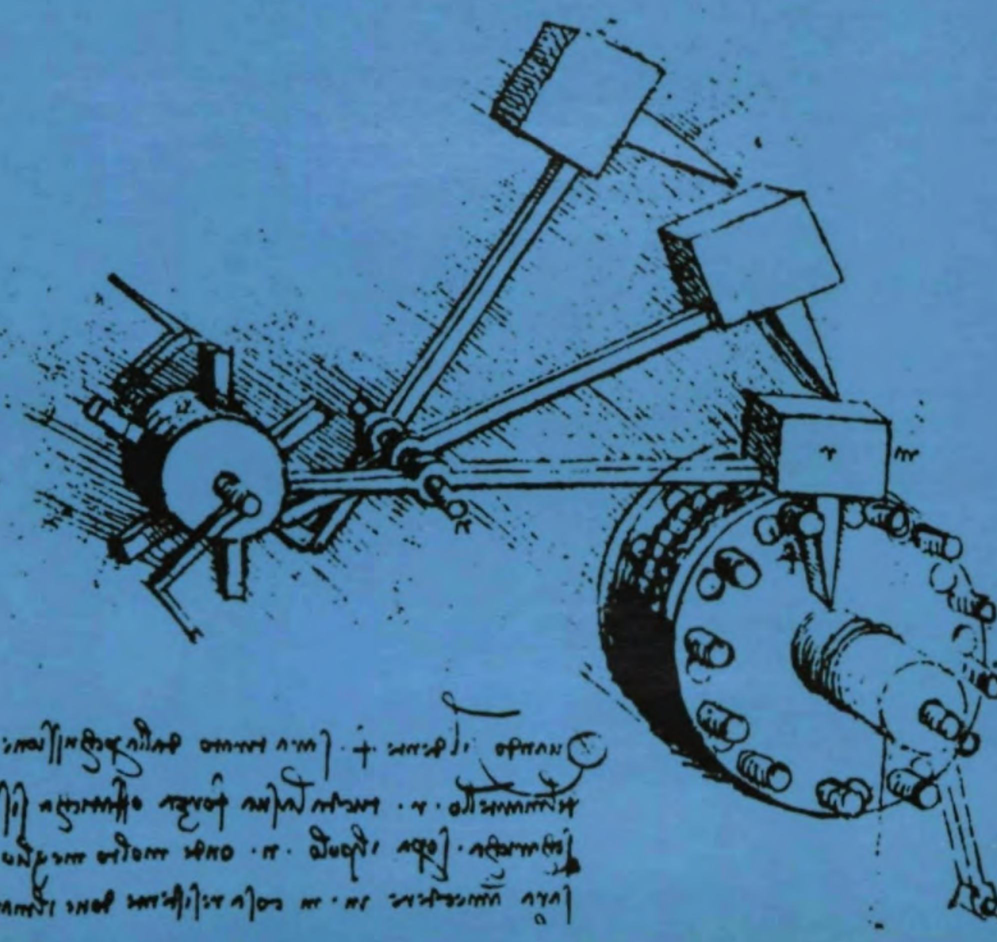

Analysis of Straight and Involute Tooth Forms

Influence of Relative Displacements Between Pinion and Gear on Tooth Root Stresses of Spiral Bevel Gears

Design and Manufacture of Plastic Gears — Machining Installation and Gear Sound Measurement

Longitudinal Load Distribution Factor of Helical Gears

Material Selection and Heat Treat

Guess who builds more multi-axis CNC hobbing machines for automotive-size gears?

American Pfauter, of course.

For example, our new PE150 represents the best of high production capability plus flexibility for hobbing gears up to 6-in. Because of high dynamic rigidity, it's capable of using the latest in TiN and carbide tool technology. Setup times are reduced as much as 85% because change gears and mechanical gear trains have been replaced with trouble-free electronic controls.

Simple CNC operation is assured with a variety of available software. Dialogue programming covers all operational sequences, walks the operator through data entry and alerts him to conflicting or illogical data. A diagnostic program simplifies maintenance procedures by detecting and displaying errors directly on the CRT.

Flexible automation is a reality with the PE150's integral workhandling system which combines unsurpassed speed and versatility—even where medium or small production lots dictate frequent retooling during one shift.

Faster tool change is accomplished with the quick hob change system which saves more than 90% of tool changing time while assuring hob concentricity independent of operator skill. A tool magazine with automatic changer is also available.

Shorter machining times. Shorter changeover times. Faster tool change. Reduced idle times. Lower operating costs. All at a price no higher than conventional hobbing machines. For additional information, contact American Pfauter Ltd., 925 East Estes Avenue, Elk Grove Village, IL 60007 U.S.A. (312-640-7500).

AMERICAN PFAUTER LIMITED

World-class gearmaking technology in hobbing • grinding • shaping • hard gear finishing • inspection • gear cells and systems

CIRCLE A-1 ON READER REPLY CARD

INDUSTRY FORUM

"INDUSTRY FORUM" provides an opportunity for readers to discuss problems and questions facing our industry.

Please address your questions and answers to: INDUSTRY FORUM, GEAR TECHNOLOGY, P. O. Box 1426, Elk Grove Village, IL 60007.

Letters submitted to this column become the property of GEAR TECHNOLOGY. Names will be withheld upon request; however, no anonymous letters will be published. Opinions expressed by contributors are not necessarily those of the editor or publishing staff.

Dear Editor:

In response to Ed Uberts letter, we have come a long way in gearing since WWII. The Europeans do use long addendum pinions in many cases. This modification does improve load capacity, sliding conditions and the working life of a gearset. When modifying a pinion tooth it is necessary to modify the geartooth or adjust the center distance accordingly but we will leave that to the designers.

I have found that Dr. Werner Vogel who compiled the book entitled "Involutometry & Trigonometry" has all of the information necessary to accurately calculate measurements over rolls for Helicals or Spurs. His derivation of the formulas is concise and complete. The span measurement method with the books supplied by MAAG of Zurich, Switzerland are also accurate so long as the facewidth allows you to use vernier calipers in the case of high helix angles.

Some of the better hand held calculators have software Engineering packages that are programmed to do the calculations with the imput of the necessary variables.

Mitchell J. Hilow,
Manuf. Eng. & Gearing
Morgan Constr., Co.
Worcester, Mass.

Dear Editor:

The letter from Edward Ubert in the May/June issue caught my attention, as I have worked in the area of gear geometry for many years (although only from the U.S. viewpoint).

We at Foote-Jones/Dresser (Chicago) also use many gears of non-standard geometry, not only of our own design, but also as reproductions of gears designed elsewhere. Theories of gear geometry are outlined in Van Keuren, *Precision Measuring Tools*, Dudley, *Gear Handbook*, Khiralla, *On the Geometry of External Involute Spur Gears*, Buckingham, *Analytical Mechanics of Gears*, etc., but applying these to an arbitrary geometry so as to avoid "surprises" at assembly is not a trivial task. However, we have created a tool to do this by coding the theory into an interactive computer program, which will parse any parallel shaft, external gear set geometry in seconds. Because I have reviewed the derivations in the above literature, run the program against those from other sources and employed it thru gear assembly, I am confident that it and the basic theory are analytically correct. However, in performing measurement over wires in conjunction with program, the wire diameter must be chosen, of course, so that the wires protrude above the o.d. sufficiently to avoid interference between top land of teeth and calipers, and also so that the wires make contact in the region of the pitch line because, were they to contact a modified region of the flank (near tip or root), they would not be measuring the involute.

Regarding tooth modification, if one member of a set has modified addendum, the addendum of the other member must be correspondingly modified (or else the center distance must "float"). Thus, generally there is no interchangability when "every gear is modified to some extent."

The "addendum modification coefficient" concept Mr. Ubert mentions is not unique to Europeans, but is just one method of manipulating a design. Of course, the rules of gear geometry do not follow AGMA, DO or BS, but rather the laws of mathematics.

If Mr. Ubert would like, I would be glad to give him wire measurements for some sets he would consider to be test cases, to check his calculation method.

Sincerely,
Henry Tideman
Supervisor,
Computer & Engineering Analysis
Foote-Jones Gear Division

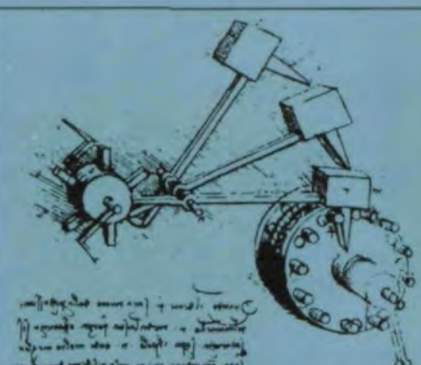

COVER

The Advanced Technology of
LEONARDO DA VINCI
1452-1519

Before Leonardo created his famous 'machines', he developed many simple tools. These devices were derived from his scientific observations and later became the parts of his machines. He was particularly fascinated by the conversion of reciprocal to rotary motion and the use of reducing gears. Leonardo might be called the father of the machine tool. Today we would say Leonardo was increasing 'profitability' by using automation to bring his day into the industrial age.

The cover sketch illustrates a set of gears to control a counterweight. It is not known how he planned to use this, but it was one of many such studies of complex systems of gears, springs, and counterweights, possibly to be used in his improvement of timepieces.

GEAR TECHNOLOGY
The Journal of Gear Manufacturing

CONTENTS — PAGE NO.

FEATURES

DEPARTMENTS

July/August 1985 — Vol. 2, No. 4

SUBSCRIPTION INFORMATION: GEAR TECHNOLOGY is distributed free of charge to **qualified** individuals and firms in the gear manufacturing industry. To continue receiving your subscription, complete and mail the application card found elsewhere in this magazine. Subscription rates for nonqualified individuals and firms are: $30.00 in the United States, $50.00 for foreign countries. Back issues are $7.00 in the United States, $15.00 for foreign countries. Subscription requests to RANDALL PUBLISHING CO., INC., P.O. BOX 1426 Elk Grove, IL 60007, (312) 437-6604.

MANUSCRIPTS: We are requesting technical papers of every sort from manufacturers of gear making machinery and related equipment, universities, and engineers. Articles should be of an educational and training nature with general appeal to anyone having anything to do with the purchase of materials or machinery, or the design, manufacture, testing or processing of gears. Subjects sought are solutions to specific problems, explanations of new: technology, techniques, designs, processes, and alternative manufacturing methods. These can range from the "How to . . ." of gear cutting **(BACK TO BASICS)** to the most advanced technology. All manuscripts submitted will be carefully considered. However, the Publisher assumes no responsibility for the safety or return of manuscripts. Manuscripts must be accompanied by *a self-addressed, self-stamped envelope, and be sent to GEAR TECHNOLOGY, The Journal of Gear Manufacturing, P.O. Box 1426, Elk Grove,* IL 60007, (312) 437-6604.

GEAR TECHNOLOGY (ISSN 0743-6858) is published bimonthly as a reference source of technological developments in the gear industry. It welcomes independent opinion, but the opinions expressed by authors and contributors to GEAR TECHNOLOGY are not necessarily those of the editor or publishing staff, and we assume no responsibility for the validity of claims in connection with items printed. Application to mail at second-class postage rates is pending at Elk Grove, Illinois and at additional mailing office.

POSTMASTER: Send address corrections to GEAR TECHNOLOGY, 1425 Lunt Ave., P.O. Box 1426, Elk Grove, IL 60007.

A job well done

Why have so many important gear companies purchased BHS-HÖFLER gear grinding machines?

Because they appreciate extremely high accuracy, output and technical back-up!

We train their planning, operating and maintenance staff, install and run off machines to all guaranteed specifications.

Our engineering department will assist in gear design, fixturing tooling and process calculation.

We maintain profitable gear production by providing immediate service and parts from our Clinton, N. J. Corporation.

A job well done

Now, if you assume all this is expensive, why don't you try us? You will be surprised.

BHS HÖFLER

BHS - DR.-ING. HÖFLER CORP., 65 Route 22, Clinton, N. J. 08809
Phone: (201) 735-8995, Telex: 380 576

CIRCLE A-4 ON READER REPLY CARD

EDITORIAL

Photo by Jennifer Short

Almost overnight, America's industry found itself competing against an onslaught of lower cost imported products. For this reason, the need to improve the quality of our products and simultaneously reduce their cost became imperative. Manufacturers needed to quickly acquire vast amounts of knowledge about new manufacturing methods, techniques, designs, materials, machines and manufacturing systems.

It was with this in mind that late last summer I looked with anticipation to the upcoming fall technical sessions being hosted by SME, ASME and AGMA. (The SME and AGMA sessions meet annually and the ASME conference is held once every four years.) You would think that with the wealth of knowledge to be gained and the industry interaction available, these conferences would have had terrific attendance, right? Wrong! Not counting people representing the machine tool manufacturers, suppliers and those presenting papers, only 250 or 300 people attended these three conferences. I was surprised, however, by the large percentage of foreign attendees at the ASME conference. Many Japanese attended along with visitors from Germany, France, Holland, China, Egypt, England, Italy and many more. They thought it important enough to come to the United States, present papers, and receive the conference information.

It's time for a change of attitude, a change of priorities, and possibly things are changing. AGMA just held a technical conference in April in Indianapolis. In contrast to their earlier conferences, this one was oversubscribed and potential attendees had to be turned away.

What changed? Is business better? Has optimism improved? Are attitudes changing regarding ongoing education and the need to seek information from all sources? Probably the answer is "all of the above". It certainly isn't because the subjects and papers being presented are any better, or more timely. Many of the papers presented at the poorly attended conferences were reprinted on these pages, gathering excellent comment. Hopefully, this is the beginning of a new trend.

AGMA's upcoming Fall Technical Conference, October 14th through 16th in San Francisco, and the SME Gear Processing and Manufacturing Clinic, November 12th through 14th in Detroit, offer the opportunity to start or continue the necessary educational process. Look over the subjects carefully. If you don't see subjects that will help you, write to these organizations and tell them what kind of information you need. They want to help, but in turn, they need your support and your attendance. From each conference that you attend, you will acquire new information, but the real gains are cumulative and come from attending these conferences over a long period of time.

Is this the answer to the onslaught of competition? I don't know. But without keeping up to date on the technique and developments presented at these and other conferences, we don't stand a chance.

Thank You

Michael Goldstein
Editor/Publisher

Dynamic Analysis of Straight and Involute Tooth Form

by
Hsiang H. Lin
Ronald L. Huston
Department of Mechanical & Industrial Engineering
University of Cincinnati
Cincinnati, Ohio 45221

John J. Coy
Propulsion Laboratory
AVRADCOM Research and Technology Laboratories
NASA-Lewis Research Center
Cleveland, Ohio 44135

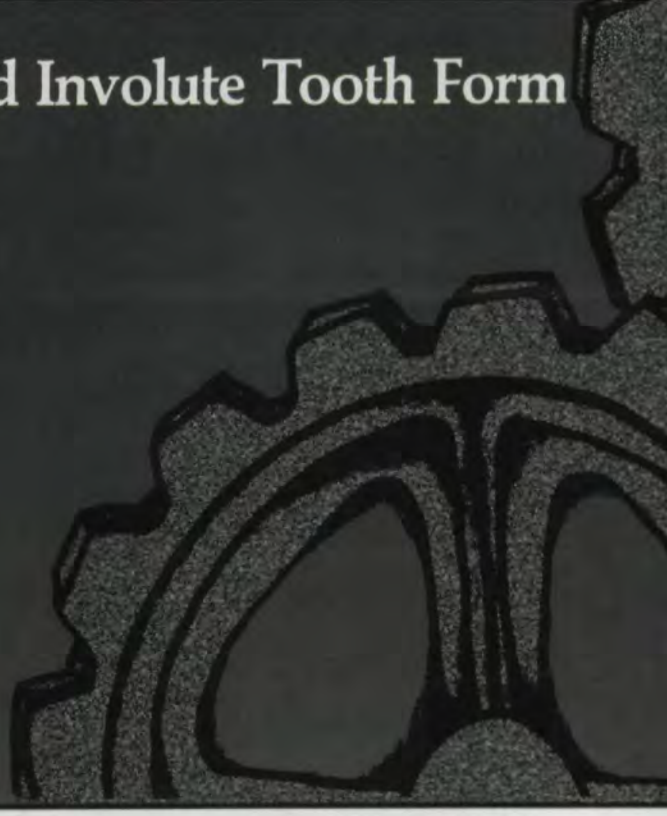

Abstract

The effect of load speed on straight and involute tooth forms is studied using several finite-element models. It is found that for rapidly rotating gears and sprockets, the load speed along the tooth surface can significantly affect the tooth vibration. Indeed, it is found that for sufficiently high load speeds and for sufficiently slender tooth forms, the tooth deflection can, at times, be directed opposite to the load direction.

Comparisons are made of various dynamic models of gear and sprocket teeth. It is shown that for stubby tooth forms there is considerable difference between results obtained with finite element models and results obtained with Timoshenko beam models.

Finally, it is shown that gear or sproket vibrations can be induced by the shape of the tooth form itself. This effect becomes increasingly significant at higher speeds.

Introduction

Recently there has been increased interest in the dynamic characteristics of gear and sprocket teeth. Performance, noise, wear, and life considerations have all stimulated interest in tooth dynamics. In this paper, we consider the dynamical effects of a moving load along the surfaces of straight and involute tooth forms.

Several researchers have considered various aspects of this problem. For example, Nagaya and Uematsu[1] recently (1981) studied effects of moving load speeds on the deflection of a tapered, cantilever, Timoshenko beam. Their analysis is based upon approximations developed earlier by Nagaya.[2] Much earlier research by Attia[3] (1959) and Utagawa and Harada[4] (1961) led to an analysis of tooth response as a function of load postion but not load speed. Later Wallace and Weireg[5] (1973) used the finite element method together with Hertzian type contact to study dynamic loading. Still later, Cornell and Westervelt[6] (1978), using a method developed by Richardson[7] and Howland[8] studied dynamic tooth stresses by modeling meshing gear teeth by variable springs with inertias of rigid bodies. They showed that tooth profile modification, inertia, damping, and resonance can all affect the tooth stresses.

TABLE I. Interaction of Dynamic Parameters of Gears and Sprocke

	Tooth Errors and Modifications	Gear Speed	Transmitted Load	Contact Ratio	Conta Positi
Dynamic Load	L	N	I	I	U
Efficiency	U	L	I	N	U
Dynamic Stress	N	U	L	I	U
Tooth Deflection	U	U	L	I	U
Gear or Sprocket Vibration	U	N	U	U	U

NOTATION: L – Linearly Proportional Relation
N – Nonlinear Relation

A summary of the interation of the various parameters affecting tooth dynamics, as reported in the literature, is given in Table I.

In the analysis of this paper, we use the finite element method to study the effect of load speed and slenderness ration on the dynamic responses of tapered beams. We then examine the dynamic response of involute tooth forms to moving loads.

Dynamic Analysis of Tapered, Truncated Beams

Using Timoshenko beam theory, Nagaya and Uematsu[1] considered the problem of a force P moving with constant speed V along the centerline of a tapered, truncated, cantilever beams as depicted in Fig. 1. The beam cross section is rectangular. To simulate a gear tooth the half angle β is taken as 20°. The truncated length $(L-a)$ is 2.25M where M is the

Mesh Stiffness	Rim Thickness	Gear or Sprocket Inertia	Damping	References
U	U	L	I	3, 4, 6, 10, 12, 13, 15
U	U	U	U	14, 22, 23
U	I	U	U	6, 9, 16, 17
I	I	U	U	20
U	U	U	U	18, 25

I – Inversely Proportional Relation
U – Unknown or Random Relation

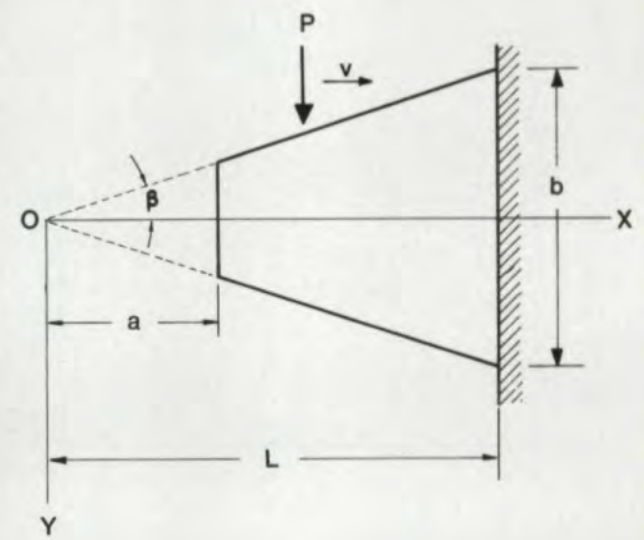

Fig. 1—Tapered, Truncated, Cantilever Beam.

module of the gear. Then the base b of the beam, simulating the root of the tooth, is 2.48M. Nagaya and Uematsu[1] have shown that as V is increased, the centerline deflection differs substantially from the static deflection. Indeed, when V is 1% of the longitudinal wave propagation speed ($\sqrt{E/p}$), the centerline deflection is in the negative Y direction for a major portion of the span at various load positions, and even beneath the load itself.

To further examine this phenomenon, we constructed a three-dimensional, finite-element model of the beam as shown in Fig. 2. The mesh contains 120 "8-node brick" elements and 288 nodes. The model was given a unit thickness in the Z-direction. The elastic constant E was 30×10^6 psi (s.07x10″ N/m^2), the weight density γ was 0.283 lb/in^3 (7.83×10^3 kg/m^3), giving a wave propagation speed V* of 2.024×10^5 in/sec (5.14×10^3 m/sec). The beam was loaded in the positive Y-direction with a unit load moving at 0.001V*, 0.005V*, and 0.01V*. The centerline displacement was then determined. The results are shown in Fig. 3 for four load positions.

By comparing these results with those of Nagaya and Uematsu[1] it is seen that the magnitude of the displacements differ substantially. Moreover, the displacements are always positive with the finite-element model. The primary reason for the difference is the effect of the thickness of the beam. Indeed, for this beam the slenderness ration, defined as $\sqrt{AL^2/I}$, is only 6.0, where A is the average beam cross section area, L is the beam length and I is the average second moment of area of the beam cross section about a line parallel to the Z-direction and intersecting the centerline.

To examine the effects of the slenderness ratio, three other finite-element models were developed. First, a stepped beam model with a slenderness ratio of 49.0 was constructed. The model consists of 15 beam elements with different thicknesses as depicted in Fig. 4. The model was given the same loading as the tapered beam of Fig. 1. The displacements of the centerline and the tip were computed. Figs. 5 and 6 show the

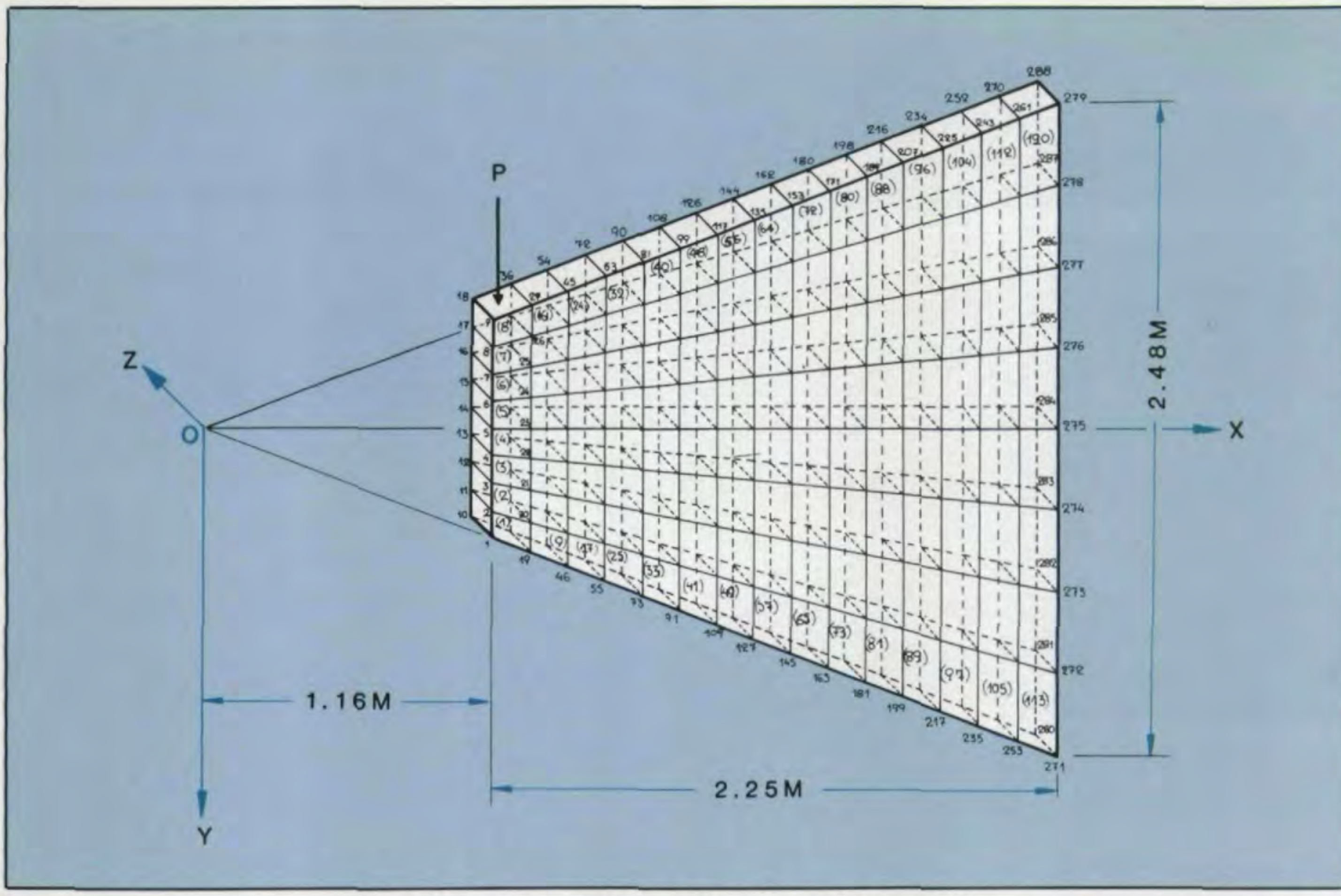

Fig. 2 – A Finite Element Mesh for the Beam of Fig. 1 (M is Gear Module).

results. Finally, straight, thin beam models were constructed with slenderness ratios of 26 and 78. With the same loading as before, the centerline and tip deflections were computed. Figs. 7, 8, and 9 show the results.

A comparison of the results of Figs. 3, 5, 6, 7, 8, and 9, together with those of Nagaya and Uematsu[1], show that, as expected, the slenderness ratio has a significant effect upon the beam response to the moving load. However, the finite-element models show that a relatively high slenderness ratio is required for significant negative V-deflection of the centerline.

Dynamic Analysis of Involute Tooth Forms

Many gears and sprockets have involute tooth forms. That is, the tooth profile is in the shape of an involute to a circle. If a gear or sprocket has an infinite radius (a "rack"), the involute form is a straight line. Thus, a tapered, truncated cantilever beam is a good model of a rack gear or sprocket tooth. However, for circular gears and sprockets, a preferable model has the curved shape of an involute. To develop such a model, we constructed a finite-element grid as shown in Fig. 10. The model consists of 104 8-node brick elements with 242 nodes. The model represents a 20° involute 20-tooth gear or sprocket with a diametral pitch of 1.0.

A unit load was applied to the surface to simulate the meshing loading. The load was applied near the root of the tooth, at the base circle, and then moved with a speed V along the surface toward the tip. The local speed was not constant, but instead was governed by the expression:

$$V = R_B \omega^2 t \tag{1}$$

where R_B is the base circle radius and ω is the gear or sprocket angular velocity. When the time t is zero, the load is at the base circle. [Equation (1) is developed in the Appendix.]

Figs. 11 and 12 show the radial and transverse displacements of various surface nodes for an angular speed of 100 rpm.

Discussion and Conclusions

The foregoing results show that slender beams may produce erroneous conclusions for many tooth forms – especially for short stubby teeth. Indeed, if the root thickness is approximately equal to the tooth depth, the slenderness ratio is too small for conventional beam theory to be valid – even with thickness modifications.

Next, it is seen that the load speed along the tooth can have a significant effect on the deformation and it can induce vibrations. For sufficiently thin tooth forms, or for sufficiently high load speeds, the centerline deflection can even be directed *opposite* to the load. This is especially important for high speed

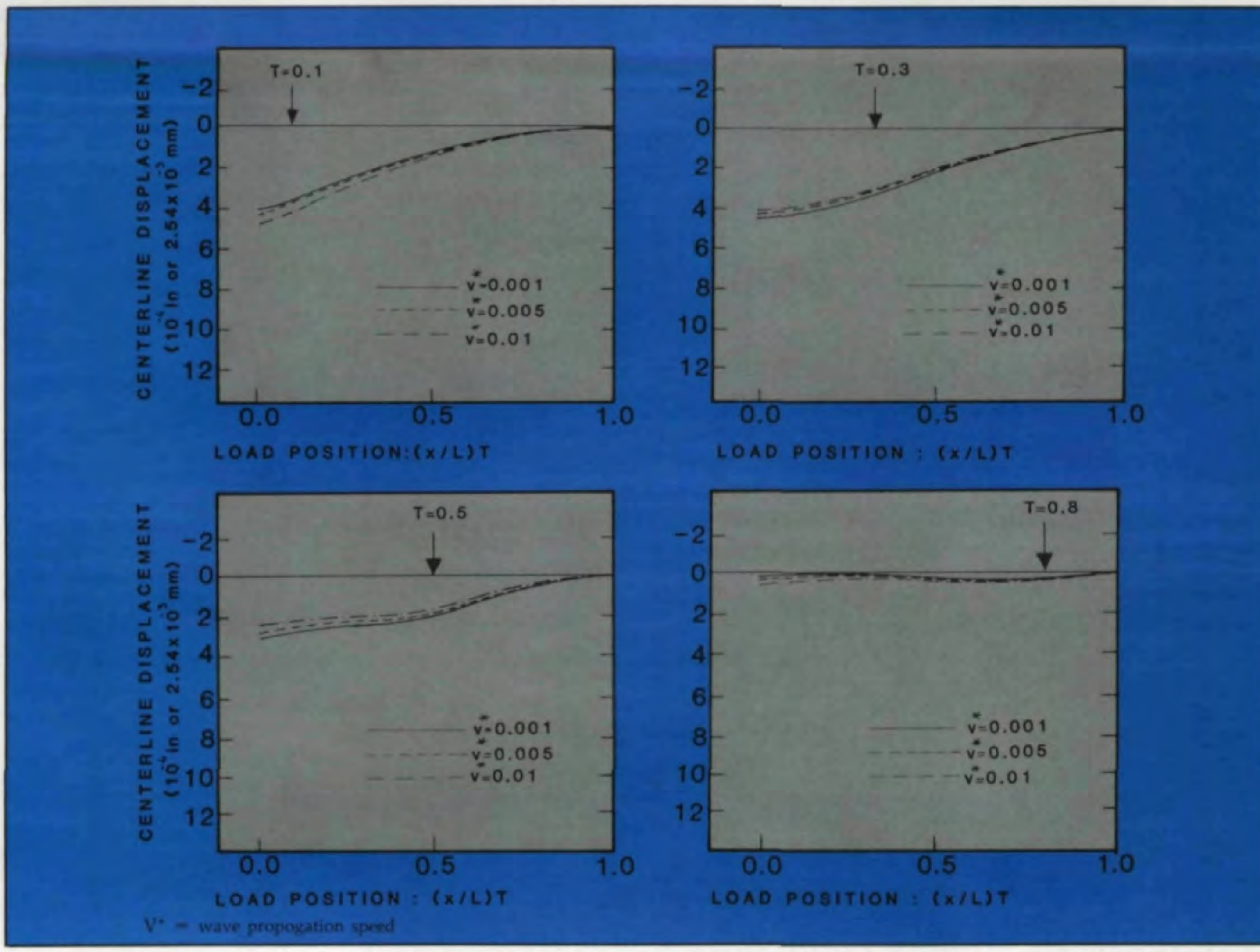

Fig. 3 – Centerline Displacements for the Beam of Fig. 1 for Various Load Speeds and Positions.

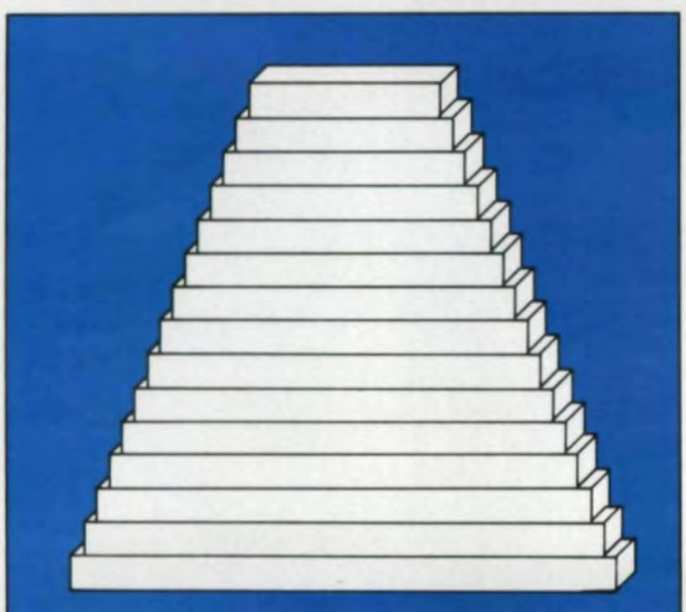

Fig. 4 – Stepped Beam Model.

gears and sprockets since tip relief and tooth design modifications for dynamic effects are generally based upon the static load deflection curve. This curve closely resembles the low speed curves of Figs. 3, 5, 7, and 8. Thus, for higher load speeds (for example, greater than 0.005V*), the design modifications may lead to *deleterious* as opposed to beneficial effects.

Third, Figs. 11 and 12 show that disengagement of the load may also induce significant vibration. Indeed, for rapidly rotating gears and sprockets, this vibration could lead to interference and impact during subsequent engagement.

Finally, the shape of the tooth itself can affect the load speed and thus induce vibration. For involute tooth forms, the load speed is proportional to the time of engagement and to the square of the rotation speed. This means that the induced vibration and other dynamic effects become much more pronounced as the gear or sprocket rotational speed is increased.

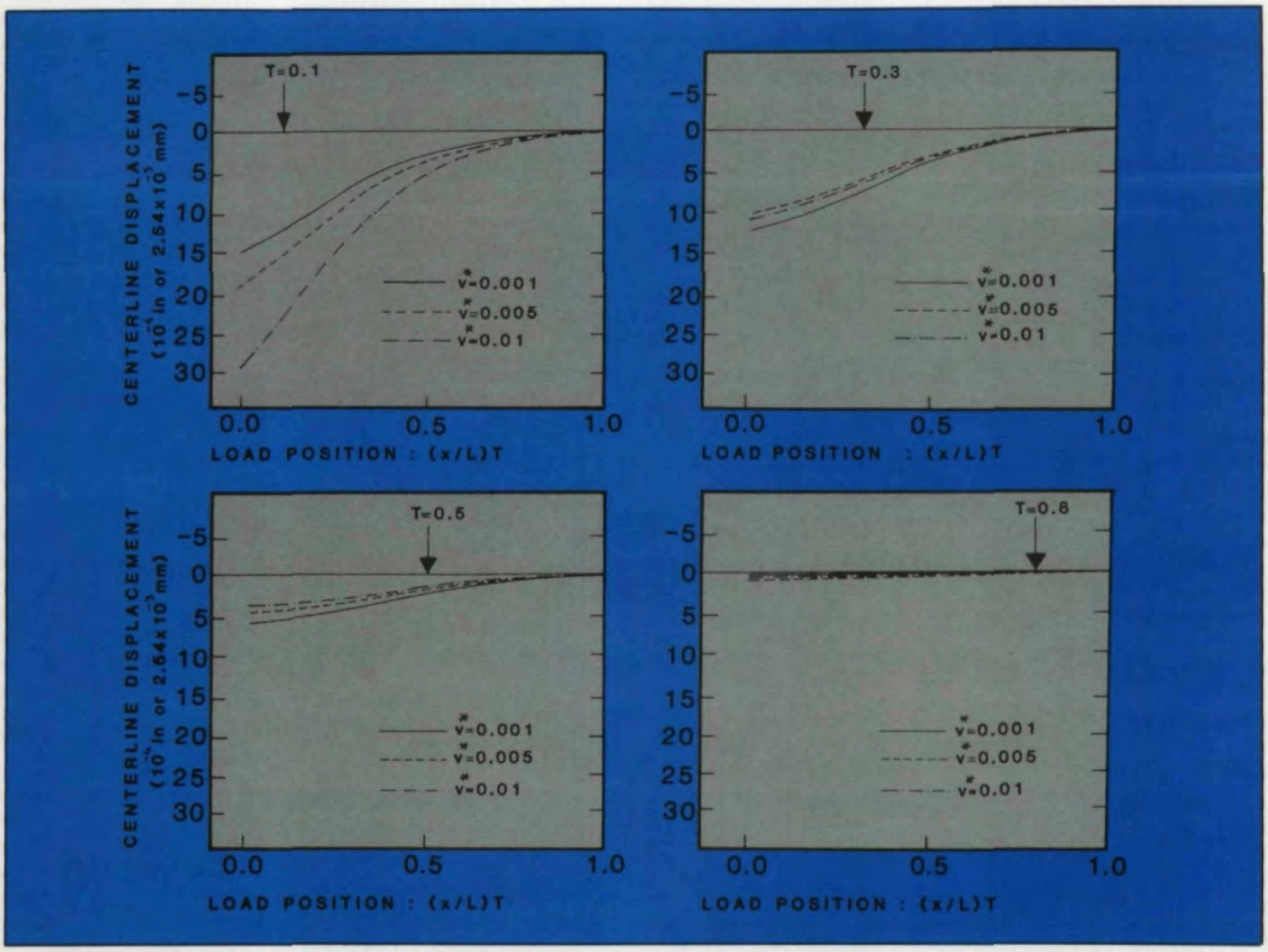

Fig. 5 – Centerline Displacements for the Stepped Beam of Fig. 4 for Various Load Speeds and Positions.

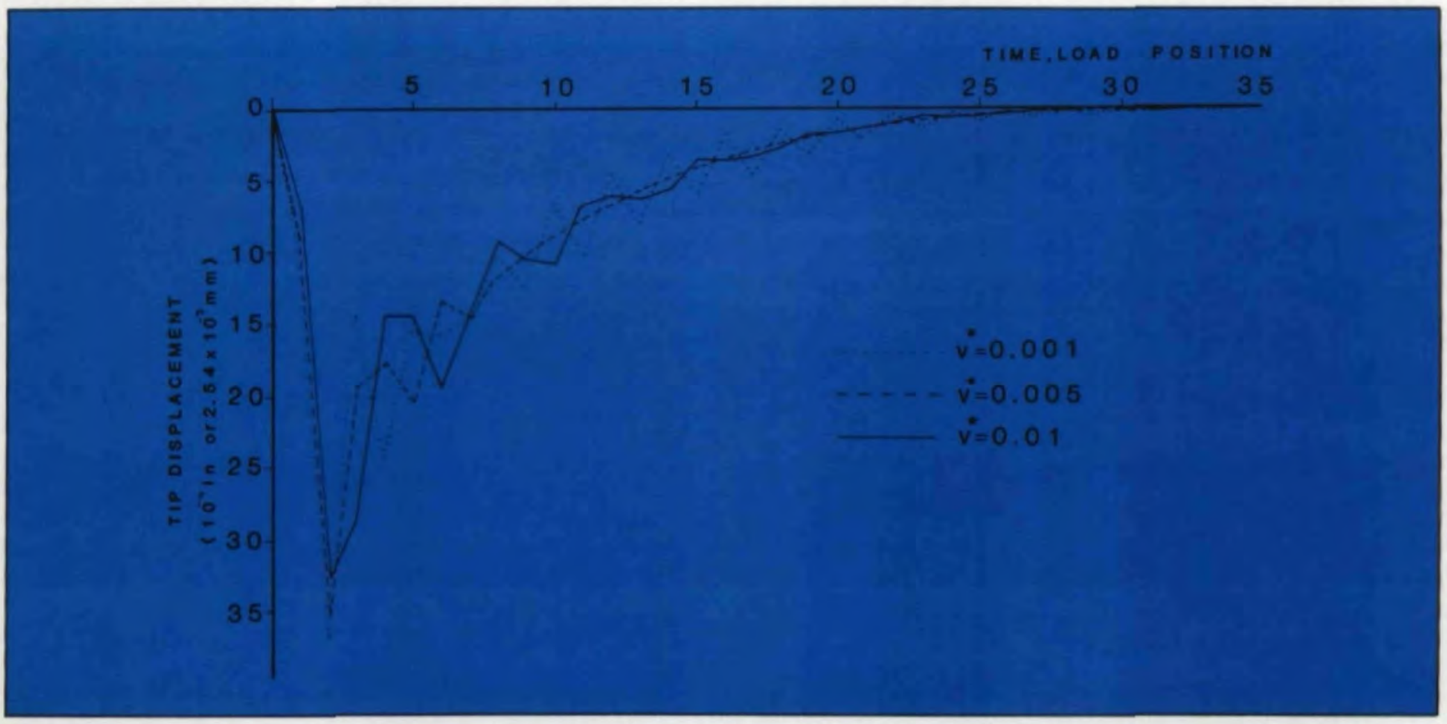

Fig. 6 – Tip Displacements for the Stepped Beam of Fig. 4 for Various Load Speeds.

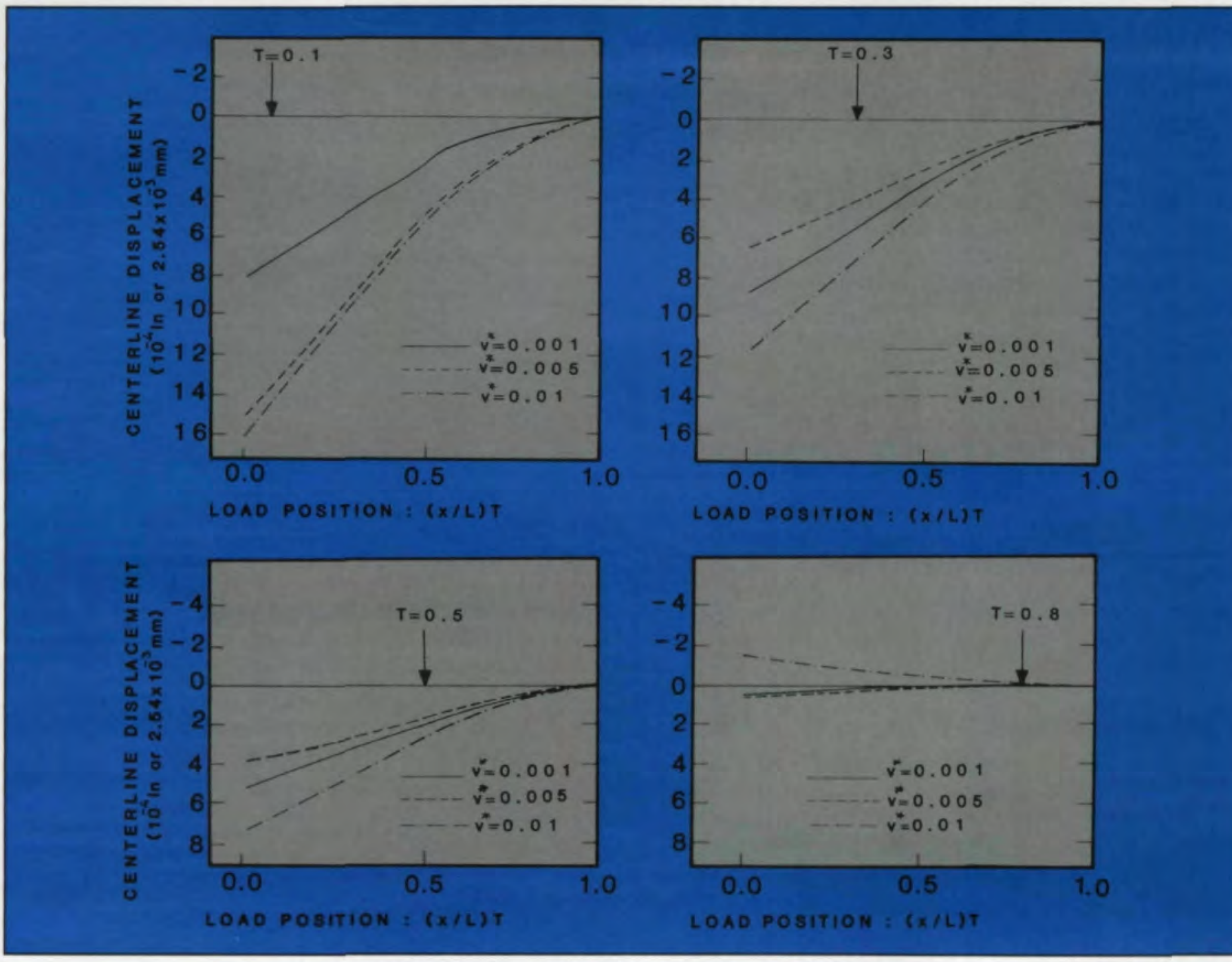

Fig. 7 – Centerline Displacement for a Straight Beam with Slenderness Ratio: 26.

APPENDIX

Moving Load Along an Involute Tooth Form

Recall that an involute to a circle may be viewed as the locus of the end point of a cord being unwrapped around the circle. Consider the clockwise involute I to the circle C shown in Fig. 13. Let $\underset{\sim}{p}$ locate a typical point P of I relative to O, the center of C. Then, if $\underset{\sim}{r}$ and $\underset{\sim}{t}$ are the radial and tangential vectors as shown, $\underset{\sim}{p}$ may be written as:

$$\underset{\sim}{p} = \underset{\sim}{r} + \underset{\sim}{t} \tag{A1}$$

Let X and Y be Cartesian coordinate axes with origin at O and with accompanying unit vectors $\underset{\sim}{n}_x$ and $\underset{\sim}{n}_y$. Let the Y-axis pass through the origin O of I. Finally, let ϕ be the angle between $\underset{\sim}{r}$ and the X-axis. Then, $\underset{\sim}{p}$ may be expressed in terms of $\underset{\sim}{n}_x$, $\underset{\sim}{n}_y$, and ϕ as:

$$\underset{\sim}{p} = (r\sin\phi - r\phi\cos\phi)\underset{\sim}{n}_x + (r\cos\phi + r\phi\sin\phi)\underset{\sim}{n}_y \tag{A2}$$

where r is the radius of C. Hence, the X-Y coordinates of P are:

$$x = r(\sin\phi - \phi\cos\phi) \text{ and } y = r(\cos\phi + \phi\sin\phi) \tag{A3}$$

The arc length along I from its origin O to a typical point P is then:

$$s = \int_O^\phi [(dx/d\phi)^2 + (dy/d\phi)^2]^{1/2} d\phi = r\phi^2/2 \tag{A4}$$

From the properties of involute geometry [26], since the normal to I at P is tangent to C (See Fig. 13), P is the contact point of the involute tooth form with its mating tooth form. Therefore, the speed V of the contact point, and hence the load, along the tooth is:

$$V = ds/dt = r\phi(d\phi dt) = r\omega^2 t \tag{A5}$$

where $\omega(=d\phi dt)$ is the angular speed of the gear or sprocket.

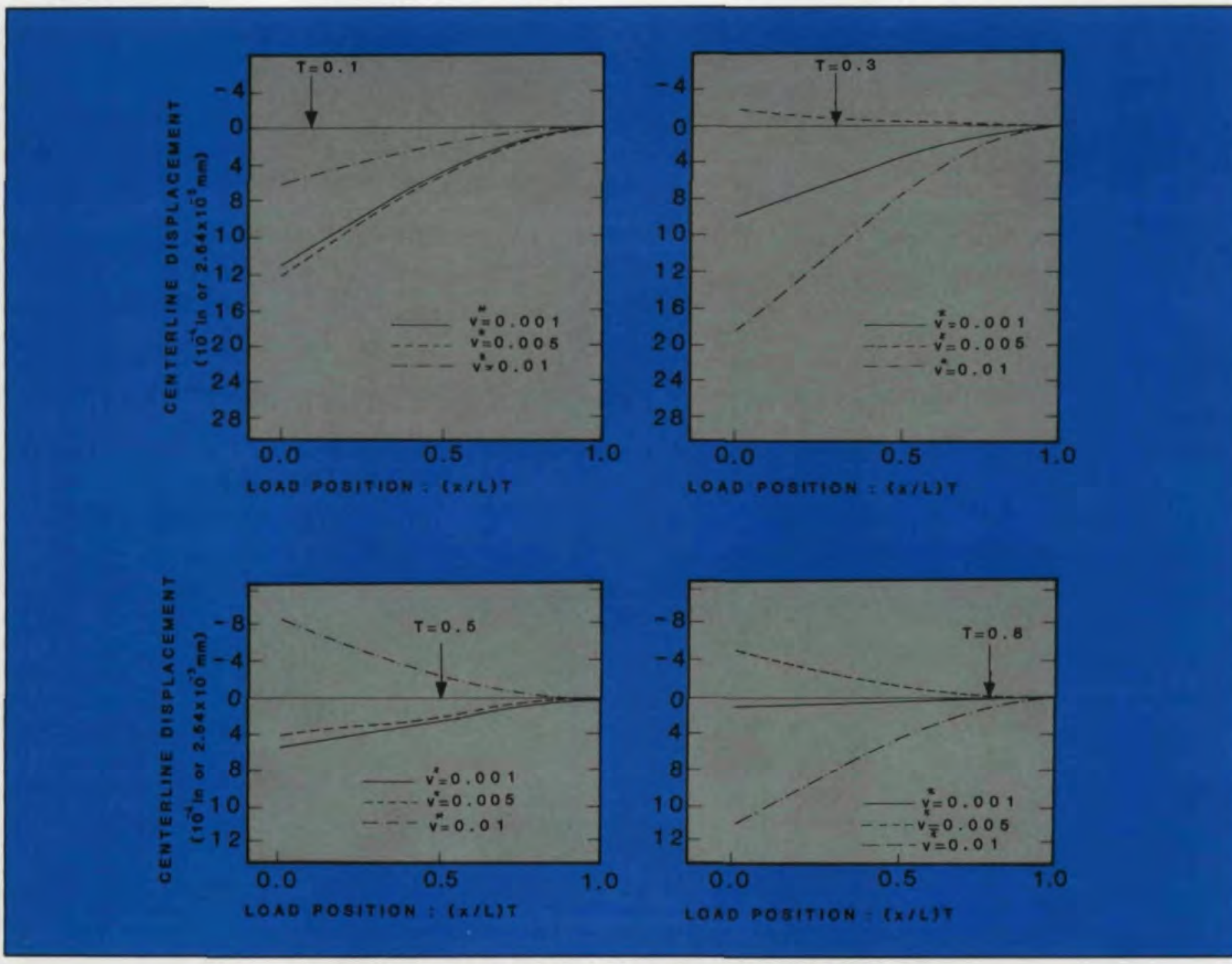

Fig. 8—Centerline Displacement for a Straight Beam with Slenderness Ratio: 78.

References

1. NAGAYA, K., and UEMATSU, S., "Effects of Moving Speeds of Dynamic Loads on the Deflections of Gear Teeth," *Journal of Mechanical Design*, Vol. 103, 1981, pp. 357-363.
2. NAGAYA, K., "Approximate Dynamic Analysis of Timoshenko Beams and Its Applications to Tapered Beams," *Journal of the Acoustical Society of America*, Vol. 66, 1979, pp. 794-800.
3. ATTIA, A. Y., "Dynamic Loading of Spur Gear Teeth," *Journal of Engineering for Industry*, Vol. 81, 1959, pp. 1-9.
4. UTAGAWA, M. and HARADO, T., "Dynamic Loads on Spur Gear Teeth at High Speed," *Bulletin of the JSME*, Vol. 4, 1961, pp. 706-713.
5. WALLACE, D. B., and SEIREG, A., "Computer Simulation of Dynamic Stress, Deformation, and Fracture of Gear Teeth," *Journal of Engineering for Industry*, Vol. 95, 1973, pp. 1108-1114.
6. CORNELL, R. W., and WESTEVELT, W. W., "Dynamic Tooth Loads and Stressing for High Contact Ratio Spur Gears," *Journal of Mechanical Design*, Vol. 100, 1978, pp. 69-76.
7. RICHARDSON, H. H., "Static and Dynamic Load, Stresses and Deflection Cycles in Spur Gear Systems," Sc.D. Thesis, Massachusetts Institute of Technology, 1958.
8. HOWLAND, J. S., "An Investigation of Dynamic Loads in Spur-Gear Teeth," M.S. Thesis, Massachusetts Institute of Technology, 1972.
9. HOUSER, D. R., and SEIREG, A., "An Experimental Investigation of Dynamic Factors in Spur and Helical Gears," *Journal of Engineering for Industry*, Vol. 92, 1970, pp. 495-503.
10. HOUSER, D. R., and SEIREG, A., "Evaluation of Dynamic Factors for Spur and Helical Gears," *Journal of Engineering for Industry*, Vol. 92, 1970, pp. 504-515.
11. YADA, T., "Relation of Frictional Loss of Gear to Speed and Torque," *Bulletin of the JSME*, Vol. 16, pp. 872-880.
12. ICHIMARU, K., and HIRANO, F., "Dynamic Behavior of Heavy-Loaded Spur Gears," *Journal of Engineering for Industry*, Vol. 96, pp. 373-381.
13. KASUBA, R., and EVANS, J. W., "An Extended Model for Determining Dynamic Loads in Spur Gearing," *Journal of Mechanical Design*, Vol. 100, 1978, pp. 69-76.
14. MARTIN, K. F., "The Efficiency of Involute Spur Gears," *Journal of Mechanical Design*, Vol. 103, 1981, pp. 160-169.

(continued on page 22)

Influence of Relative Displacements Between Pinion and Gear on Tooth Root Stresses of Spiral Bevel Gears

H. Winter and M. Paul
Technical University, Munich, West Germany

Introduction

The manufacturing quality of spiral bevel gears has achieved a very high standard. Nevertheless, the understanding of the real stress conditions and the influences of certain parameters is not satisfactory. This refers to the influence of geometric data (like flank curvature, crowning, spiral angle, etc.) or mounting conditions on stress distribution and load capacity. The design of bevel gears in general is based on experience. The investigation of tooth root stresses at spiral bevel gears, described in this paper, was initiated under these aspects. This research program started in 1981 at the FZG, Munich (Forschungsstelle für Zahnräder und Getriebebau – Gear Research Laboratory). It is financed by the DFG (Deutsche Forschungs-Gemeinschaft – German Research Association). The research method follows a line of similar basic studies on tooth root stresses for spur [1] and helical[2] gears and is also mainly based on experimental investigations.

The main objective was to gain reliable information on the amount, direction, and distribution of root stresses in spiral bevel gears by direct measurements. Especially the influence of size and location of the contact pattern on the working conditions of a bevel gear set should be investigated. In this connection, the influence of the amount of crowning of the pinion teeth should be examined. The results of this investigation were intended to provide data for verification of similar theoretical calculations[3] and, therefore, to present a contribution to a more accurate and realistic calculation of the load capacity of bevel gears.

The measuring method is explained and some general results on the distribution of tooth root stresses are discussed. In particular, the influence of various contact patterns achieved by defined relative displacements between pinion and gear are described.

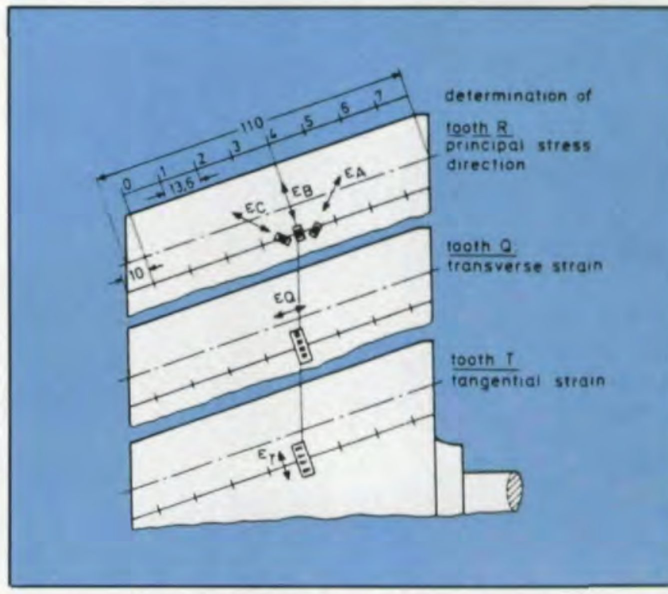

Fig. 1 – Type and position of the strain gages.

Measuring Method

In the fillet surface of a loaded tooth, there is a two-dimensional stress status. Therefore, the principal (maximum) stresses can be evaluated by following the rules of Mohr's circle:

$$\epsilon_{1,2} = \frac{\epsilon_T - \epsilon_Q}{2} \pm \frac{\epsilon_T - \epsilon_Q}{2\cos(2\psi)} \tag{1}$$

$$\sigma_{12} = E(\epsilon_{12} + \nu\epsilon_{21})/(1 - \nu^2) \tag{2}$$

For an experimental determination of the principal stresses δ_1 and δ_2 at any point in the root fillet, three measurements (ψ, ϵ_T, ϵ_Q) must be determined. ψ specifies the principal stress direction. ϵ_T and ϵ_Q are strains oriented in perpendicular directions.

Corresponding to these relations different types of strain gages had to be used to determine the strain elements. The arrangement of the gages is shown in Fig. 1. On tooth *R*, strain gage rosettes are applied to evaluate the principal stress direction (angle ψ). These rosettes are approximately positioned at the height of the 30 deg-tangent-point (see Fig. 4). The teeth *Q* and *T* are fitted by 10-element strip gages having a grid length of 0.51 mm (0.020 in.). On tooth *Q* , the

---

AUTHORS:

PROF.DR.-ING. HANS WINTER *has studied as an associate of Prof.Dr.-Ing.h.c. Gustav Niemann. He received his Doctoral degree at the Technical University of Munich. In 1956, he began his work in the German gear industry: Zahnradfabrik, Friedrichshafen (Calculation, research, manufacturing), Demag, Duisburg (Research, development, design, selling). Since 1969 he has been the head of the Laboratory of Gear Research and Gear Design (FZG) at the Technical University of Munich.*

MR. MICHAEL PAUL *is the Chief Engineer at the Gear Research Laboratory (FZG). From 1978 to 1984 he was an assistant at this laboratory and was involved in research of tooth root stresses of spiral bevel gears. Mr. Paul studied engineering at the Technical University of Munich.*

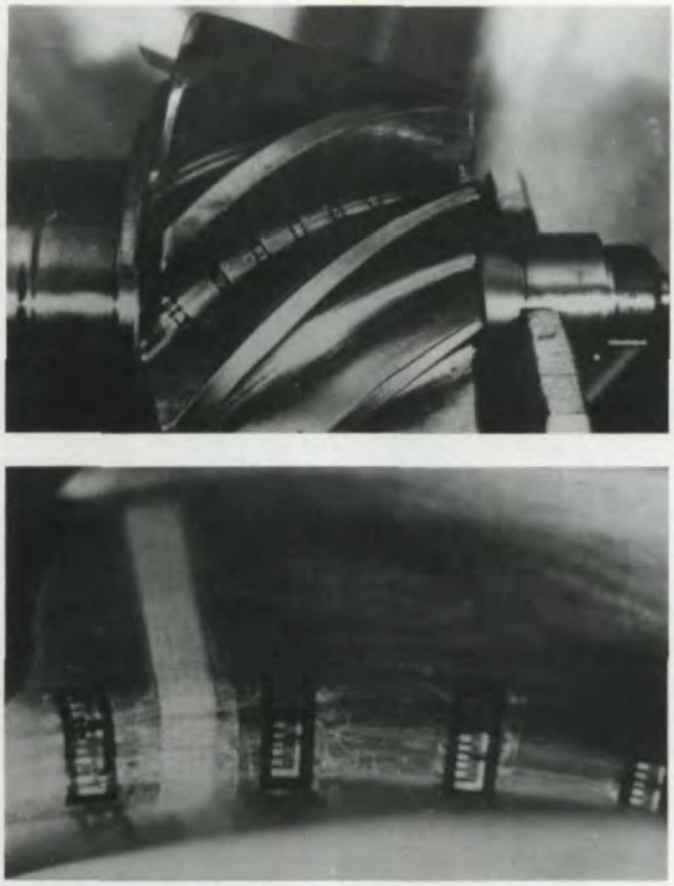

Fig. 2 — Pinion tooth with 10-element strip gages (before they were wired).

measuring direction of the grids is oriented lengthwise, and on tooth T in the direction of the tooth height. These strip gages cover nearly the whole root curvature, so that the stress distribution across the root fillet can be determined.

To determine the stress distribution across the facewidth, eight of these gages are fitted on each measuring tooth. Fig. 2 shows the strain strips on one pinion tooth before they were wired. Wiring such a large number of strain gages was a severe problem since the normal meshing of the mating teeth could not be disturbed. Only the small clearance space provided at the bottom was available. Considering this fact, a test gear set having a large module (normal module in midfacewidth = 12 = 2.12 DP) had to be chosen. For essential geometric data, see Fig. 3. This test gear set represents a typical gear design. The gears were manufactured by Klingelnberg und Söhne, Germany.

Fig. 4 gives a summary of the relationship between the different measuring data in detail. Determination of the principal stress direction ψ by using three rosette strains is explained in Fig. 4(b). Fig. 4(a) shows the relationship between ψ and the strip gage strains ϵ_T and ϵ_Q.

It has to be considered that the principal directions estimated by the rosettes are theoretically valid for only one level of the root depth. The transverse and tangential strains were measured across the whole area of the root fillet; so the combination of data taken from different tooth height levels might not be correct. To estimate the eventual error,

nomenclature	pinion	gear
number of teeth	11	36
normal module in midfacewidth	12	
outer transverse module	17.50	
outer pitch diameter /mm/	192.50	630.00
mean spiral angle	34.597	
cutter radius /mm/	210.00	
excentricity (pinion) /mm/	2.5	
total contact ratio (theoretical)	2.8	
addendum modification	0.34	-0.34
thickness modification	0.025	-0.025
material	17 CrNiMo 6 (through hardened)	

Fig. 3 — Main data of the test gear set.

on one tooth the rosettes were bonded on different levels, and it was found that the difference of the principal directions in the area covered by one strip gage is largely negligible. Therefore, this approximation seems to be tolerable.

The combination of measuring data received from three different teeth requires that loading conditions are equal on these teeth. Fig. 5 shows how the measuring teeth of the gear were selected considering the adjacent pitch error. These teeth which were selected, showed a minimum pitch fluctuation with their neighboring teeth. So for these teeth, one can assume that the conditions referred to the load distribution on several pairs, in contact at the same time, might be largely the same.

Loading Device

The loading of the large test gears required a rigid test rig. This is shown in Fig. 6. To apply torque, the gear is loaded against the blocked pinion by using a hydraulic system.

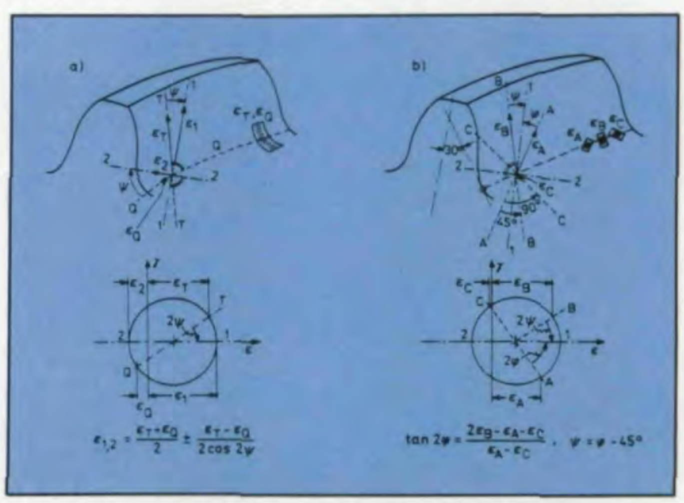

Fig. 4 — Determination of the prinicpal strains from the measuring data.

Nomenclature

f_a = pinion offset deviation, mm
$f_{v1,2}$ = axial displacement of pinion/wheel, mm
f_Σ = shaft angle deviation, degree
E = modulus of elasticity, N/mm^2 (E = 210 000 N/mm^2)
T_1 = pinion torque, Nm
$\epsilon_{1,2}$ = principal strains, μm/m
$\epsilon_{A,B,C}$ = rosette strains, μm/m
ϵ_Q = transverse strains, μm/m
ϵ_T = tangential strains, μm/m
ν = Poisson's ratio (ν = 0.3)
$\sigma_{1,2}$ = principal stresses, N/mm^2
σ_T = stress in depth wise direction, N/mm^2
φ = angle between ϵ_A and ϵ_1, deg
ψ = angle between ϵ_B and ϵ_1 deg

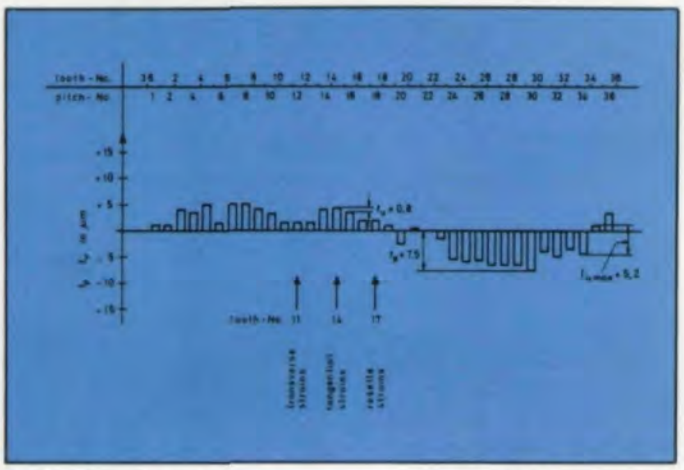

Fig. 5 – Determination of the measurement gear teeth suitable for considering the adjacent pitch errors.

Measurements along the whole path of contact were made stepwise while holding the pinion in different rotary positions. That meant that the load was applied statically on discrete lines of contact to which the corresponding stress distribution is related. Therefore, all results discussed in this paper refer to the static loaded condition.

The test rig provides for accurate adjustments of defined positions and displacements of the pinion and gear. By an additional mechanism, the deflections under load can be set back.

General Results on the Distribution of Tooth Root Stresses

Before discussing the influence of displacements on tooth root stresses, some general results should be mentioned. Fig. 7 shows the distribution of the tensile strains across the root fillets of pinion and gear, plotted in the normal section. The stress curves are nearly the same as those of cylindrical gears. Looking at the gear, it becomes obvious that the maximum tension appears almost exactly at the 30-deg. tangent point.

Fig. 6 – Loading device for determination of tooth root stresses at bevel gears.

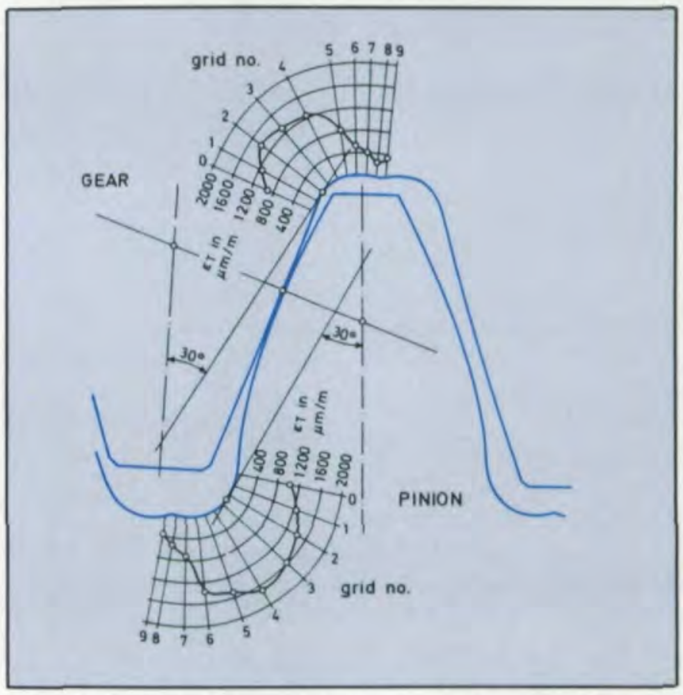

Fig. 7 – Distribution of the tangential strains over the root fillet: (measuring point 4; mesh position 4, compare Fig. 9; torque T_1 = 8000 Nm).

On the pinion, the point of maximum stress is somewhat closer to the root circle. These results were well confirmed by finite element analysis applied to the actual tooth profiles. Moreover, it was found that the point of maximum strain is nearly independent of the bending arm and largely constant across the face width.

Therefore, in the following evaluation, the strain and stress distributions are plotted for the level in the root fillet where the maximum stresses occur.

In Fig. 8, the distributions of the tangential and transverse strains are plotted for different mesh positions, i.e. for different lines of contact. It can be seen that the maximum tangential strains occur approximately at the center of the line of contact. At that point, the transverse strains have their (negative) minimum. That means that the depthwise tension is accompanied by a lengthwise contraction.

It has to be pointed out that the scales used in Fig. 8 for the transverse and tangential strains differ in about one magnitude. The transverse strains are relatively small and are equal to about 5 percent of the maximum tangential strains. This is an effect of the relatively short line of contact compared to the total face width; so the unloaded ends of the teeth largely obstruct the transverse strains.

The principal stresses received by a combined evaluation of the tangential, transverse, and rosette strains are plotted for the pinion in Fig. 9. The arrows qualitatively show the

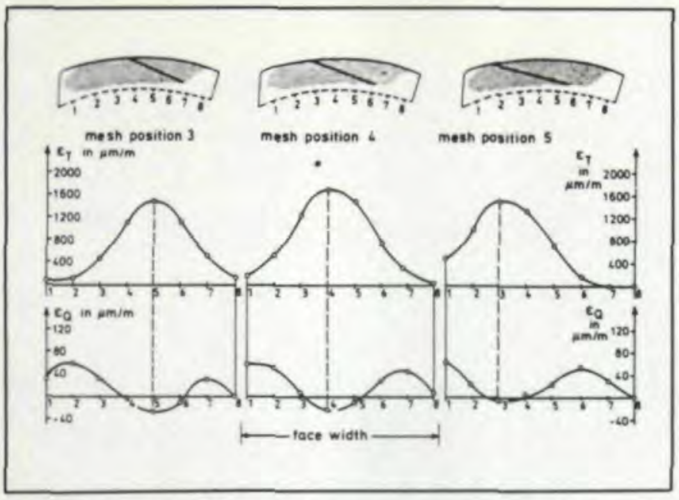

Fig. 8 – Distribution of the tangential and transverse strains over the facewidth at the pinion (torque $T_1 = 8000$ Nm).

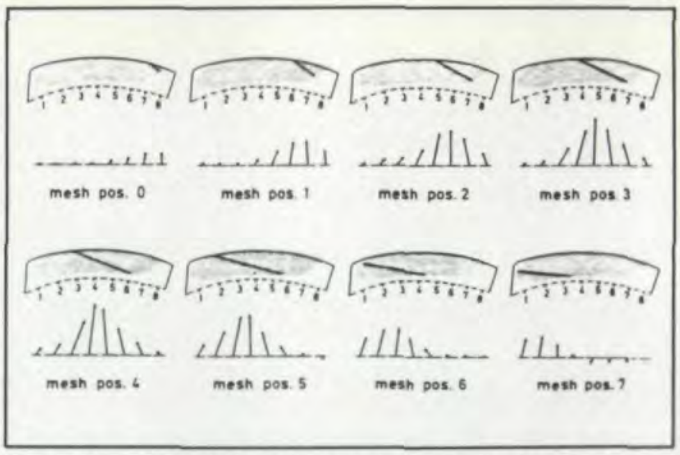

Fig. 9 – Value (qualitatively) and orientation of the absolute greater principal stresses.

magnitude and orientation of the (absolute) greater principal stresses. It is obvious that in each mesh position the stresses are directed toward one common point. This point is located approximately at the center of the corresponding line of contact. That means that the maximum stress in each position is oriented approximately in the depthwise direction. Therefore, the real tension status can be closely approximated by straight bending, if only the maximum stresses are of interest. The calculation methods, which are based on such a straight bending, seem to represent a good approximation. The same results were found for the gear.

In Fig. 10, the stress distribution over the facewidth and for the whole contact cycle is plotted for the pinion and the mating gear. These measurements were made with the original rating position of the contact pattern. The pinion torque was 8000 Nm, which corresponds approximately to the fatigue limit of an equivalent case hardened gear set.

Looking first at the pinion it can be seen that the contact begins at the toe with light load (mesh position 0; corresponding lines of contact see Fig. 9). After that, the stresses gradually increase while the stress concentration shifts toward the heel. The maximum stress appears in mesh position 4, nearly in the middle of the face width (see the hatched area). At this position, a nearly symmetric stress distribution over the facewidth is observed. Subsequently, the stresses decrease until the heel goes out of contact.

The corresponding plot for the gear looks quite different. We observe an extensive area of compressive stresses at the beginning of the contact (see screened field). These stresses are caused by the loading of the neighboring tooth. They amount to about 35 percent of the maximum tensile stress, i.e. in this region there is an alternating loading in the root of gear. On the pinion, only a small area of compressive stresses is found amounting to about 15 percent of the maximum tensile stress.

Corresponding to the position of the line of contact, the tensile stresses at the gear first appear at the toe and then extend gradually over the facewidth. The maximum stresses appear in mesh positions 4 and 5. Both have about the same amount and they are located at midfacewidth, respectively, shifted somewhat toward the heel.

In general, the plotted stress curve for the gear is flatter than for the pinion. In the test gear set, the maximum stress at the gear was about 25 percent lower.

Load Distribution With Multiple Teeth Contact

The total contact ratio of spiral bevel gears normally exceeds a value of 2. That means that there are always two, sometimes three, teeth in mesh simultaneously. The tangential force is distributed on two or three teeth.

The influence of load distribution on the tooth root stresses was determined by measurements with single and multiple tooth contact.

Fig. 11 shows the stress curve for single (broken line) and multiple tooth contact (full line) plotted across the face width. In mesh positions 2 and 6, there are two pairs of teeth in contact and the load is distributed almost equally. If one tooth is removed (by milling) the stresses at the root of the remaining tooth increases to about twice the value with double contact. With mesh position 4, where three pairs of teeth are simultaneously in contact, the root stresses in the case of single contact are about the same as with multiple contact.

The teeth before and behind, having short lines of contact only, carried a very small portion of the total load.* As the maximum stress occurs in this position, it can be stated that a high theoretical contact ratio (in case of the test gears ≈ 2.8) does not essentially reduce the maximum tooth root stresses.

In Fig. 12, the percentages of load carried by one tooth in the course of the contact is plotted. The load is smoothly taken over from the tooth before (*V*) and given further to the tooth behind, and there is a short period of time when tooth (*M*) has to carry nearly the total load (for this example about 98 percent).

*The complete distribution of root stresses in the loaded area is much more complicated than can be described by Fig. 11. So tensile and compressive tooth root stresses overlap each other when the teeth before and behind carry a portion of the total load. This has to be taken into account with regard to the load capacity. Moreover, it has to be considered that the length of the line of contact is increased if the total load is applied to one pair of teeth only. The results in Fig. 12 include this more detailed consideration.

You are cordially invited to learn from the best . . . ask the man who's been there

ITW Illitron

Gear Systems . . .

3601 WEST TOUHY AVENUE
LINCOLNWOOD, ILLINOIS 60645
312-761-2100

The Society of Manufacturing Engineers (S.M.E.) has approved this School for Professional Credits toward the S.M.E. Recertification Program. Credits are awarded on the basis of one credit per content hour.

GEAR TRAINING PROGRAM

1. BASIC FUNDAMENTALS

1. **Gear History**
   - A. Cycloidal Teeth
   - B. Involute Teeth
   - C. Gear Cutting Machines
   - D. Gear Cutting Tools
2. **Gear Types**
   - A. Parallel Axis
   - B. Intersecting Axis
   - C. Skew Axis
3. **Gear Ratios**
4. **Involute Gear Geometry**
   - A. Nomenclature
   - B. Involutary — Contact Ratio, etc.
   - C. Helical Gears — Lead — Helical Overlap
5. **Gear Tooth Systems**
   - A. Full Depth
   - B. Full Fillet
   - C. Stub Depth
6. **General Formulae**
7. **Mathematics — (I.T.W. Trig Book)**

2. HI SPEED STEELS

- A. Common Types
- B. Special Types
- C. Heat Treatment — Metallurgy — Forgings
- D. Controls
- E. Surface Treatments
- F. Special Cases

3. CUTTING THE GEAR

1. **Forming**
   - A. Milling
   - B. Broaching
   - C. Shear Cutting
2. **Generating**
   - A. Shaping
     - a) Rack Type
     - b) Circular Type
     - c) Machine Types and Manufacturers
     - d) Schematic — Principles
     - e) Speeds — Feeds
     - f) Machine Cutting Conditions
   - B. Hobbing
     - a) The Hobbing Machine
     - b) Types and Manufacturers
     - c) Schematic — Differential and Non-Differential
     - d) Speeds — Feeds
     - e) Climb Cut — Conventional Cut
     - f) Shifting — Types
3. **The Hob as a Cutting Tool**
   - A. How It Cuts
   - B. Tolerances and Classes
   - C. Multiple Threads
   - D. Hob Sharpening and Control
   - E. The Effect of Hob and Mounting Errors on the Gear
4. **The Shaper Cutter as a Cutting Tool**
   - A. Know Your Shaper Cutters
   - B. Design Limitations
   - C. Sharpening
   - D. The Effect of Cutter Mounting and Errors on the Gear
   - E. Manufacturing Methods
5. **Tool Tolerance Vs. Gear Tolerance**
   - A. Machining Tolerances
   - B. Gear Blank Accuracy and Design Limitations

4. FINISHING THE GEAR

1. **Gear Finishing — Before Hardening**
   - A. Shaving
     - a) The Shaving Cutter
     - b) Types of Shaving — Conventional, Underpass, Diagonal
     - c) Crown Shaving
     - d) Shaving Cutter Modifications
     - e) Co-ordinating Tool Design — The Shaver and Pre-Shave Tool
     - f) Re-Sharpening
     - g) Machines
   - B. Rolling
2. **Gear Finishing after Heat Treat**
   - A. Honing
   - B. Lapping
   - C. Grinding
     - a) Methods — Formed Wheel-Generating — Threaded Wheel
     - b) Machine Types

5. GEAR INSPECTION

1. **Functional**
   - A. Gear Rollers
   - B. Gear Charters
     - a) Reading the Chart
     - b) Tooth-to-Tooth Composite Error
     - c) Total Composite Error
   - C. Master Gears
     - a) Tolerances
     - b) Designs
     - c) Special Types
2. **Analytical**
   - A. Size — Tooth Thickness
   - B. Runout
   - C. Spacing
   - D. Lead
   - E. Involute
3. **Automatic and Semi-Automatic**
   - A. How They Work
   - B. What Can Be Checked
   - C. How Fast
4. **Chart Interpretation — Analytical and Functional**
   - A. Reading the Charts
   - B. Which Errors Affect Other Elements
   - C. How to Correct the Error the Chart Shows

6. INDIVIDUAL INSTRUCTION AND SPECIFIC PROBLEMS OR PLANT TOUR

This Program is flexible and changed to meet the needs of each group.

The 4-day program consists of a coordinated series of lectures given by the Engineering, Production and Inspection staffs of Illinois Tool Works Inc. They represent over sixty years of experience in gear and tool specialization.

The sessions are conducted with a technique and approach that leads to interesing discussion and participation. Starting with the basic fundamentals, the program is directed into those areas of greatest interest and value to the people attending the particular session. The groups are kept small so that this object is readily accomplished.

As mentioned, the planned program lasts four days. One-half of the fourth day is for individual discussion of specific problems in a detailed manner with members of the Illinois Tool Works' staff.

More than 3,500 individuals from hundreds of companies representing manufacturing, engineering, inspection and management, have come to Chicago for these programs. They have been conducted on a monthly basis since 1958. Classes have also been conducted in Europe. We are certain that this well rounded program has helped all of them to a better job and also given them a better understanding of engineering, manufacturing and inspection.

All those attending are assigned to the same hotel. This promotes friendly contact and discussion of mutual problems and interests. Tuition for the course includes transportation from the hotel to ITW and back, one group dinner, all continental breakfasts and all lunches.

We hope we may include your company in one of our Training Programs.

CIRCLE A-5 ON READER REPLY CARD

1985 Monthly Four Day Seminars

May	6- 9	September	16-19
June	10-13	October	14-17
July	15-18	November	11-14
August	19-22	December	2- 5

TUITION FEE: $550.00

Additional students, same company, same class $500.00.

Includes the transportation from the hotel to ITW and back, one group dinner, hospitality meeting, continental breakfasts, and all lunches.

For additional information contact:
ROBERT H. MODEROW
Manager, Training
312-761-2100

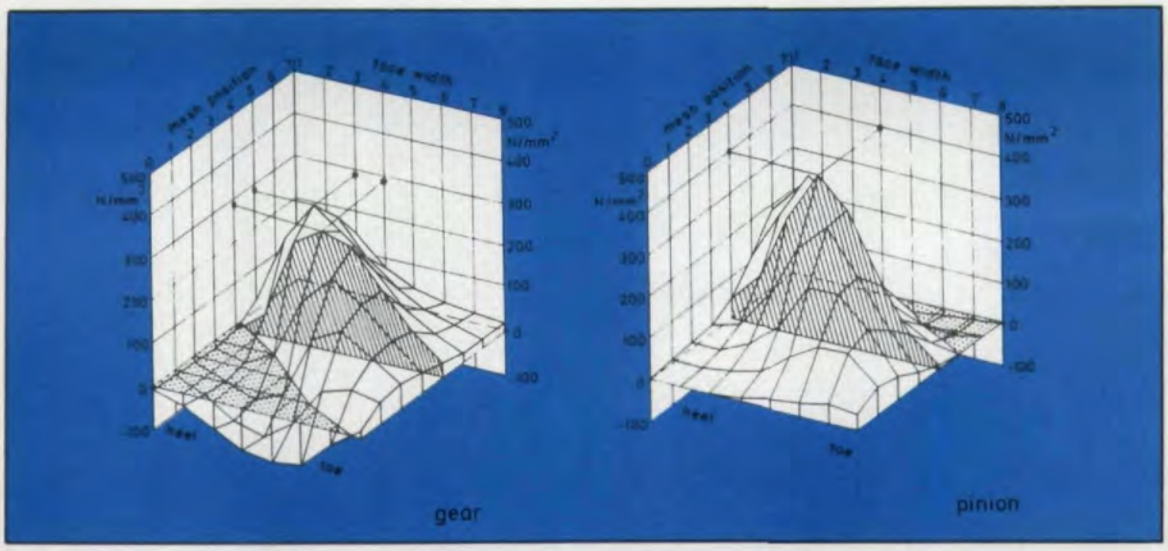

Fig. 10 – Stress distribution over facewidth and time of contact (torque $T_1 = 8000$ Nm).

Influence of Pinion and Gear Displacements on the Tooth Root Stress

Fig. 13 shows the definitions for the various relative displacements between pinion and wheel. All these displacements can be exactly adjusted in the test rig. As an example, the influence of an axial displacement of the pinion (f_{v1}) on the tooth root stresses shall be discussed. The results were achieved with a gear set having a usual length and position of the contact pattern.

Fig. 14 shows the contact patterns occurring when the mounting distance of the pinion was varied. It is easy to recognize that the light load contact pattern shifts appreciably axially and also in the depthwise direction.

If the discrete lines of contact arising from loading the teeth in the different mesh positions are combined, the contact pattern for the loaded flank is obtained. This pattern tends to move in the same way as with a light load, but the amount of the displacement is smaller. Even if the extreme positions ($f_{vl} = \pm$ 0, 8mm) are considered, the contact patterns under load nearly cover the total facewidth. On the other hand, quite a different load pattern in the depthwise direction is obtained.

Fig. 14 indicates that the stress at the end of the teeth is strongly influenced by these displacements. Fig. 15 demonstrates this for the pinion in mesh position 6. At that moment, the corresponding line of contact is positioned toward the heel. The curves indicate that there is a large increase in stress for the position of $f_{vl} = -$ 0, 8, i.e. when the contact pattern is shifted toward the heel. Compared to the stress curve for the nominal contact pattern, (full line in Fig. 15) the increase is in the order of 60 percent.

When evaluating this effect, one has to consider that the maximum stress over the whole time of contact does not appear at the moment shown in Fig. 15 (see Fig. 10).

To give a more general view in Fig. 16, the stresses were compared for those mesh positions where the maximum stresses occur. These maximum stress positions always are observed in mesh positions 4 or 5; i.e. when the lines of contact are positioned approximately in midfacewidth. As shown in Fig. 11, the tooth has to carry nearly the total load at that moment. Hence, it follows that in spite of the displacements, and although the centers of the contact patterns are spread over a wide range, the point of stress concentration is hardly moved from midfacewidth. On the pinion, this area of

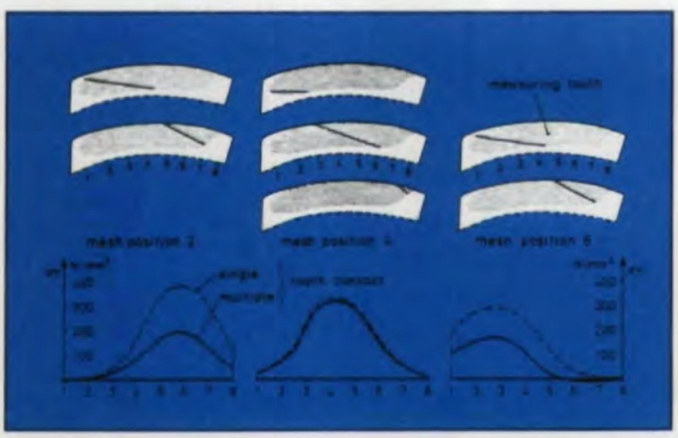

Fig. 11 – Stress distribution across the facewidth at the pinion root in case of single and multiple tooth contact (torque T_1 = 4000 Nm).

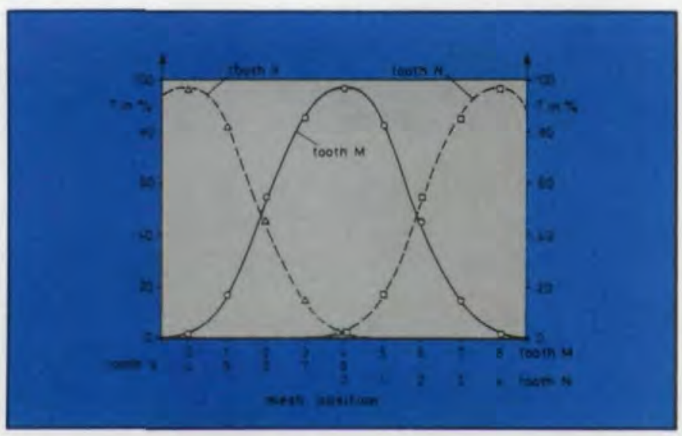

Fig. 12 – Load distribution onto meshing teeth in multiple teeth contact (torque T_1 = 4000 Nm).

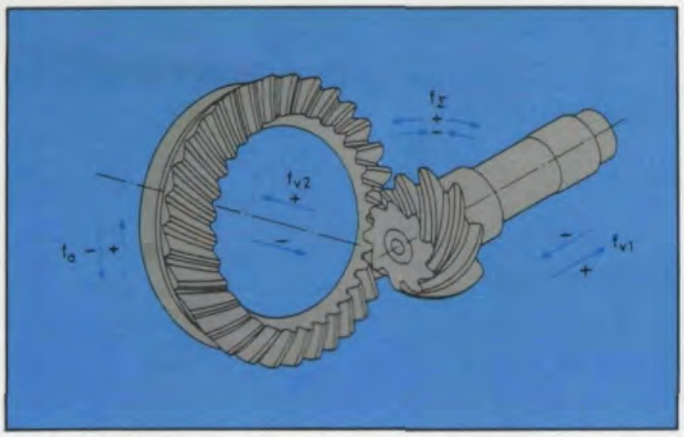

Fig. 13 – Definitions of relative displacements between pinion and wheel

maximum stress is quite narrow. This observation corresponds with experience from a large number of damage cases at bevel or hypoid gears in service. Nearly always the cracks started at the pinion teeth in the middle of the face width.

Due to the axial displacement of the pinion (f_{vl}), the maximum stresses vary in a range of about 16 percent for the gear and 20 percent for the pinion.

Fig. 17 covers a summary of the influences of the other displacements, defined in Fig. 13. For this comparison, the stress distribution curves were evaluated in the same way as shown in Fig. 15. From such curves, the maximum stresses were taken. It becomes obvious that axial displacements of the pinion (f_{vl}) and misalignments (offset) of the axes (f_a) have the strongest influence. Deviations of the shaft angle (f_Σ) and of the mounting distance of the wheel (f_{v2}) have a minor influence.

Further, one can see that the pinion stresses are always higher than the gear stresses. Of course, this effect is partly due to the design of the present test gear set, but obviously the main reason is the special load distribution over the line

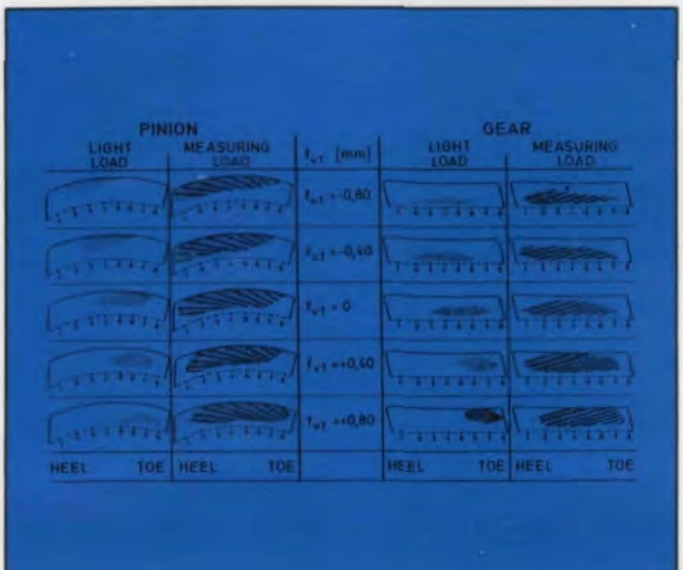

Fig. 14 – Contact patterns for different axial displacement of the pinion.

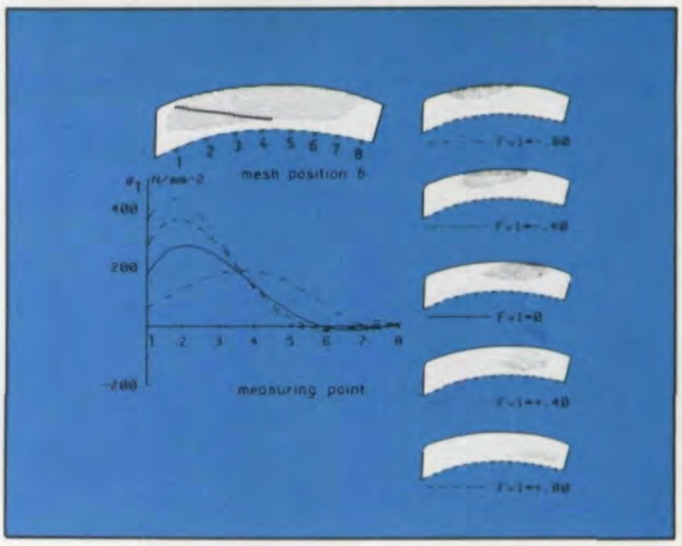

Fig. 15 – Stress distribution due to axial displacement of the pinion.

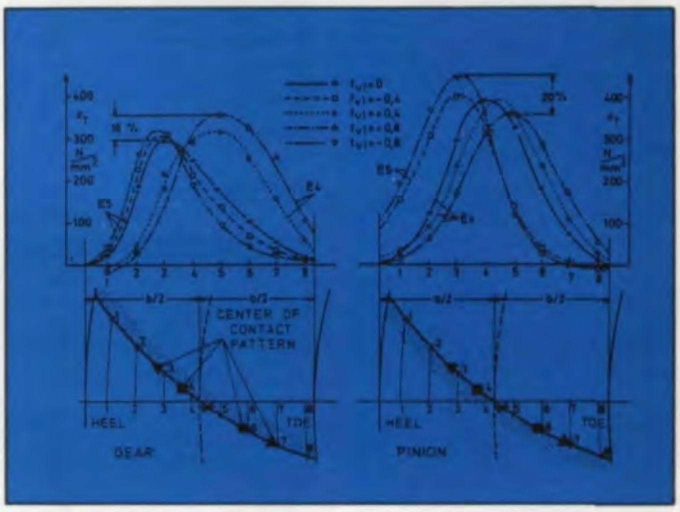

Fig. 16 – Maximum tooth root stress for various pinion mounting distances.

of contact. Previous measurements have shown that the load is more or less concentrated at the outer end of the line of contact for *all* displacements. For a left-hand spiral on the pinion, the outer end of the line of contact is located at the pinion tip and near the root of the gear (see lines of contact in Fig. 14). Therefore, very different bending arms are acting at the pinion and the gear, and the root stress differs correspondingly. It is intended to continue investigations on this interrelationship between load distribution and different relative deviations and deflections of the gears.

Moreover, it was found that a shifting of the contact pattern toward the toe (positive values of f_{vl} and f_a) results in a decrease of pinion root stress. In case of the variation of f_{vl}, this is accompanied by an increase of the gear root stresses. For the test gear set, optimum conditions were achieved for a (light load) contact pattern shifted approximately 25 percent of the facewidth toward the toe.

Nearly the same conditions, according to contact pattern and root stresses, were obtained by an offset deviation of $f_a \approx +0.5$ mm.

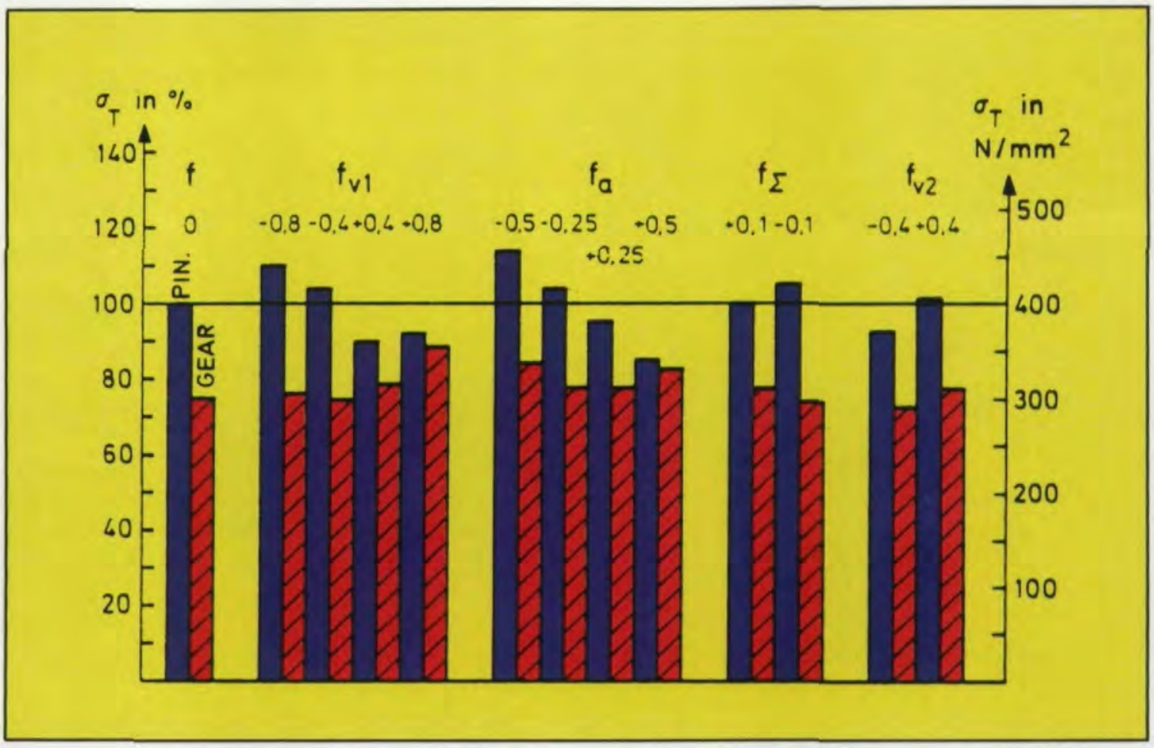

Fig. 17 – Influence of relative displacement between pinion and wheel on tooth root stresses.

Of course, the quantitative results referring to the relationship between the amount of displacement and the amount of stress increasing or decreasing are influenced by the special rigidity and mounting conditions of the test stand. This test rig is very rigid; therefore, the deflections under load are quite small. Since larger displacements, which for instance might correspond to weak aluminum housings, can be adjusted, also results valid for weak mounting conditions are achieved. For this the range of displacements adjusted for the measurements, as shown in Fig. 17, was chosen so wide that it exceeds the amount of deflection which usually might appear even in very weak configurations.

These results give a survey on the behavior of the test gear set under different working conditions. And as these results are intended to be a basis for the verification of theoretical calculations by finite element method, (e.g. the research work "Kegelradkette" of the Technical University Aachen) they can make a contribution to an improvement of the calculation of load carrying capacity of bevel gears in general.

Summary

A method for the experimental examination of tooth root stresses on spiral bevel gears has been described. The principal stresses were derived from strip strain gages and strain gage rosettes measurements.

Some basic results, referring to the stress distribution over the root fillet and along the facewidth and to the load distribution between the meshing teeth, have been discussed. It was found that the maximum stresses appear approximately at the middle of the facewidth, if the total load is carried by one pair of teeth. This result was hardly influenced by different positions of the contact patterns due to various displacements between pinion and wheel. The maximum stresses were always observed in (approximately) midfacewidth.

The maximum differences in root stresses could be achieved by varying the mounting distance of the pinion and the offset between the axes of pinion and gear. Differences up to about 20 percent in maximum stress were observed.

Common experience was confirmed on the test gear set: under light load the contact pattern should be displaced somewhat towards the toe. In this case, balanced stresses with relative low values on pinion and wheel were observed.

References

1. HIRT, M., "Einfluss der Zahnfussausrundung auf Spannung und Festigkeit von Geradstirnrädern," diss., Tu, München, 1976.
2. BROSSMANN, U., "Über den Einfluss der Zahnfussausrundung und des Schrägungswinkels auf Beanspruchung und Festigkeit schrägverzahnter Stirnräder," diss., Tu München, 1979.
3. NEUPERT, B., "Berechnung der Zahnkräfte, Pressungen und Spannungen von Stirn- und Kegelradgetrieben," diss., TH Aachen, 1983.

This article was contributed by the Power Transmission & Gearing Committee and was presented at the Design Engineering Technical Conference of the American Society of Mechanical Engineers. Paper No. 84-Det-98.

DYNAMIC ANALYSIS OF STRAIGHT . . .

(continued from page 12)

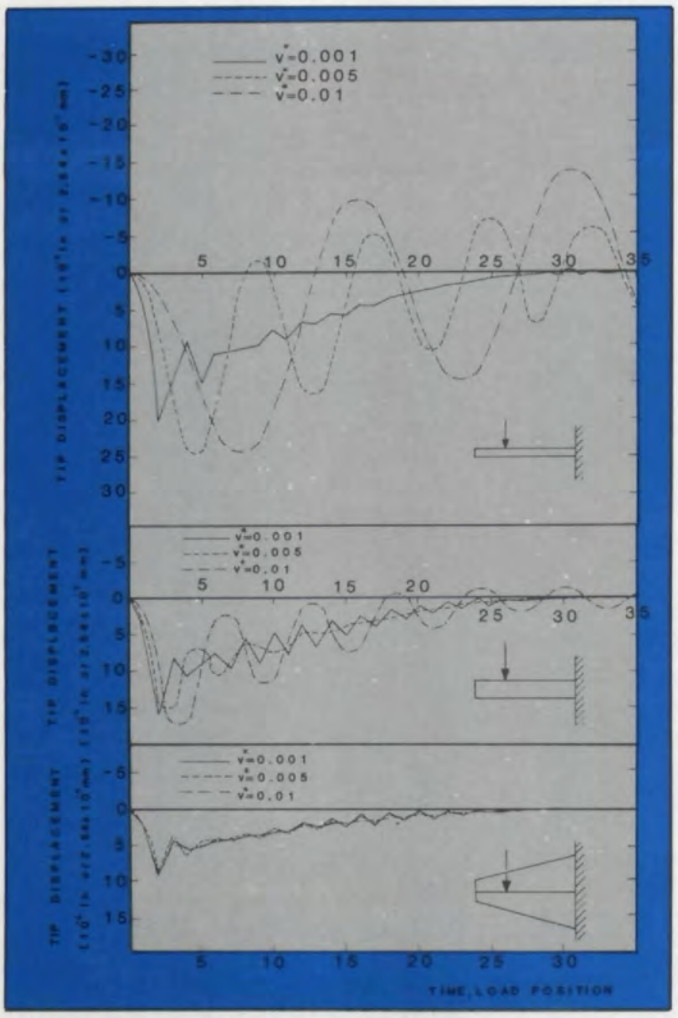

Fig. 9 – Comparison of Tip Displacements for Thin and Tapered Beam Models.

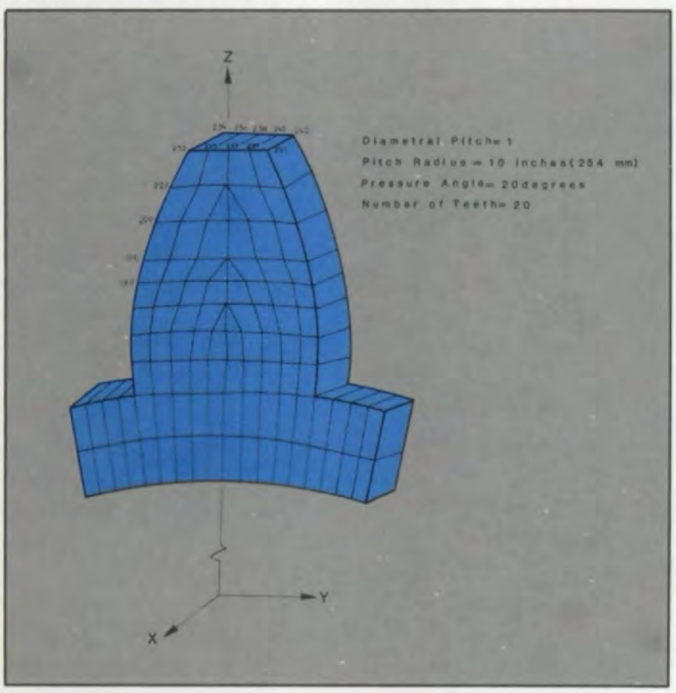

Fig. 10 – Finite Element Model of an Involute Tooth Form.

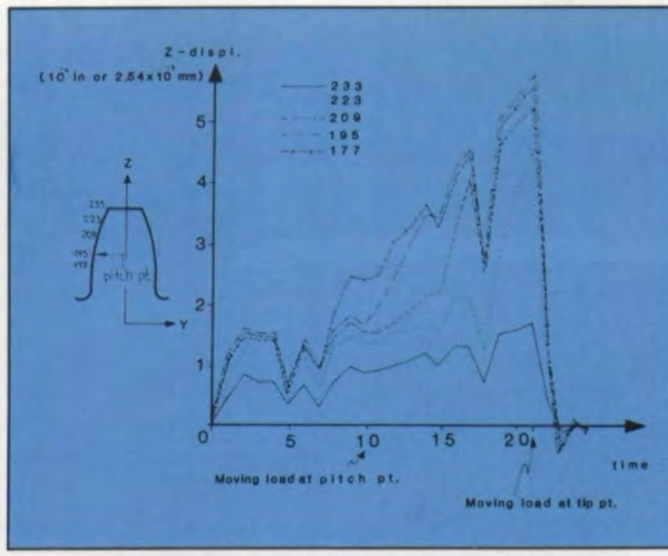

Fig. 11 – Radial Displacement of Involute Tooth.

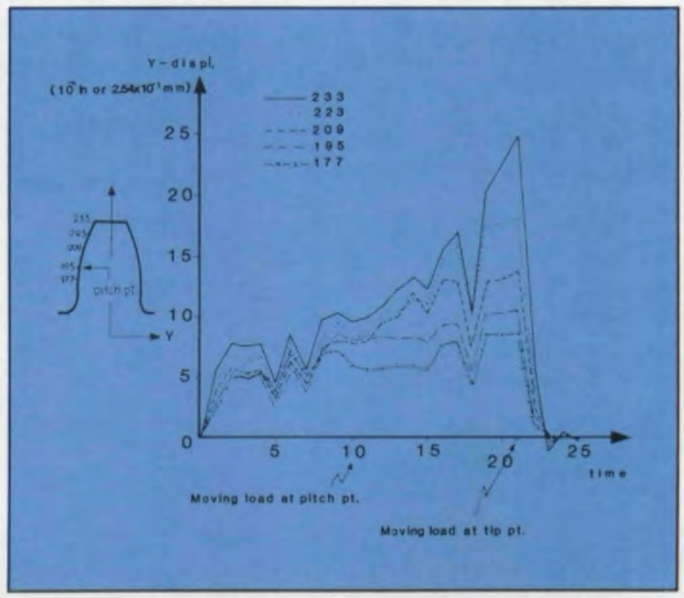

Fig. 12 – Transverse Displacement of Involute Tooth.

15. WANG, K. L., and CHENG, H. S., "A Numerical Solution to the Dynamic Load, Film Thickness, and Surface Temperatures in Spur Gears, Part I, Analysis, *Journal of Mechanical Design,* Vol. 103, 1981, pp. 177-187.

16. ODA, SATOSKI, NAGAMURA, K., and AOKI, K., "Stress Analysis of Thin Rim Spur Gears by the Finite Element Method," *Bulletin of the JSME,* Vol. 24, 1981, pp. 1273-1280.

17. ARAI, N., HARADA, S., and AIDA, T., "Research on Bending Strength Properties of Spur Gears with a Thin Rim," *Bulletin of the JSME,* Vol. 24, 1981, pp. 1642-1650.

18. KIYONO, S., FUJII, Y., and SUZUKI, Y., "Analysis of Vibration of Bevel Gears," *Bulletin of the JSME,* Vol. 24, 1981, pp. 441-446.

19. TOBE, T., "Dynamic Loads on Spur Gear Teeth," *Bulletin of the JSME,* Vol. 4, 1961, pp. 417-422.

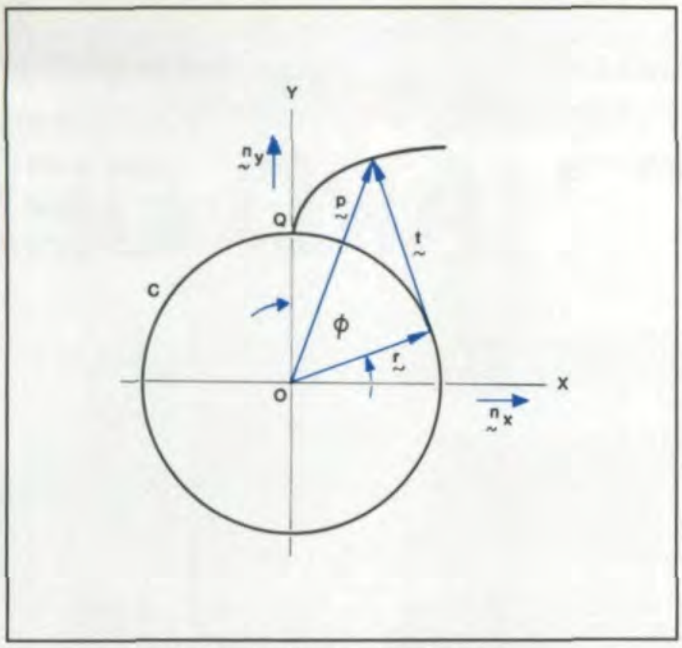

Fig. 13 – Involute I and Base Circle C.

20. ATTIA, A. Y., "Deflections of Spur Gear Teeth Cut in Thin Rims," *Journal of Engineering for Industry*, Vol. 86, 1964, pp. 333-342.

21. AZAR, R. C., and CROSSLEY, F. R. E., "Digital Simulation of Impact Phenomena in Spur Gear Systems," *Journal of Engineering for Industry*, Vol. 99, 1977, pp. 792-798.

22. RADZIMOUSKY, E. I., MIRAREFI, A., and BROWN, W. E., "Instantaneous Efficiency and Coefficient of Friction of an Involute Gear Drive," *Journal of Engineering for Industry*, Vol 95, 1973, pp. 1131-1138.

23. RADZIMOUSKY, E. I., MIRAREFI, A., "Dynamic Behavior of Gear Systems and Variation of Coefficient of Friction and Efficiency During the Engagement Cycle," *Journal of Engineering for Industry*, Vol. 97, 1975, pp. 1274-1281.

24. UDOGUCHI, T., OKAMURA, H., KANO, T., and NOZUE, Y., "An Error Analysis of Various Finite Element Patterns," *Bulletin of the JSME*, Vol. 16, 1973, pp. 1803-1813.

25. KIYONO, S., AIDA, T., and FUJII, Y., "Vibration of Helical Gears, Part I, Theoretical Analysis," *Bulletin of the JSME, Vol. 21, 1978, pp. 915-922.*

26. *BUCKINGHAM, E., Analytical Mechanics of Gears*, Dover, New York, 1963.

Acknowledgement: *The work reported herein was partially funded under NASA Lewis Research Center Grant No. 3188 with the University of Cincinnati.*

This paper was originally presented at the American Society of Mechanical Engineers Technical Meeting 1984 – DET-226

E-1 ON READER REPLY CARD

AUTHORS:

MR. HSIANG LIN *is a Research Assistant, Department of Mechanical and Industrial Engineering, at the University of Cincinnati. He received his B.S. in Mechanical Engineering in 1974 from National Chung-Hsing University, Taiwan, R.O.C., and his M.S. in Mechanical Engineering in 1980 from the University of Cincinnati. After undergraduate study, Mr. Lin served as a Mechanical Engineering Officer at the Chinese Naval Ordinance Center in Kaohsiung, Taiwan for two years. From 1976 to 1977, was with the SHARP Corporation, Taiwan branch. From 1977 to 1978, joined the faculty of National Chung Hsing University as a Teaching Assistant in Mechanical Engineering. Current research interests are computer-aided design, vibrations dynamics, and finite element methods.*

DR. RONALD L. HUSTON *is Professor of Mechanics, Dept. of Mechanical and Industrial Engineering, and Director, Institute for Applied Interdisplinary Research, University of Cincinnati. He joined the faculty at the University of Cincinnati in 1962. Additionally, he has served as Visiting Professor of Mechanics at Stanford University, Division Director, Division of Civil and Mechanical Engineering at the National Science Foundation in Washington, D.C., and as Acting Senior Vice President and Provost, University of Cincinnati. Dr. Huston has edited three books, and he is the author of a textbook on Finite Element Methods, and over 100 technical papers. A Licensed Professional Engineer in Ohio, he holds a B.S., M.S. and Ph.D. in Engineering Mechanics from the University of Pennsylvania.*

DR. JOHN J. COY *is employed by the U.S. Army Aviation Systems Command's Propulsion Laboratory at the NASA Lewis Research Center, Cleveland, Ohio. He has been doing research at NASA on helicopter drive trains since 1974 and is currently Acting Head, Rotorcraft Section in the Aeronautics Directorate. He earned BS, MS, and PhD degrees in Mechanical Engineering at the University of Cincinnati. A licensed professional engineer in Ohio, he is a member of the ASME, Chairman of the ASME Power Transmission and Gearing Committee, and a member of the NATO/AGARD Propulstion Energetics Panel. Author or co-author of over 50 technical papers, he has been on the faculty of Rose Hulman Institute of Technology and the University of Cincinnati, and has been a consultant for industry and goverment agencies.*

CIRCLE A-7 ON READER REPLY CARD

The State of the Art...

HURTH CNC HARD GEA

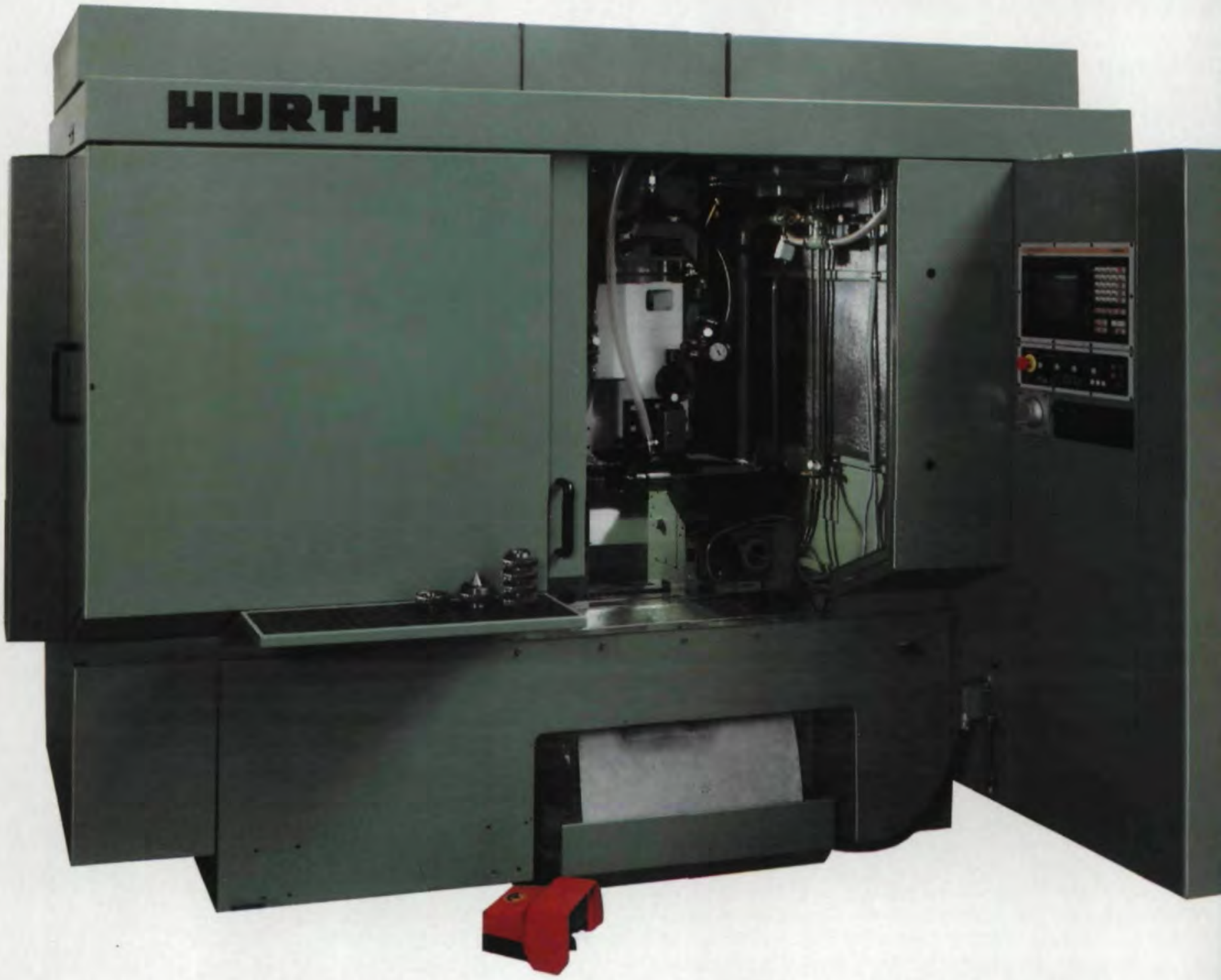

The HURTH hard finishing process is an entirely new approach to gear manufacture and finishing because it enables the manufacturer to alter the geometry of the teeth while smoothing the tooth flank surfaces of external and internal hardened gears. This process can correct errors in profile, spacing and lead, as well as such parameters as radial runout, pitch and cumulative pitch. The end product is a more accurate, smoother, quieter-running gear.

To accomplish this, the tool flank and the work gear flank being machined are positively guided in such a way that the workpiece and tool are rigidly linked during machining with the tool performing a plunge-feed motion for stock removal. All right-hand flanks are finished first. The machine then reverses and finishes left-hand flanks. This single-flank contact means no broken-out tool teeth due to workpiece defects and permits correction or "redesign" of the workpiece gear during finishing.

The tool, either Borazon® or ceramic, is conditioned and profiled for the work gear geometry and desired stock removal by using a coated dressing master. Dressing takes no longer than the time required to finish one workpiece and each dressing removes a minimal amount of material from the tool surfaces.

R FINISHING MACHINES

The hard finishing process gives the widest range of applications of all post-hardening gear finishing methods. Adjacent shoulders or collars rarely pose serious problems.

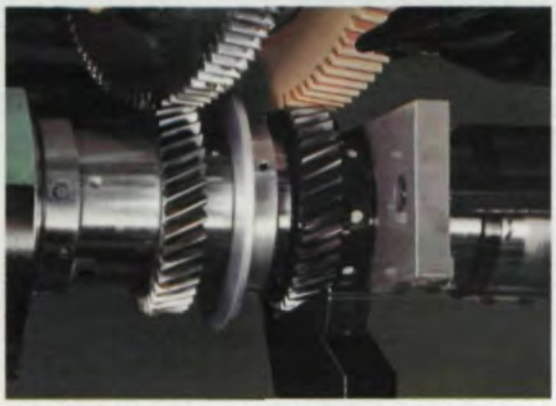

This illustration shows the tool finishing the work-piece gear and the external master gears engaged to control the operation.

Other advantages of the process:

- AGMA Class 14 achievable.
- Definitely no grinding burns.
- Tool marks run diagonally to gear diameter.
- Permits machining of gear teeth adjacent to shoulders.
- Equipment is ideal for automated work handling.

Please write or phone for details on this revolutionary new process.

STARCUT SUPPLIED PRODUCTS FOR PRODUCTIVITY

Star Machine Tools

Standard and CNC Hob Sharpeners
Shaper Cutter Sharpeners
Standard Gun Drilling Machines
CNC Drill and Reamer Sharpeners
Keyseaters

Star Cutting Tools

Hobs
Form-Relieved Cutters
Gun Drills
Gun Reamers
Keyseat Cutters

Gold Star Coatings

Hurth Machine Tools

Standard & Automatic Keyway and Slot Milling Machines
Automatic Spline Shaft Milling Machines
CNC Precision Boring and Milling Machines
CNC Gear Hobbing Machines
CNC Gear Shaving Machings
Shaving Cutter Grinding Machines
Gear Testing Machines
CNC Gear Tooth Chamfering Machines
Gear Deburring Machines
CNC Hard Gear Finishing Machines

Stieber Precision Clamping Tools

Planring Flexible Machining Systems

Since 1927

Star

STARCUT SALES, INC.
23461 Industrial Park Drive
Farmington Hills, MI 48024
313/474-8200 Telex 230-411

The Design and Manufacture of Plastic Gears

Part II

Machining, Installation and Gear Sound Measurement

by
John H. Chen and Frank M. Juarbe
The Polymer Corporation
Reading, Pennsylvania 19603

ABSTRACT

Advancements in machining and assembly techniques of thermoplastic gearing along with new design data has lead to increased useage of polymeric materials. Information on state of the art methods in fabrication of plastic gearing is presented and the importance of a proper backlash allowance at installation is discussed. Under controlled conditions, cast nylon gears show 8-14 dBA, lower noise level than three other gear materials tested.

Introduction

In Part I, which was presented in the May/June issue of *Gear Technology*, the latest design parameters for endurance strength as a function of diametral pitch, pressure angle, pitch line velocity, lubrication and life cycles were reported.

Machined gears of cast or extruded thermoplastics (such as nylons, acetals, and UHMWPE) ranging in size from 50 mm to over 2 meters (2"-84") in diameter are increasingly used for power transmission applications. The plastic gear blanks are machined to required dimensions and then cut by hobbing, shaping, form milling or other methods.

AUTHORS:

DR. JOHN H. CHEN *is Project Leader for The Polymer Corp. where he has been employed since 1968. During this time he has been involved in various aspects of product development and application testing of thermoplastics. Dr. Chen received his BSME from Taiwan College of Engineering and his Dr. -Ing. degree from the Technical University of Aachen, West Germany. He is the author of over 30 technical papers in the field of plastic engineering, and holds patents in manufacturing methods of nylon parts. Additionally he is a member of the American Society of Mechanical Engineers, American Society of Testing Materials, Society of Plastics Engineers, and chairman of Plastics Gearing Committee of ASME Design Division.*

MR. FRANK M. JUARBE *has been with Polymer Corp. for the past ten years as Product Manager where he has been involved in the development of Cut Tooth Plastic Gearing and Sprockets. Prior to his work at Polymer, he has over twenty years experience in related engineering fields. Mr. Juarbe is a member of the American Gear Manufacturers Association and the American Society of Mechanical Engineers.*

Some information pertaining to machining plastic gearing is available.[1-4] Most metal working equipment can be adapted or modified to fabricate plastic gearing.

Over the years, empirical data in improved techniques for machining plastics has developed. The improvements in manufacturing and installation, along with new design data resulted in increased utilization of polymeric materials and in prevention of premature failures.

Tools and techniques for machining plastics are illustrated. Emphasis is placed on variations between machining plastic and metal gears. The importance of proper installation and backlash allowance are discussed.

Low acoustic impedance[5] and sound dampening characteristics make thermoplastic gearing a choice in combating industrial noise pollution. Sound measurements were conducted on cast nylon 6, bronze, phenolic and cast iron gears, and the results reported.

Plastic Gear Construction and Fabrication

Extruded or cast gear blanks are produced sufficiently oversize to allow for machining to the finished dimensions of the gear.

Gears up to 20 cm (8") outside diameter are often constructed entirely of extruded thermoplastic or cast nylon; however, consideration must be given to the gear configuration and type of service. For plastic gear rings exceeding 20 cm in diameter, or for gears in relatively severe service, it is suggested that a metal hub be utilized. The inside diameter of the gear ring blank must be machined accurately to match the frame diameter, allowing an interference fit when assembled. In addition, the plastic gear ring must be securely bolted to the frame to prevent movement.

General Machining

Normally, standard metal working equipment can be effectively used for machined thermoplastic gears. Therefore, machining techniques for engineering plastic gears are similar to those employed for metals; however, there are several important differences due to certain characteristics of polymeric materials. For optimum results, certain characteristics unique to thermoplastic must be recognized and allowances for these made. One of these characteristics is the generation of frictional heat. Generated heat must be kept to a minimum or removed by coolants. Tools must be kept sharp and provided with generous clearances. In general, very high speeds with relatively low feeds produce the best results. Also, polymers exhibit a relatively low modulus of elasticity and are rather flexible when compared to metals. Provision must be made to prevent flexing of stock away from the cutting tools, and clamping or gripping pressures must be held to a minimum. Clamping pressures and fixtures must not overstress the material, yet must be adequate to prevent chatter. Between rough and finish machining, a 24 to 48 hour normalizing at room temperature is a popular procedure. Large plastic parts such as gear rings and/or gear segments must be securely fastened to a metal hub or frame prior to final machining.

Tolerances of plastic gears must be liberal in comparision to metals. As an example, a 25.4 mm (1") diameter bore might be specified for a tolerance of ±0.05 mm (±0.002"). Variations in plastic materials must be considered when developing specifications for gears.

Drilling and Reaming

Drilling holes in plastic can cause difficulties not normally encountered with metals. The melting point of engineering thermoplastics in the range of 175° to 265°C (347/510°F) is considerably lower than metals, so the use of dull drills or drilling "dry" must be avoided. The use of adequate coolant with frequent withdrawal of the drill to prevent chip build-up will prevent this potential problem. Fig. 1 and Table 1 show typical drill design and speed in RPM for drilling plastics. Normal feed rates are 0.1-0.4 mm (0.004" to 0.015") per revolution. Large diameter holes are usually machined in two or more stages.

The relative softness of plastic materials require the use of oversize reamers to allow for close-in of the hole. Speed and feed rates should approximate those used for drilling, with a minimum removal of 0.12 to 0.25 mm (0.005"-0.010"). The use of coolant will also aid in improving surface finish.

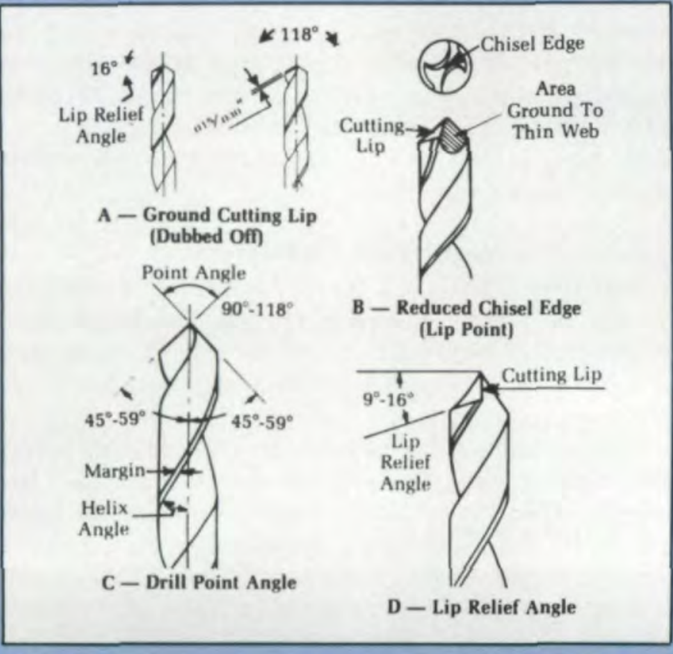

Fig. 1 – Drill Design

Table 1: Drill Speed Size Chart

Drill Sizes (USAS B94.11 1967)	RPM
No. 60 thru 33	5,000
32 thru 17	3,000
16 thru 1	2,500
1.6 mm (1/16")	5,000
3.2 mm (1/8")	3,000
4.8 mm (3/16")	2,500
6.4 mm (1/4")	1,700
8.0 mm (5/16")	1,700
9.5 mm (3/8")	1,300
11.1 mm (7/16")	1,000
12.7 mm (1/2")	1,000
A thru D	2,500
E thru M	1,700
N thru Z	1,300

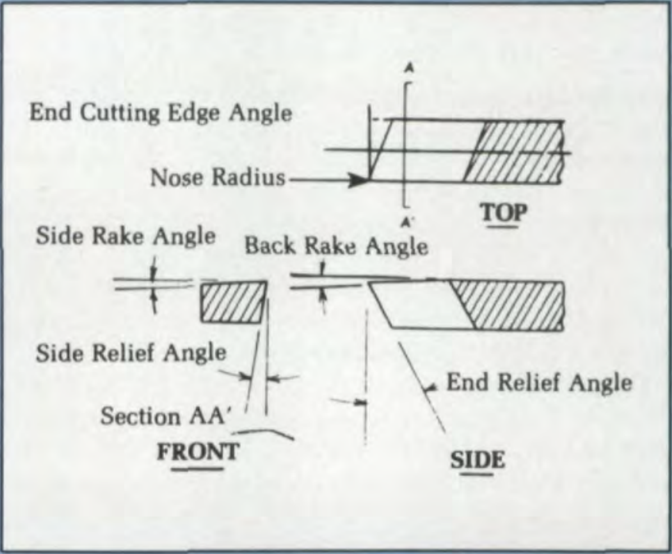

Fig. 2 – Cutting Tool Design

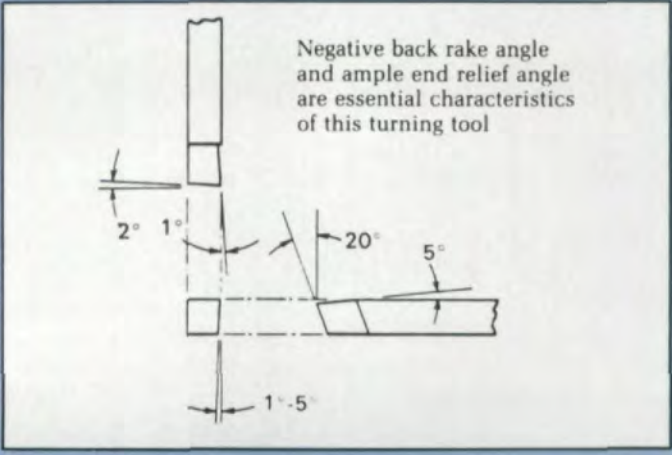

Fig. 3 – Cutting Tool Design

Turning and Boring

Plastic blanks are usually machined at cutting speeds of 600 to 900 surface ft. per minute. Roughing cuts up to 10 mm (3/8") at 0.4 mm feed (0.15" per revolution, and finishing cuts 1.5-3.0 mm (1/16" to 1/8") at 0.08-0.18 mm (0.003" to 0.007") per revolution are suggested as starting rates. Proper clamping pressure, fixturing, cutting tools and coolant combine to result in trouble-free machining.

Fig. 2 and 3 show typical carbide cutting tool design. Fig. 4 shows typical high speed steel cut-off tool design.

Gear Cutting

Hobbing, shaping and form milling are methods commonly used for cutting plastic gear teeth. Tooling and fixtures should be similar to those used for metal gears. Standard high speed steel cutters can be used satisfactorily to cut gear teeth in plastics. Carbide hobs, however, will exhibit longer cutting life and are preferred for long production runs and for gears with many teeth. Selection of appropriate speeds and feeds for milling or hobbing plastics will depend largely on judgement gained from experience. Suggested feeds and speeds are offered in Table 2 only as a guide to what may be considered ordinary practice. Table 3 is a checklist describing various machining difficulties and causes.

Gear finishing operations such as shaving, grinding, honing or lapping are normally not utilized for plastic gears. The tooth surface finish from gear hobbing and/or shaping is adequate for most applications precluding the need for subsequent finishing.

Installation and Backlash Allowance

Properly designed, manufactured and installed plastic gearing work well in practice and will show minimal wear.

One of the most frequent design errors made in converting from a metal gear to a plastic gear is not allowing sufficient backlash. Insufficient backlash in plastic gearing can cause heat buildup and tooth deflection which lead to interference and premature failures including wear, pitting, tooth profile deformation and melting[5].

Backlash of metal gearing was established using generally recognized tolerances for gear tooth and center distances, and lubricating film thickness. For plastic gearing, in addition, thermal expansion in tooth thickness, elastic deflection and creep deformation of the teeth at operating temperatures are significant enough to be taken into consideration.

Table 2: Gear Cutting Speeds and Feeds		
Cutting Method	Surface Cutting Speed	Feed Rate
Hobbing	3.05-4.57 m/s (600-900 ft./min.)	1.5-3.0 mm/rev. (0.060"-0.120"/rev.)
Shaping	0.9-1.0 m/s (175-200 ft./min.)	.13-.25 mm/stroke (0.005"-0.010"/stroke)
Milling	3.05-4.57 m/s (600-900 ft./min.)	75-200 mm/min. (3"-8"/min.)

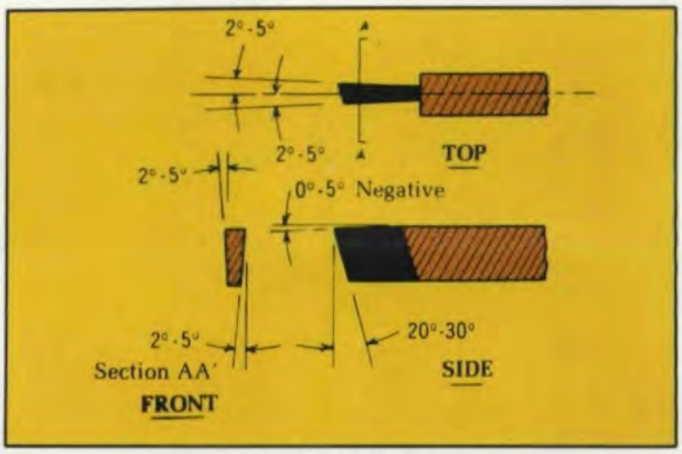

Fig. 4 – Cut-Off Tool Design

The following formula can be utilized to calculate the necessary operating backlash for thermoplastic gearing in open air systems.

Backlash Allowance
$$= 0.100''/P \qquad \text{Eq. (1)}$$
where P = diametral pitch

In an enclosed system, thermal expansion of pitch radius due to temperature increase in the gear box is to be added to the backlash allowance, then:

Backlash Allowance
$$= 0.100''/P + 1.82\, D_p \bullet \Delta T \times 10^{-5} \qquad \textit{Eq. (2)}$$
where D_p = pitch diameter

The backlash allowance is provided in order of preference, by center distance adjustment, or by tooth thinning of the mating metal gears, or by tooth thinning of the plastic gears, or by any combination of the three.

When installing thermoplastic gears, care must be taken to insure that the gear mesh has been checked for the appropriate backlash prior to operating the gear system. It is suggested that the plastic gear and the mating gear be checked at 90° intervals through one complete rotation to insure both gears are running true and are not mounted on bent shafts or defective bearings.

Gear Sound Measurement

Gear noise is a problem in many industries, but complex factors are involved in noise generation. The design of the entire system, for example, must be thoroughly investigated to isolate noise sources which can then be addressed with suppression techniques.

Thermoplastic gearing involves three acoustic implications. First, a plastic/metal gear mesh will generate much lower impact noise than a metal/metal gear mesh, due to sound dampening characteristics of polymeric materials. Secondly, the mesh impact is further reduced by multiple pairs of teeth sharing the load. Third, since the material has a lower acoustic impedance, sound transmission is poor and any noise waves generated are well attenuated.

Sound levels of cast nylon 6 (filled with MoS_2), grey cast iron (AGMA 30), bronze (SAE CA932A) and phenolic laminate (ANSI/ASTM D709, II Grade C) for 10P gears meshing with a steel driving pinion was measured in dBA at a pitch line velocity of 10.2 m/s (2,000 fpm) and at different torque levels. With the outer cover of the test machine removed, a monitoring microphone was set 30.5 cm (12") from the mesh point of the gears. The center distance of the mating gears was maintained at 88.93 mm (3.501") for all tests.

A sound level meter equipped with piezo-electric microphone, which gives it a frequency range from 20 Hz to 10 kHz was used. The sound meter has built-in A, B, and C weighing networks and conforms to type II of ANSI (American National Standard Institute) S 1.4 – 1971 and IEC (International Electrotechnical Commission) R 123-1961 specifications. The noise amplitude was measured as sound pressure in dB (decible) at the A scale, which is close to the human ear perception. A description of the four-square test machine was given in Part I of this paper.

Sound level in dBA at different torque measurements are illustrated in Fig. 5. When 100 inch-lbs. torque was applied,

(continued on page 48)

Table 3: Machining Difficulties and Causes

CHECK LIST

DRILLING

Difficulty	Common Causes
Tapered hole	1. Incorrectly sharpened drill 2. Insufficient clearance 3. Feed too heavy
Burnt or melted surface	1. Wrong type drill 2. Incorrectly sharpened drill 3. Feed too light 4. Drill dull 5. Web too thick
Chipping of surfaces	1. Feed too heavy 2. Clearance too great 3. Too much rake (thin web as described)
Chatter	1. Too much clearance 2. Feed too light 3. Drill overhang too great 4. Too much rake (thin web as described)
Feed marks or spiral lines on inside diameter	1. Feed too heavy 2. Drill not centered 3. Drill ground off-center
Oversize holes	1. Drill ground off-center 2. Web too thick 3. Insufficient clearance 4. Feed rate too heavy 5. Point angle too great
Undersize holes	1. Drill dull 2. Too much clearance 3. Point angle too small
Holes not concentric	1. Feed too heavy 2. Spindle speed too slow 3. Drill enters next piece too far 4. Cut-off tool leaves nib, which deflects drill 5. Web too thick 6. Drill speed too heavy at the start 7. Drill not mounted on center 8. Drill not sharpened correctly
Burr at cut-off	1. Cut-off tool dull 2. Drill does not pass completely through piece
Rapid dulling of drill	1. Feed too light 2. Spindle speed too fast 3. Insufficient lubrication from coolant

CUTTING OFF

Difficulty	Common Causes
Melted surface	1. Tool dull 2. Insufficient side clearance 3. Insufficient coolant supply
Rough finish	1. Feed too heavy 2. Tool improperly sharpened 3. Cutting edge not honed
Spiral marks	1. Tool rubs during its retreat (use same fall on cam as rise) 2. Burr on point of tool
Concave or convex surfaces	1. Point angle too great 2. Tool not perpendicular to spindle 3. Tool deflecting (use negative rake) 4. Feed too heavy 5. Tool mounted above or below center
Nibs or burrs at cut-off point	1. Point angle not great enough 2. Tool dull or not honed 3. Feed too heavy
Burrs on outside diameter	1. No chamfer before cut-off 2. Tool dull

TURNING & BORING

Difficulty	Common Causes
Melted surface	1. Tool dull or heel rubbing 2. Insufficient side clearance 3. Feed rate too slow 4. Spindle speed too fast
Rough finish	1. Feed too heavy 2. Incorrect clearance angles 3. Sharp point on tool (slight nose radius required) 4. Tool not mounted on center
Burns at edge of cut	1. No chamfer provided at sharp corners 2. Tool dull 3. Insufficient side clearance 4. Lead angle not provided on tool (tool should ease out of cut gradually, not suddenly)
Cracking or chipping of corners	1. Too much positive rake on tool (use negative rake) 2. Tool not eased into cut (tool suddenly hits work) 3. Dull tool 4. Tool mounted below center 5. Sharp point on tool (slight nose radius required)
Chatter	1. Tool much nose radius on tool 2. Tool not mounted solidly enough 3. Material not supported properly 4. Width of cut too wide (use two cuts)

Longitudinal Load Distribution Factor of Helical Gears

T. Tobe, Professor
K. Inoue, Associate Professor
Faculty of Engineering, Tohoku University,
Sendai, Japan

This paper deals with the longitudinal load distribution and the bending moment distribution of a pair of helical gears with a known total alignment error. The load distribution along the contact lines is calculated by the finite element method based on the plate theory including transverse shear deformation. Empirical formulas for both longitudinal load distribution factor and bending moment distribution factor are proposed for practical use. The load distribution factor in AGMA 218.01 is examined, and it is concluded that the load distribution factor is close to the calculated results if the value of unity is taken as the transverse load distribution factor.

Introduction

The contact lines of a pair of helical gears move diagonally on the engaged tooth faces and their lengths consequently vary with the rotation of the gears. The load distribution along the contact lines is one of the most important factors for gear design, and some investigators have analyzed this problem.

Hayashi[1] and Niemann and Schmidt[2] solved numerically integral equations to obtain the load distribution. Niemann and Richter[3] proposed an experimental formula of the load distribution which was obtained by the photoelastic method. Conry and Seireg[4] developed a mathematical programming technique to estimate the load distribution and to obtain optimum profile modification. Kubo and Umezawa[5] obtained tooth bearings by means of the finite difference method. The authors developed a finite element technique based on the plate theory including the transverse shear deformation to calculate the deflection of gear teeth,[6] then estimated the longitudinal load distribution factor $K_{H\beta}$ and determined the optimum amount of arc shaped crowning for both spur gears[7] and helical gears

In a previous article[8], the longitudinal load distribution factor was defined as the ratio of the maximum load intensity to the average load on the contact lines at the worst position. Although the definition is logical, it is difficult to foresee the worst position. The average load is, therefore, generally unknown and the load distribution factor in the previous article is inconvenient for the practical use in gear design. In this article, this weak point is improved by introducing the average load on the contact lines of the minimum length. Formulas for both load distribution factor and bending moment distribution factor are proposed. A comment is also given on the transverse load distribution factor in AGMA 218.01[9].

Assumptions for the Calculation of the Load Distributions

The load distributions discussed in this article are for the involute helical gears which are generated by the basic rack (pressure angle = 20 deg, whole depth = $2.25m_n$ and the radius of tip corner = $0.375m_n$) recommended in ISO 53-1974 as well as JIS B 1701-1973.

Although the tooth of helical gears is essentially twisted, the effect of twist on the flexibility of tooth and the bending moment is assumed to be negligible. The thrust component of transmitted load is also assumed to be neglected. According to the assumptions, the cantilever plate with the flexural rigidity of the tooth is adopted as an adequate model. The plate is approximately represented by assembling 12 (in the direction of tooth height) x 21 max (in the direction of face

AUTHORS:

DR. TOSHIMI TOBE *is Professor Emeritus of Tohoku University. He graduated from Tohoku Imperial University in 1944, and in 1957 he received the degree of Dr. Eng. Subsequently he studied the strength of gears under Professor G. Niemann at the Technical University at Munich. From 1964-1985 he was a Professor at Tohoku University. He is a member of JSME, JSLE, and JSPE.*

DR. KATSUMI INOUE *is an Associate Professor of Tohoku University in the Department of Precision Engineering. He earned his undergraduate and graduate degrees from Tohoku University, and in 1977 he received the degree of Dr. Eng. Dr. Inoue is a member of JSME.*

width) rectangular elements whose thicknesses vary linearly in the direction of tooth height. The deflection of the plate was calculated by FEM including both the transverse shear deformation and the deformation at the elastic built-in edge of the plate[6]. Since the helical gear tooth does not have full thickness near the end of tooth trace, the thickness at the centroid of element is adopted to estimate the flexibility at the part of tooth. The characteristic of a helical gear tooth is mainly involved in the inclination of the contact lines. In the middle plane of a tooth, the angle β_{tm} between the contact line and the tooth trace is presented by the following expression,

$$\tan \beta_{tm} = \sin \beta_b \tan \alpha_t \cos \alpha_n \qquad (1)$$

where α_t is the transverse pressure angle. The fundamental equations[7, 8] are summarized in Appendix 2.

Variations of the Load Intensity and the Bending Moment With the Rotation of Gears

An example of the contact lines in the plane of action is illustrated in Fig. 1. The transverse base pitch p_{bt} is divided into six equal parts. The lines with the same number are a set of contact line and the mesh advances in numerical order. The position of each line is indicated by the distance ζ along the side of the plane of action.

The load distributions of the pair of gears: $m_n = 5$, $z_1 = z_2 = 20$, $\beta = 20$ deg, $b_1 = b_2 = 68.89$ ($\epsilon_\beta = 1.5$), were calculated at every position of mesh shown in Fig. 1. The variations of the maximum load $p_{\max}$ and the maximum bending moment $m_{\max}$ of a tooth are shown in Fig. 2. The transmitted load is $P_{nt}/b = 600$ N/mm. The direction of total alignment error F_β and the rotation of gear 1 are illustrated in the figure. The abscissa indicates the position of the contact line, that is, $\zeta/(\epsilon_\alpha + \epsilon_\beta)\, p_{bt} = 0$ and 1 mean the initiation and the end of meshing, respectively. Since a set of contact lines whose interval is p_{bt} are in mesh simultaneously, the maximum load on the contact lines and the maximum bending moment of gear 1 vary as shown in Fig. 3. The total length of contact lines L, the mean load p_m and the load sharing factor ψ are also shown in the figure. In the case of $F_\beta = 0$, $p_{\max}$ and $M_{\max}$ reach maximum at the position where L is minimum. When the gears have total alignment error, the worst meshing positions for the load distribution are fairly close to the position of $L = L_{\min}$. The

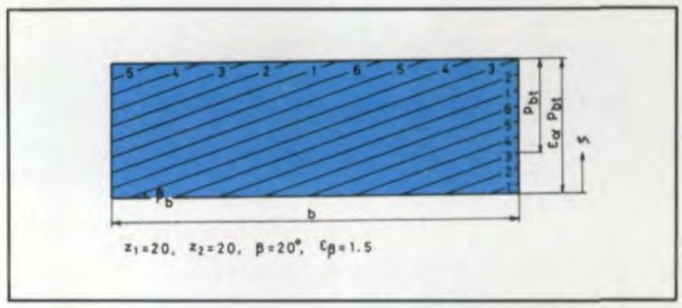

Fig. 1 – Contact lines on the plane of action ($m_n = 5$, $b = 68.89$, $p_{bt} = 15.59$, $\epsilon_\alpha = 1.44$)

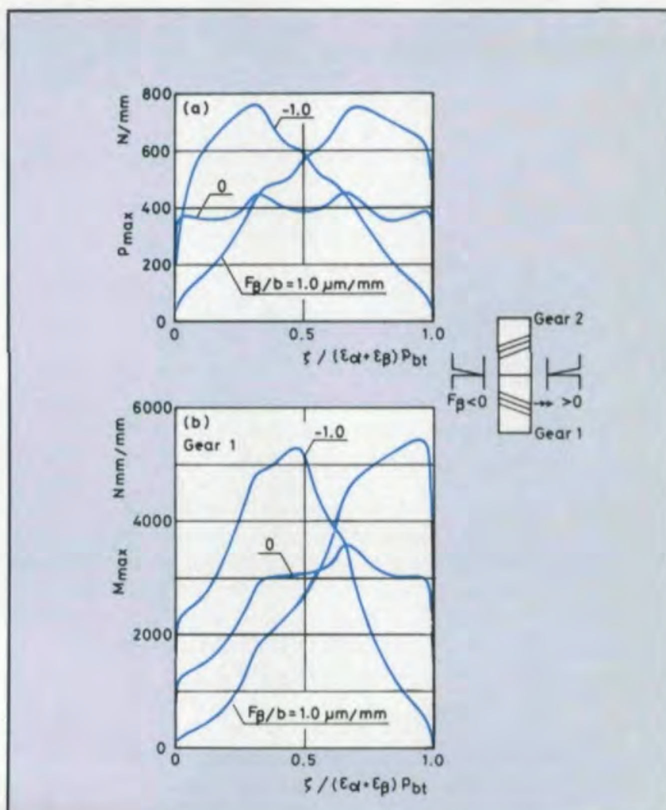

Fig. 2 – Variations of the maximum load on a tooth (a) and the maximum bending moment (b) $(m_n) = 5$, $z_1 = z_2 = 20$, $\beta = 20$ deg, $\epsilon_\beta = 1.5$, $P_{nt}/bm_n = \mathrm{N/mm^2}$)

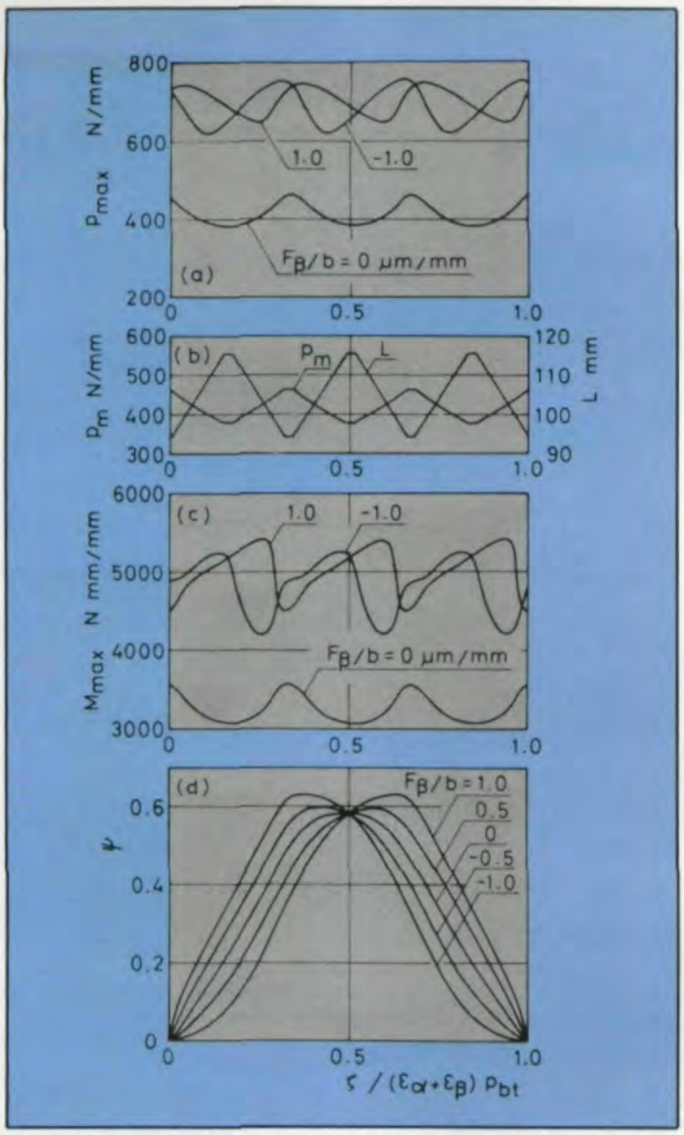

Fig. 3 – Variations of the maximum load intensity p_{max} (*a*), mean load p_m and the total length of contact lines L (*b*), the maximum bending moment M_{max} (*c*) and the load sharing factor ψ (*d*) of the pair of gears shown in Fig. 2.

worst positions for the bending moment, on the contrary, are shifted and they do not coincide with the worst positions for the load distribution. The worst positions ζ^* of both load distribution and bending moment are shown in Fig. 4. In the case of $F_\beta/b = 1.0$ μm/mm, ζ^* increases linearly with the increase of the face width. On the contrary, ζ^* in case of $F_\beta/b = -1.0$ μm/mm is approximately constant. The increase, like a step shown in the figure, means the boundary where the worst position shifts from the region of the single-tooth meshing to double-teeth meshing.

Longitudinal Load Distribution Factor

In the previous paper,[8] the longitudinal load distribution factor was defined as the ratio of the maximum load intensity to the average load which was uniformly distributed on the contact lines at the worst position. Although the definition is logical, the worst position may not be foreseen and the average load is generally unknown.

In order to improve this weak point, the following definition of the longitudinal load distribution factor is adopted in this paper:

$$K_{H\beta} = p_{max}/p_{ref} \tag{2}$$

where p_{max} is the maximum load intensity and p_{ref} is the reference load intensity which is represented as follows:

$$p_{ref} = p_n/L_{min} = (P_{nt}/\cos\beta_b)/L_{min} \tag{3}$$

The load distribution factor $K_{H\beta}$ of the pair of gears $z_1 = z_2 = 20$, $\beta = 20$ deg is shown in Fig. 5. The direction of total alignment error had little effect on $K_{H\beta}$. In most cases of $F_\beta = 0$, $K_{H\beta}$ is not equal to unity. However, $K_{H\beta}$ for $F_\beta = 0$ is assumed to be unity in this paper, since the error is not very significant. From the calculated results in the figure, the following expression can be obtained:

$$K_{H\beta} = 1.00 + \alpha_H\,(|F_\beta|/b)^{1.2} \tag{4}$$

Nomenclature

- A = dimensionless value in relation to the ratio of L_{min} to face width, see equation[5] and Appendix 1
- b = face width, (mm)
- C_m = load distribution factor in AGMA 218.01
- C_{mf} = face load distribution factor in AGMA 218.01
- C_{mt} = transverse load distribution factor in AGMA 218.01
- F_β = total alignment error, (μm)
- $K_{H\beta}$ = longitudinal load distribution factor
- $K_{m\beta}$ = bending moment distribution factor
- L_{min} = minimum total length of lines of contact, (mm)
- m_n = normal module, (mm)
- M = bending moment at the root per unit length (N mm/mm)
- p = load intensity or tooth normal load per unit length of the contact line (N/mm)
- p_{bt} = transverse base pitch (mm)
- p_n = tooth normal load in the normal plane, (N)
- P_{nt} = tooth normal load in the transverse plane, (N)
- z = number of teeth
- α_n = normal pressure angle, (deg)
- β = helix angle, (deg)
- β_b = base helix angle, (deg)
- ϵ_α = transverse contact ratio
- ϵ_β = overlap ratio
- ζ = distance from the initiation of meshing to the position of contact line, (mm)
- ψ = load sharing factor

Subscripts 1 and 2 represent pinion and gear, respectively.

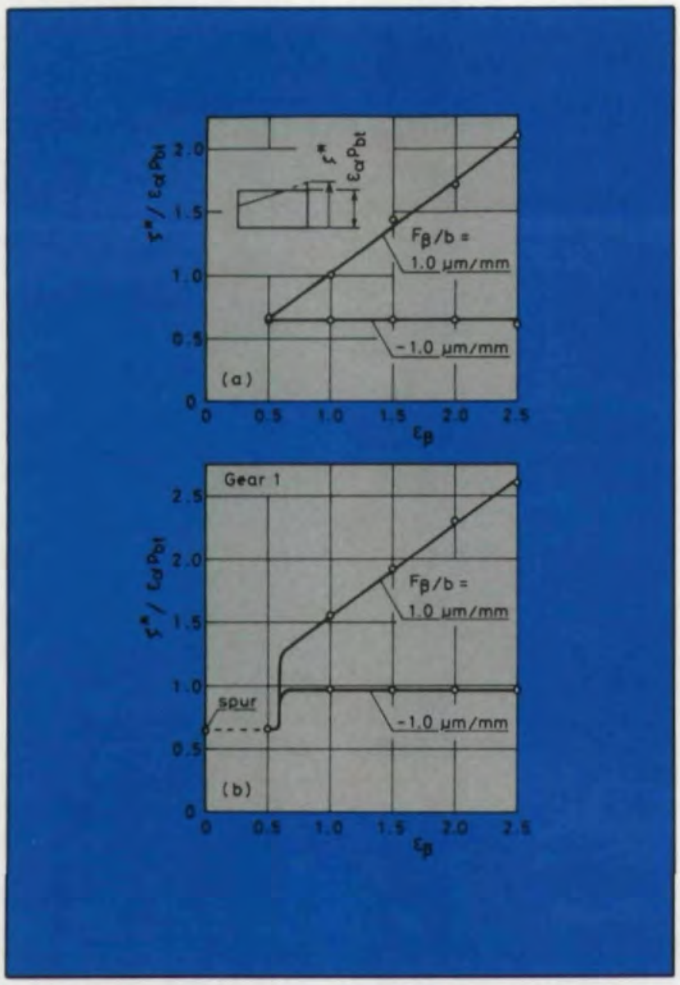

Fig. 4 – Worst position ζ^* of helical gears in relation to load intensity (*a*) and bending moment (*b*)

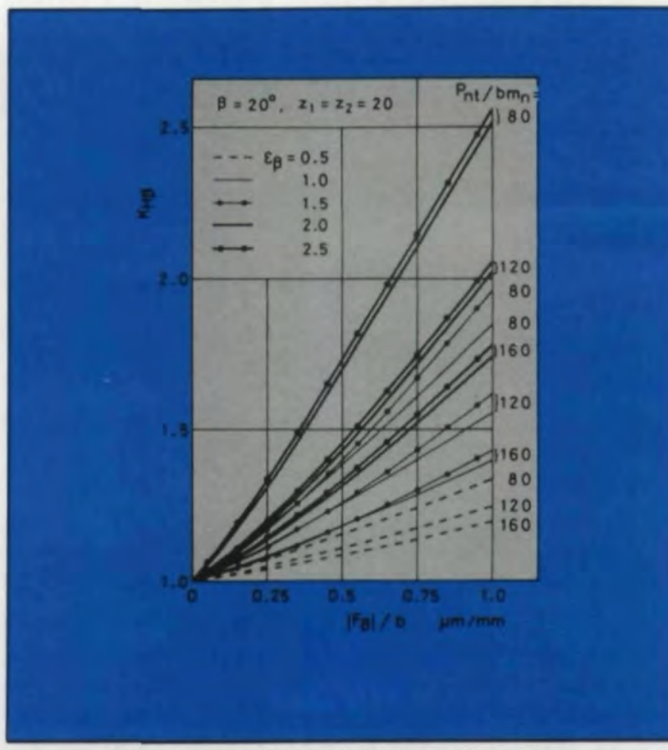

Fig. 5 – Longitudinal load distribution factor $K_{H\beta}$

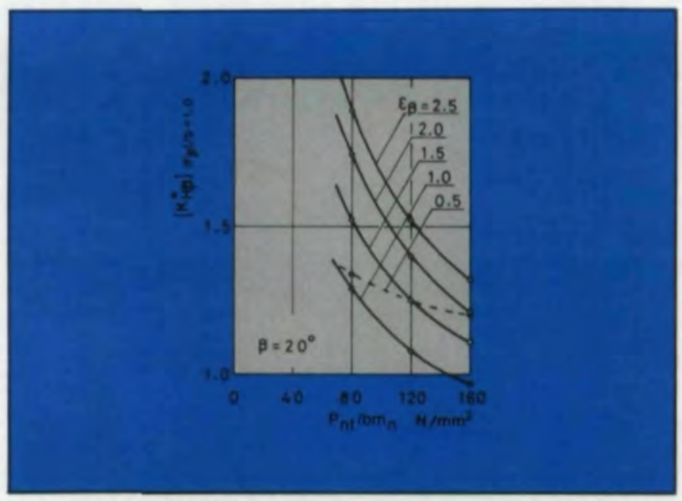

Fig. 6 – Modified load distribution factor $K_{H\beta}{}^*$ of gears $z_1 = z_2 = 20$ with the effective alignment error $|F_\beta|/b = 1.0$ μm/mm

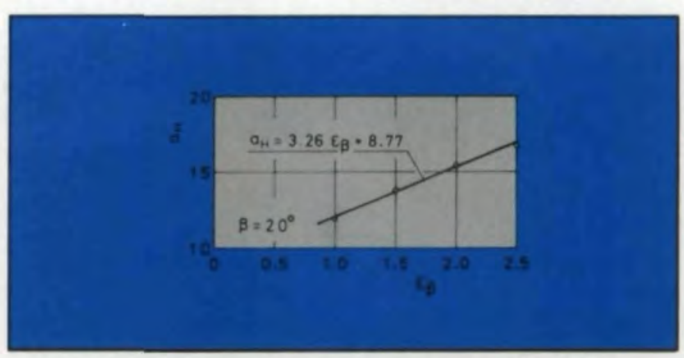

Fig. 7 – Value of a $_H$ ($a_H = [K_{H\beta}{}^*]_{|F_\beta|/b\,=\,1.0} \sqrt{P_{nt}/bm_n}$)

where α_H is estimated from the value of $K_{H\beta}$ for $|F_\beta|/b = 1.0$ μm/mm. Introducing the dimensionless value

$$A = (L_{\min} \cos\beta_b)/b \tag{5}$$

equation (2) is transformed as follows:

$$K_{H\beta}{}^* = K_{H\beta}/A = p_{\max}/(P_{nt}/b) \tag{6}$$

$K_{H\beta}{}^*$ for $|F_\beta|/b = 1.0$ μm/mm is shown in Fig. 6. The relation between $\alpha_H = [K_{H\beta}{}^*]_{|F_\beta|/b\,=\,1.0}\sqrt{P_{nt}/bm_n}$ and ϵ_β is shown in Fig. 7 and the following expression can be derived for $\epsilon_\beta \geqq 1.0$:

$$[K_{H\beta}{}^*]_{|F_\beta|/b\,=\,1.0} = (3.26\epsilon_\beta + 8.77)/\sqrt{P_{nt}/bm_n} \tag{7}$$

From equations (4) to (7), the approximate expression of $K_{H\beta}$ for the pair of gears of $\beta = 20$ deg is obtained. In the same way, similar expressions for gears of $\beta = 10$ deg and 30 deg are obtained. These are arranged and the empirical formula is finally determined as follows:

$$K_{H\beta} = 1.00 + \left(\frac{\phi_H \epsilon_\beta + 8.77}{\sqrt{P_{nt}/bm_n}} A - 1.00\right)(|F_\beta|/b)^{1.2} \tag{8}$$

$$\phi_H = 160\,\beta^{-1.3}$$

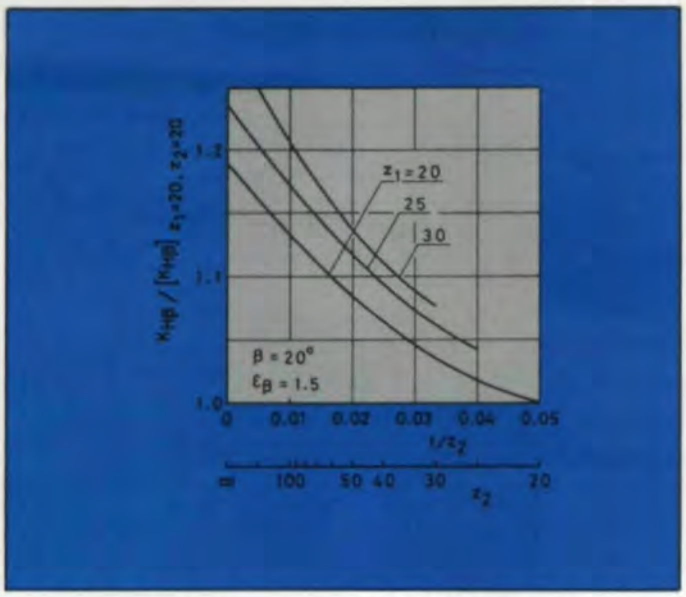

Fig. 8—Effect of gear ratio on the load distribution factor

The formula is valid for gears of $z_1 = z_2 = 20$, 10 deg $\leqq \beta \leqq 30$ deg, $1.0 \leqq \epsilon_\beta \leqq 2.5$; $80 \leqq P_{nt}/bm_n \leqq 160$ N/mm^2 with the restriction that the value in the first parentheses of expression[8] is positive. The maximum error is about 5 percent except for the gears of narrow face width.

An example of the effect of gear ratio on $K_{H\beta}$ is shown in Fig. 8. It is obtained for the gears with the total alignment error of $|F_\beta|/b = 0.5$ and 1.0 μ/mm. The transmitted load is $P_{nt}/bm_n = 80$ to 160 N/mm.^{2} The effect shown in the figure is rather significant. It is the reason that the reference load of gears with larger number of teeth is light since the L_{min} is proportional to the transverse contact ratio ϵ_α. The maximum load intensity p_{max}, however, is not strongly influenced by gear ratios. For example, p_{max} of gears $z_1 = 20$ and $z_2 = 100$ is only about 5 percent greater than that of gears $z_1 = z_2 = 20$.

The effect of shaft stiffness for straddle- and overhung-mounted gears on the load distribution factor has already been reported.[8] The load distribution can be estimated from the resultant error which is the sum of the initial alignment error and the additional alignment error due to shaft deflection. The formula,[8] therefore, is valid for straddle- and overhung-mounted gears by substituting the resultant error into F_β.

The comparison between $K_{H\beta}$ of the present method and the load distribution factor C_m in AGMA 218.01 is shown in Table 1. The value of AGMA 218.01 (the stiffness $G = 1.4 \times 10^4$ MPa is used) are close to the calculated results, especially in the case of $\beta = 20$ deg.

Table 1 Comparison of the load distribution factor

(1) Empirical formula (8) ($z_1 = 20$, $z_2 = 20$)

β	P_{nt}/bm_n \ $\lvert F_\beta \rvert/b$	$\epsilon_\beta = 1.0$: 0.5	1.0	1.5: 0.5	1.0	2.0: 0.5	1.0	2.5: 0.5	1.0
$\beta =$ 10°	80	1.81	2.87	1.95	3.18	2.41	4.24	2.57	4.61
	120	1.58	2.34	1.70	2.60	2.07	3.45	2.20	3.76
	160	1.45	2.03	1.54	2.25	1.87	2.99	1.98	3.26
15°	80	1.54	2.25	1.59	2.35	1.89	3.04	1.96	3.21
	120	1.36	1.84	1.40	1.92	1.64	2.48	1.70	2.62
	160	1.26	1.59	1.29	1.66	1.50	2.15	1.55	2.27
20°	80	1.41	1.93	1.42	1.97	1.63	2.46	1.68	2.55
	120	1.25	1.58	1.27	1.61	1.44	2.01	1.47	2.09
	160	1.16	1.37	1.17	1.40	1.32	1.74	1.35	1.81
25°	80	1.31	1.72	1.32	1.74	1.48	2.10	1.50	2.16
	120	1.18	1.41	1.18	1.42	1.31	1.71	1.33	1.76
	160	1.09	1.22	1.10	1.23	1.21	1.48	1.23	1.53
30°	80	1.24	1.55	1.24	1.56	1.36	1.83	1.38	1.88
	120	1.12	1.27	1.12	1.27	1.21	1.49	1.23	1.53
	160	1.04	1.10	1.04	1.10	1.13	1.29	1.14	1.33

(2) AGMA 218.01 ($G = 1.4 \times 10^4$ MPa)

β	P_{nt}/bm_n \ $\lvert F_\beta \rvert/b$	$\epsilon_\beta = 1.0$: 0.5	1.0	1.5: 0.5	1.0	2.0: 0.5	1.0	2.5: 0.5	1.0
$\beta =$ 10°	80	1.64	2.29	1.97	2.78	2.27	3.21	2.54	3.59
	120	1.43	1.86	1.64	2.27	1.86	2.62	2.07	2.93
	160	1.32	1.64	1.48	1.97	1.64	2.27	1.81	2.54
15°	80	1.42	1.85	1.64	2.25	1.85	2.60	2.06	2.91
	120	1.28	1.56	1.42	1.85	1.56	2.12	1.71	2.38
	160	1.21	1.42	1.32	1.64	1.42	1.85	1.53	2.06
20°	80	1.31	1.62	1.47	1.93	1.62	2.23	1.78	2.49
	120	1.21	1.41	1.31	1.62	1.41	1.83	1.52	2.03
	160	1.16	1.31	1.23	1.47	1.31	1.62	1.39	1.78
25°	80	1.24	1.48	1.36	1.72	1.48	1.96	1.60	2.20
	120	1.16	1.32	1.24	1.48	1.32	1.64	1.40	1.80
	160	1.12	1.24	1.18	1.36	1.24	1.48	1.30	1.60
30°	80	1.19	1.39	1.29	1.58	1.39	1.77	1.48	1.97
	120	1.13	1.26	1.19	1.39	1.26	1.52	1.32	1.64
	160	1.10	1.19	1.15	1.29	1.19	1.39	1.24	1.48

Comments on the Transverse Load Distribution Factor in AGMA 218.01

In AGMA 218.01, the load distribution factor C_m is defined by the product of the transverse load distribution factor C_{mt} and the face load distribution factor C_{mf}.

$$C_m = C_{mt} C_{mf} \tag{9}$$

C_{mf} is defined as the ratio of the peak load intensity to the average load. C_{mt} is related to the load sharing, but the definition is not given. The value of unity is used because standardized procedures to evaluate the influence of C_{mt} have not been established.

The contact stress number s_c can be represented as follows:

$$s_c \propto \sqrt{\frac{W_t}{F} \frac{C_m}{C_c} \frac{m_N}{C_\psi^2}} \tag{10}$$

In the case of $m_F\ (= \epsilon_\beta) > 1.0$, $C_\psi = 1.0$ and $m_N = F/L_{min}$. Substituting these values into equation,[10] the following expression is obtained:

$$s_c \propto \sqrt{\frac{W_t}{L_{min}} \frac{C_m}{C_c}} \tag{11}$$

In order to estimate s_c on the basis of the maximum tangential load w_{max}, C_m should equal to w_{max} / (W_t/L_{min}) and it coincides with the definition of $K_{H\beta}$ in this paper.

If C_{mf} is assumed here to be defined as the ratio of the peak load to the mean load on the contact line where the peak load exists

$$C_{mf} = w_{max}/(\psi W_t/l) = p_{max}/(\psi P_n/l), \tag{12}$$

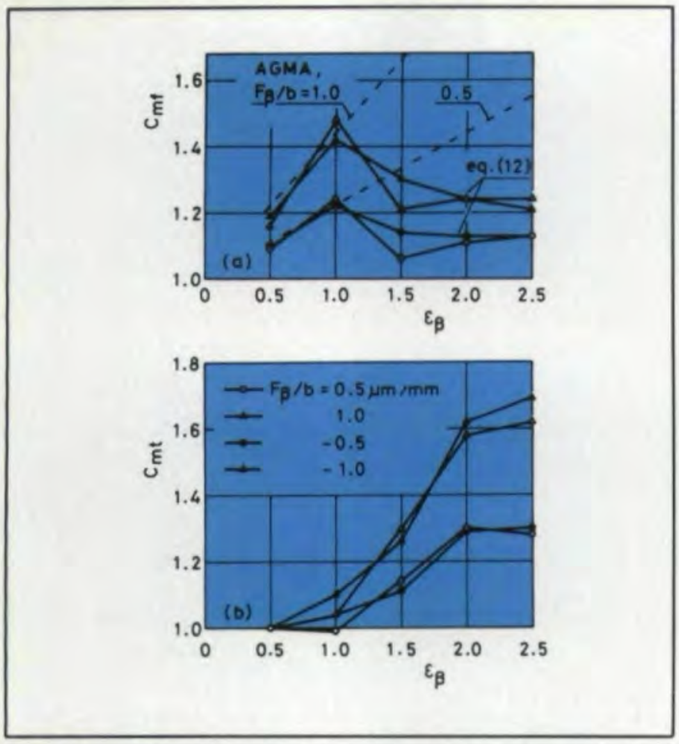

Fig. 9 – Estimated face load distribution factor C_{mf} (*a*) and transverse load distribution factor C_{mt} (*b*) of gears β = 20 deg, P_{nt}/bm_n = 120 N/mm[2]

C_{mt} is represented as follows:

$$C_{mt} = C_m/C_{mf} = (w_{max}/(W_t/L_{min})/C_{mf} = \psi/(l/L_{min}) \quad (13)$$

where ψ and l denote the load sharing factor and the length of contact line on the tooth where w_{max} exists. This idea, apart from the propriety of equation,[12] would be consistent with the definition of C_{mt} which is related to the load sharing. Following these definitions, C_{mf} and C_{mt} are estimated from the results of calculation and they are shown in Fig. 9. In the case of $\epsilon_\beta \leqq 1.0$, estimated C_{mf} is approximately equal to the values of AGMA 218.01 and estimated C_{mt} is close to unity. C_{mt} in equation[13] is, however, exactly equal to unity only when the load distribution is uniform or the gears are in single-tooth meshing. Consequently, in the case of larger ϵ_β, estimated C_{mt} is greater than unity as shown in the figure and C_{mf} in equation[12] is too small in comparison with C_{mf} in AGMA 218.01 because of larger C_{mt}. The foregoing discussion, therefore, leads to the following conclusion: the supposed transverse load distribution factor is not unity owing to the definition, and C_{mt} should be taken as unity if the formula of C_m in AGMA 218.01 is used to estimate the maximum load intensity.

Bending Moment Distribution Factor

In AGMA's formula, the load distribution factor for bending stress K_m is equal to the load distribution factor for surface durability C_m. In ISO's formula,[10] on the contrary, the load distribution factor for bending stress $K_{F\beta}$ is reduced by the expression $K_{F\beta} = K_{H\beta}{}^N$. The authors have reported the bending moment distribution factor $K_{M\beta}$ for spur gears[7] and it was less than ISO's $K_{F\beta}$. In the case of helical gears, the meshing position where the maximum bending moment arises is generally different from the worst position of load intensity as illustrated in Figs. 3 and 4. It shows that the relation between $K_{H\beta}$ and $K_{M\beta}$ has less physical meanings as compared with the case of spur gears.

The following definition of $K_{M\beta}$ for the bending moment distribution is adopted in this paper:

$$K_{M\beta} = M_{max}/M_{ref} \quad (14)$$

M_{ref} is the reference bending moment due to the uniform load P_n/L_{min} which is imaginarily distributed along the tip

$$M_{ref} = (P_n/L_{min})l_p \quad (15)$$

where l_P is the length of moment arm and it is presented using tooth height h, chordal thickness at the tip s_{tip}, and the normal load angle at the tip μ_n,

$$l_P = h \cos\mu_n - (s_{tip}/2) \sin\mu_n \quad (16)$$

calculated $K_{M\beta}$ of the pair of gears: $z_1 = z_2 = 20$, $\beta = 20$ deg is shown in Fig. 10. The following expression can be obtained from the result

$$K_{M\beta} = [K_{M\beta}]_{|F\beta|/b=0} + ([K_{M\beta}]_{|F\beta|/b=1.0} - [K_{M\beta}]_{|F\beta/b=0}) (|F_\beta|/b) \quad (17)$$

Using A in equation,[5] $K_{M\beta}$ is transformed as follows:

$$K_{M\beta}{}^* = K_{M\beta}/A = M_{max}/((P_{nt}/b)\ l_p) \quad (18)$$

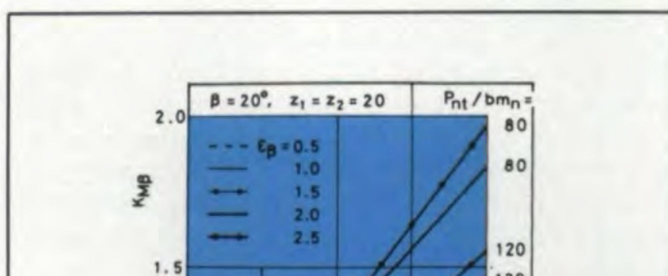

Fig. 10 – Bending moment distribution factor $K_{M\beta}$

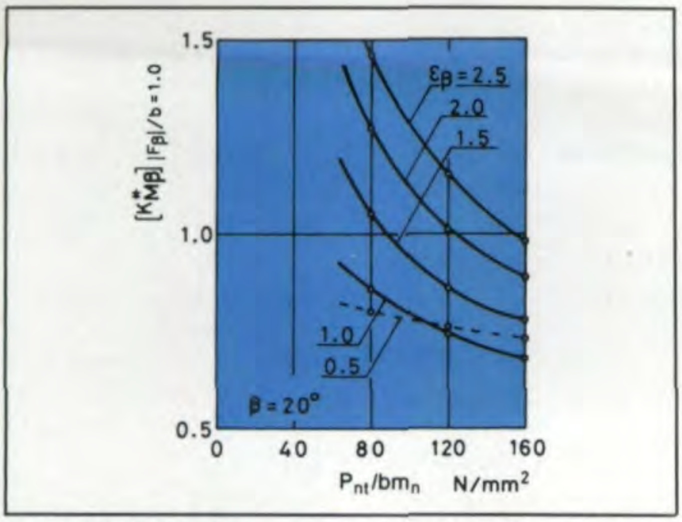

Fig. 11 – Modified bending moment distribution factor $K_{M\beta}$ of gears $z_1 = z_2 = 20$ with the effective alignment error $|F_\beta|/b = 1.0\ \mu$m/mm

$K_{M\beta}{}^*$ for $|F_\beta|/b = 0\ \mu$m/mm in approximately equal to 0.5 and the value for $|F_\beta|/b = 1.0\ \mu$m/mm is illustrated in Fig. 11. The relation between $a_M = [K_{M\beta}{}^*]_{|F_\beta|/b = 1.0} \sqrt{P_{nt}/bm_n}$ and ϵ_β is shown in Fig. 12 and the following expression can be derived for $\epsilon_\beta \geqq 1.0$:

$$[K_{M\beta}{}^*]_{|F_\beta|/b = 1.0} = (3.09\epsilon_\beta + 5.05)/\sqrt{P_{nt}/bm_n} \qquad (19)$$

From equations(17) to,(19) the approximate formula of $K_{M\beta}$ for the pair of gears of $\beta = 20$ deg is obtained. In the same way, similar formulas for the gears of $\beta = 10$ deg and 30 deg are obtained and the following formula is finally determined:

$$K_{M\beta} = A\left\{0.5 + \left(\frac{\phi_M\epsilon_\beta + 5.05}{\sqrt{P_{nt}/bm_n}} - 0.5\right)(|F_\beta|/b)\right\} \qquad (20)$$

$$\phi_M = 83.2\,\beta^{-1.1}$$

The formula is valid for the gears of $z_1 = z_2 = 20$, 10 deg $\leqq \beta \leqq 30$ deg, $1.0 \leqq \epsilon_\beta \leqq 2.5$; $80 \leqq P_{nt}/bm_n \leqq 160$ N/mm² with the restriction of $(\phi_M\epsilon_\beta + 5.05)/\sqrt{P_{nt}/bm_n} - 0.5 > 0$. The maximum error is about 6 percent except for a part of light load where the error exceeds 10 percent. Since the bending moment distribution factor is less than the load distribution factor, the effect of gear ratio shown in Fig. 8 can also be adopted in this case as the value of the safe side.

It should be noted that the factor $K_{M\beta}$ is obtained at the worst position of gears with the alignment error. As the position does not generally coincide with the worst position in the case of $F_\beta = 0$, the helical factor C_h in AGMA strength rating formula is still valid for the gears without the alignment error. The helical factor calculated by the present method has already been shown in the previous paper.(8)

Conclusions

The longitudinal load distribution on the contact lines and the bending moment distribution along the root of helical gears are calculated by FEM which is based on the plate theory including the transverse shear deformation.

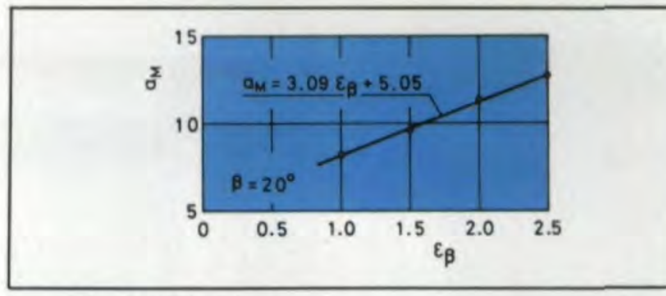

Fig. 12 – Value of a_M ($a_M = [K_{M\beta}{}^*]_{|F_\beta|/b = 1.0}\sqrt{P_{nt}/bm_n}$)

The longitudinal load distribution factor $K_{H\beta}$ caused by the effective alignment error is obtained and an empirical formula of $K_{H\beta}$ is proposed. The load distribution factor C_m in AGMA 218.01 is close to the values calculated by the present method. A formula is also proposed for the estimation of the maximum bending moment of gears with the alignment error.

A supposed definition of the transverse load distribution factor is examined and it leads to the conclusion that the transverse load distribution factor in AGMA 218.01 should be taken as unity if the formula of load distribution factor C_m is used to estimate the maximum load intensity.

References

1. HAYASHI, K., *Trans. JSME,* Vol. 28, 1962, pp. 1093-1101.
2. NIEMANN, G., and SCHMIDT, G., *VDI-Z,* Vol. 113, 1971, pp. 165-170.
3. NIEMANN, G., *Maschinenelemente II,* Springer, 1965.
4. CONRY, T. F., and SEIREG, A., *Trans. ASME,* Vol. 95, 1973, pp. 1115-1122.
5. KUBO, A., and UMEZAWA, K., *Trans. JSME,* Vol. 43, 1977, pp. 2771-2783.
6. TOBE, T., KATO, M., and INOUE, K., ASME *Journal of Mechanical Design,* Vol. 100, 1978, pp. 374-381.
7. TOBE, T., and INOUE, K., ASME paper 80-C2/DET-45, 1980.
8. INOUE, K., and TOBE, T., *Proc. Int. Symp. on Gearing & Power Transmissions,* Tokyo, Vol. 2, 1981, pp. 165-170.
9. AGMA 218.01, Dec. 1982.
10. ISO/DIS 6336/1, 1983.
11. "Calculation of the Load Capacity of Involute Cylindrical Gears," Report No. 137, *J. JSME,* Vol. 72, 1969, pp. 148-159.

Appendix 1

The minimum of total length of contact lines L_{min} is calculated by the following equation:(11)

(*a*) if $\mathrm{frc}(\epsilon_\alpha) + \mathrm{frc}(\epsilon_\beta) < 1$,

$$N_b = 1 - \frac{\mathrm{frc}(\epsilon_\alpha)\mathrm{frc}(\epsilon_\beta)}{\epsilon_\alpha\epsilon_\beta} \qquad (\epsilon_\beta \geqq 1)$$

$$N_b = 1 - \mathrm{frc}(\epsilon_\alpha)/\epsilon_\alpha \qquad (\epsilon_\beta < 1) \qquad \text{(A.2)}$$

(*b*) if $\mathrm{frc}(\epsilon_\alpha) + \mathrm{frc}(\epsilon_\beta) \geqq 1$,

$$N_b = 1 - \frac{\{1 - \mathrm{frc}(\epsilon_\alpha)\}\{1 - \mathrm{frc}(\epsilon_\beta)\}}{\epsilon_\alpha\epsilon_\beta}$$

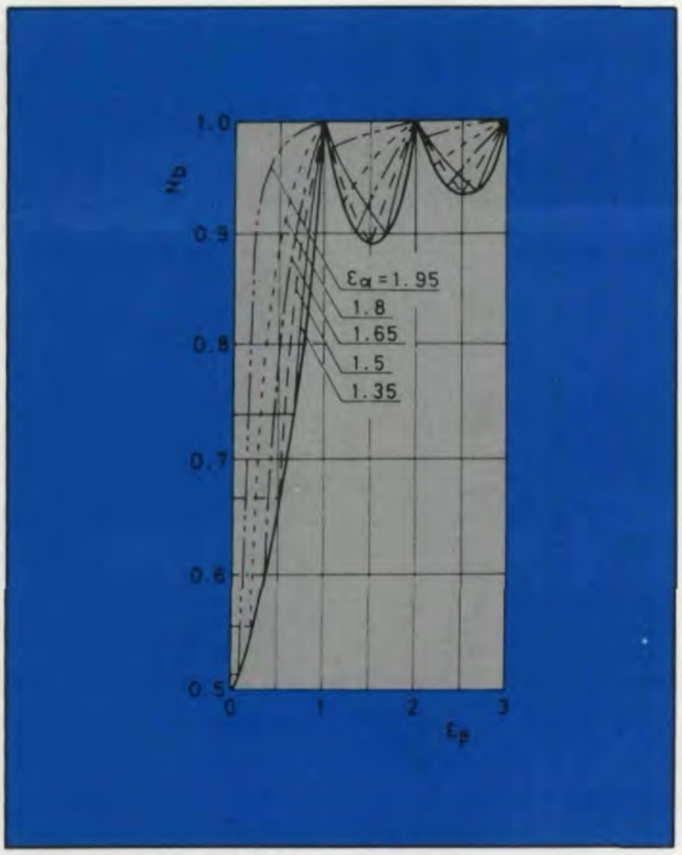

Fig. A.1 – Value of N_b

where frc (X) denotes the fraction of X. The function N_b is shown in Fig. A. 1. The dimensionless value A in equation(5) can be calculated by using N_b

$$A = \frac{L_{\min}\cos\beta_b}{b} = N_b\epsilon_\alpha \qquad \text{(A.3)}$$

In the case that the face contact ratio m_F ($=\epsilon_\beta$) in AGMA 218.01 is greater than unity, the load sharing ratio m_N is defined by $m_N = F / L_{\min}$. Therefore, A is expressed as follows:

$$A = \frac{\cos\beta_b}{m_N} \qquad \text{(A.4)}$$

Appendix 2

The matrix $[H_k]$ for gear k(k = 1, 2) is defined by $w_{k,ij}$, which is the deflection at node j on the contact line due to a unit normal load applied to node i.

$$[H_k] = [\{W_{k,1}\}, \{W_{k,2}\}, \ldots, \{W_{k,i}\}, \ldots]$$

$$\{W_{k,i}\} = (w_{k,i1}, w_{k,i2}, \ldots, w_{k,ij}, \ldots)^T \qquad \text{(A.5)}$$

$(\quad)^T$ = transposed matrix

The deflection $w_{k,ij}$ is calculated by FEM. When a pair of teeth are in mesh, the distributed load $\{P\}$ along the contact line is related to the sum of the deflection of the teeth and the relative approach due to elastic contact.

$$[H]\,\{P\} = \{w\} \qquad \text{(A.6)}$$

The elements of matrices $[H]$ and $\{w\}$ are

$$H_{ij} = H_{1,ij} + H_{2,ij} + \delta_{ij}\frac{w_{P,i}}{P_i}$$
$$w_i = w_{1,i} + w_{2,i} + w_{P,i} \qquad \text{(A.7)}$$

where $w_{P,i}$ is the relative approach at node i and σ_{ij} is Kronecker's delta. When some pairs of teeth I, II, . . . are in mesh matrices $[H_{\mathrm{I}}]$, $[H_{\mathrm{II}}]$, . . . are separately obtained. If the load on a pair of teeth is assumed to have little effect on the deflection of other pair of teeth, the matrix $[H]$ in equation (A.6) is diagonally constructed as follows:

$$[H] = \begin{pmatrix} [H_{\mathrm{I}}] & 0 & \\ 0 & [H_{\mathrm{II}}] & \\ & & \ldots \end{pmatrix} \qquad \text{(A.8)}$$

The equation (A.6) is solved under the following conditions:

$$\Sigma P_i = P_n$$
$$w_i + \frac{s_i}{1000} = (r_{b1}\theta_1 + r_{b2}\theta_2)\cos\beta_b \qquad \text{(node in contact)} \qquad \text{(A.9)}$$
$$P_i = 0 \qquad \text{(node not in contact)}$$

where s_i $[\mu m]$ is the spacing at node i caused by the effective alignment error, r_b is the radius of base cylinder and θ (rad) is the rotating angle of gear.

This article was contributed by the Power Transmission and Gearing Committee for presentation at the Design Engineering Technical Conference, October, 1984 of The American Society of Mechanical Engineers. Paper No. 84-DET-68.

MATERIAL SELECTION . . .

(continued from page 46)

and accuracy, and improved lubrication – rather than changes in material – are required to solve this problem.

Scoring

In some heavily loaded or high-speed gearing, scoring may occur under boundary film conditions. This is believed to be caused by frictional heat which reduces the lubricant protection sufficiently to allow welding and tearing of the profile.

Materials selection alone will not prevent scoring; proper lubricants and design geometry are required. This difficulty is seldom encountered in the conventional industrial gear drive. *AGMA 217.01, Oct. 1967, "AGMA Information Sheet – Gear Scoring Design Guide for Aerospace Spur and Helical Power Gears"* provides helpful recommendations for avoiding scoring.

(This article will be continued in the September/October 1985 issue of GEAR TECHNOLOGY.)

Reprinted from Modern Methods of Gear Manufacture, 4th Edition, Published National Broach and Machine Division of Lear Siegler, Inc., 17500 Twenty Three Mile Rd., Mt. Clemens, MI 48044

Factors Affecting Shaper Cutter Selection

Fellows Corp., Emhart Machinery Group
Springfield, VT 05156

EXTERNALS

How to specify the right size

When selecting cutters for external applications, the shaper cutter size is primarily dependent on the type of machine on which it will be used. A cutter should be able to clear its cutter spindle or cutter spindle adapter (depending on how the cutter is mounted) throughout its useful life. Occasionally, size is dictated by a ratio that must be maintained with the workpiece. Sometimes, larger cutters are required to avoid interferences created by workpiece design, workholding fixture, center support, etc. A shaper cutter should be only as large in diameter and thickness as the application requires. Overhang of the cutter on the cutter spindle should remain as small as possible.

INTERNALS

Problem situations and how to solve them

1. Infeed Trim—occurs when the number of teeth in the cutter is too large in relation to the number of teeth in the work. Trim shows up as a modification of the profile near the inside diameter of one or more finished teeth as shown in Fig. 1. This problem does not harm the cutting tool.
Solution: Reduce the number of teeth in the cutter.

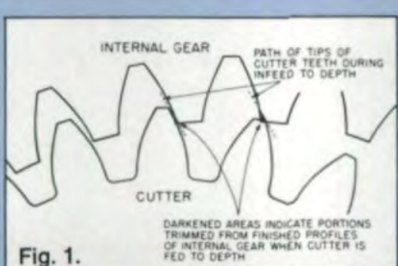

Fig. 1.

2. Finish Side Rub—caused by having a cutter too large relative to work size. Shows up as an excessive burr on the face and inside diameter of the work from the leading side of the cutter as shown in Fig. 2. This problem causes excessive wear and load on the leading side of the cutter resulting in a reduction in tool life.
Solution: Increase active p.a. by reducing cutter diameter, reduce number of teeth in cutter, decrease angle of back-off providing rub is not transferred to other side (see item 3).

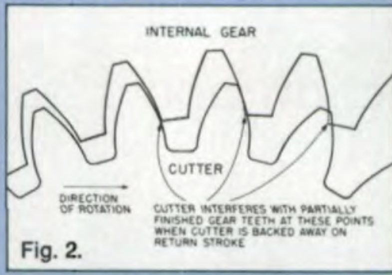

Fig. 2.

3. Infeed Rub—occurs when the cutter is too large in relation to the work or very similar to item 2, but only occurring when the cutter is infeeding. Burr produced on the inside diameter will be cut away by the time cutter reaches full depth. Excessive infeed rub will result in abnormal wear on the leading side of the cutter.
Solution: Same as for item 2.

4. Rough Side Rub—caused by the hooking action of the cutter teeth as they enter the uncut side of the work near the inside diameter. Shows up as excessive burr on the face of the gear and the inside diameter from the trailing side of the cutter. This problem causes excessive wear and/or load on the trailing side of the cutter resulting in a deterioration of tool life.
Solution: Increase the inside diameter, increase angle of back-off providing rub is not transferred to other side (see item 2) or decrease the amount of back-off.

5. Involute Tooth Form Modification—occurs when the inside diameter of the work being cut is too close to the base circle and/or the cutter is too small. Results in trimming away of involute profile to the last point of involute contact as shown in Fig. 3.
Solution: Increase inside diameter of work and/or increase size of cutter.

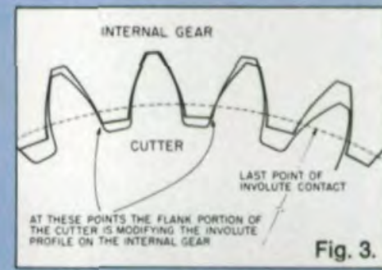

Fig. 3.

Finding The Maximum Number Of Teeth For Internal Gear Cutters

The table below may be used to determine the maximum number of teeth in a cutter for cutting a specified number of internal teeth.
NOTE:
1. 10 teeth are usually considered to be the smallest number of teeth in a gear shaper cutter, though in some cases, especially for high pressure angle splines and serrations, cutters of 5 teeth have been used.
2. The selection of number of teeth from this table will minimize the problems of trim and rub as shown above.
3. When cutting large internal gears, the cutter size must be slightly larger than the cutter spindle and/or cutter adapter during its useful life.
4. Internal gears having inside diameters less than 10° of roll from the base circle should be given special study for proper cutter design.

No. of Internal Teeth	MAXIMUM NUMBER TEETH IN CUTTER			
	14.5° PA Full Depth	20° PA Full Depth	20° PA Stub 25° PA Full Depth	30° PA Fillet Root Splines
16				9
20				13
24			10	17
28			11	21
32		10	12	25
36		13	14	29
40	14	17	18	33
44	16	21	23	37
48	18	25	27	41
52	21	29	32	45
56	24	34	36	49
60	27	38	40	53
64	30	42	45	57
68	33	46	49	61
72	36	50	53	65
80	44	58	62	73

E-6 ON READER REPLY CARD

Material Selection and Heat Treatment

by
National Broach & Machine
Mt. Clemens, Michigan

Table 1 – AGMA Standards Useful in Selecting Gear Materials

Nomenclature		
110.03	Gear-Tooth Wear and Failure (USAS B6.12-1964)	Jan. 1962
Durability		
215.01	Information Sheet for Surface Durability (Pitting) of Spur, Helical, Herringbone and Bevel Gear Teeth	Sept. 1966
217.01	Information Sheet-Gear Scoring Design Guide for Aerospace Spur and Helical Power Gears	Oct. 1965
Strength		
225.01	Information Sheet for Strength of Spur, Helical, Herringbone and Bevel Gear Teeth	Dec. 1967
Inspection		
230.01	AGMA Standard-Surface Temper Inspection Process	March 1968
Materials		
241.02	Specification for General Industrial Gear Materials—Steel (Drawn, Rolled and Forged)	Jan. 1965
242.02	Cast Iron Blanks	Sept. 1946
244.02	Nodular Iron Gear Materials	July 1965
245.01	Specification for Cast Steel Gear Materials	Jan. 1964
246.01	Recommended Procedure for Carburized Industrial Gearing	Jan. 1965
247.01	Recommended Procedure for Nitriding, Materials and Process	Jan. 1965
248.01	Recommended Procedure for Induction Hardened Gears and Pinions	Jan. 1964
249.01	Recommended Procedure for Flame Hardening	Jan. 1964

Gear materials are selected to provide the optimum combination of properties, at the lowest possible cost consistent with satisfying other requirements. Some of the important physical properties of gears are abrasion or wear resistance, toughness, static compression strength, shear strength, fatigue strength, and strength at elevated temperatures.

Because of widely varying requirements, gears are produced from a wide variety of materials. These materials include plastics such as nylon, powdered metals, brasses, bronzes, cast or ductile irons, and steels. Many types of steels, including stainless steel and tool steel, are used. Each of the materials mentioned will best satisfy some specific requirement such as corrosion resistance, extreme wear resistance, special damping qualities, ability to operate without lubrication, low cost, or producibility.

The majority of gears for automotive, aircraft, farm machinery, off-the-road equipment, and machine tool applications are produced from hardenable carbon or low-alloy steels or cast iron. Therefore, this article will cover only ferrous materials.

The choice of a gear material depends on four factors:

1. Mechanical properties
2. Metallurgical characteristics
3. Blank-forming method
4. Manufacturing process

Each of these factors must be evaluated with an eye to its effect on the three major performance criteria – durability, strength, and wear.

Mechanical Properties*

Before the optimum mechanical properties can be selected, the working stress must be determined, based on recommended allowable stresses.

This article discusses durability and strength formulas adopted by the American Gear Manufacturers Association and widely used throughout the world, Table 1. There is a fundamental relationship among most formulas, so that working and allowable stresses determined by different formulas can be used or compared.

Working stress is usually based on the fatigue or yield strength of the material. Less frequently, impact resistance, tensile strength, or brittle-fracture characteristics of the material must be considered.

For most gear trains, the limiting design consideration is profile durability (pitting resistance), gear-tooth strength (resistance to fracture), or wear. Normally, durability is the limiting consideration; but sometimes all three are of nearly equal importance.

A number of other possible modes of failure may also limit gear performance, such as scoring associated with high

*Abstracted from Machine Design, Gear Materials Design Guide, June 20, 1968.

speed and heavy loads, case crushing in carburized and hardened gearing, and micro-pitting. However, these are less likely to occur.

The AGMA gear-rating formulas for both strength and durability are basically the same for spur, helical, herringbone, and bevel gear teeth. Terms in both formulas are divided into four major groupings, associated with load, size, stress distribution, and stress.

The surface-durability or pitting-resistance formula – *AGMA 215.01, Sept. 1966, "Information Sheet for Surface Durability (Pitting) of Spur, Helical, Herringbone and Bevel Gear Teeth"* – is

$$s_c = C_p \sqrt{\underbrace{\left(\frac{W_t C_o}{C_v}\right)}_{\text{(Load)}} \underbrace{\left(\frac{C_s}{dF}\right)}_{\text{(Size)}} \underbrace{\left(\frac{C_f C_m}{I}\right)}_{\text{(Stress dist.)}}} \quad (1)$$

where

$$s_c \leqq s_{ac} \underbrace{\left(\frac{C_L C_H}{C_R C_T}\right)}_{\text{(Stress)}} \quad (2)$$

The "stress" term, Equation 2, is the most important consideration in selecting a gear material. Table 2 lists all symbols used in the strength and durability formulas. Allowable fatigue (contact) stresses, s_{ac} are shown in Table 3.

The mechanical properties for gear materials are almost always specified in terms of Brinell hardness rather than ultimate strength or test-bar properties. Location (normally the toothed portion) and number of hardness tests should also be specified. Maximum hardness is also specified in the interests of machinability and sometimes to insure a hardness difference between the mating gears; such a difference can increase wear resistance. Typical combinations are shown in Table 4.

Values of s_{ac} are based on 10^7 cycles, since most gear materials generally show the typical "knee" at or below this value. Hence, these values can be considered fatigue-strength stresses. If a gearset must operate for only a finite number of cycles, the s_{ac} values can be increased by life factor C_L, Fig. 1.

Pitting of gear teeth is considered a fatigue phenomenon. There are two kinds of pitting – initial and progressive (destructive). Corrective and non-progressive initial pitting is not considered serious and is normally to be expected until imperfections, such as high spots, are worn in.

The stresses in Table 3 are satisfactory

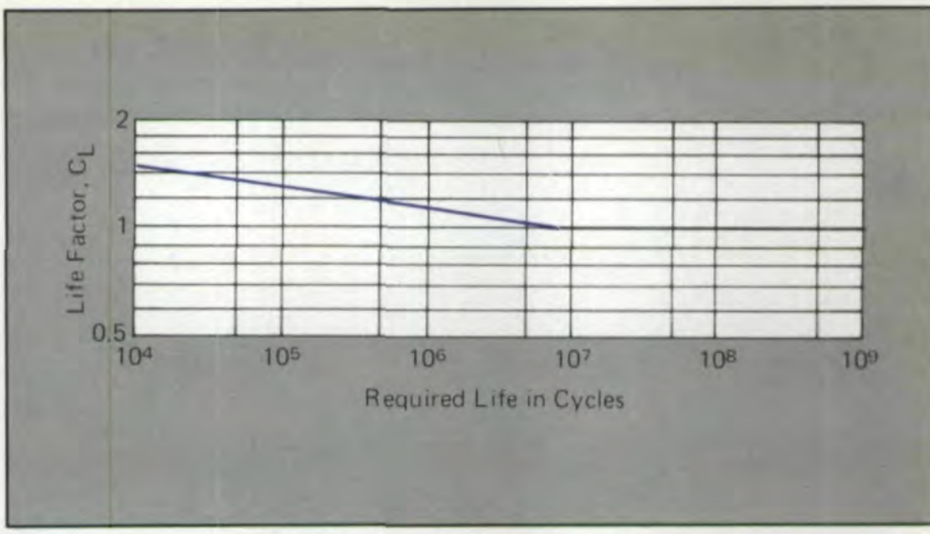

Fig. 1 – Life factor for durability rating of gears.

Table 2 – Gear Rating Factors

Factor	Strength	Durability
Load		
Transmitted load	W_t	W_t
Dynamic factor	K_v	C_v
Overload factor	K_o	C_o
Size		
Pinion pitch diameter	—	d
Net face width	F	F
Transverse diametral pitch	P_d	—
Size factor*	—	C_s
Stress Distribution		
Load-distribution factor	K_m	C_m
Geometry factor	J	I
Surface-condition factor	—	C_f
Size factor*	K_s	—
Stress		
Calculated stress	s_t	s_c
Allowable stress	s_{at}	s_{ac}
Elastic coefficient	—	C_p
Hardness-ratio factor	—	C_H
Life factor	K_L	C_L
Temperature factor	K_T	C_T
Safety factor	K_R	C_R

**Size factor is placed either in the size or stress-distribution grouping, depending upon the importance of the effect.*

Table 3 – Allowable Contact Stress (Durability)

Material	Minimum Surface Hardness	Contact Stress, s_{ac} (1000 psi)
Steel		
Through-hardened	180 Bhn	85-95
	240 Bhn	105-115
	300 Bhn	120-135
	360 Bhn	145-160
	440 Bhn	170-190
Case-carburized	55 R_c	180-200
	60 R_c	200-225
Flame or induction-hardened	50 R_c	170-190
Cast Iron		
AGMA Grade 20	—	50-60
AGMA Grade 30	175 Bhn	65-75
AGMA Grade 40	200 Bhn	75-85
Nodular Iron	165-300 Bhn	10% less than for steel with same hardness

Table 4 – Typical Gear/Pinion Hardness Combinations

	Minimum Hardness (Bhn)*											
Gear	180	210	225	255	270	285	300	335	350	375	55R_c	58R_c
Pinion	210	245	265	295	310	325	340	375	390	415	55R_c	58R_c

*Maximum hardness is usually 35 to 40 Bhn higher.

Table 5 – Recommended Safety Factors in Pitting

Required Reliability	Factor C_R
High	1.25+
Fewer than 1 failure in 100	1.00
Fewer than 1 failure in 3	0.80*

**At this value, plastic profile deformation might occur before pitting.*

Table 6 – Allowable Stress (Strength)

Material	Minimum Hardness	Allowable Stress, s_{at} (1000 psi) Spur, Helical, & Herringbone	Bevel**
Steel			
Normalized	140 Bhn	19-25	11
Quenched & temp.	180 Bhn	25-33	14
Quenched & temp.	300 Bhn	36-47	19
Quenched & temp.	450 Bhn	44-59	25
Case carb.	55R_c	55-65	27.5
Case carb.	60R_c	60-70	30
Ind. or flame through-hardened	54 Bhn	45-55*	
Ind. or flame through-hardened	54 Bhn	22	13.5
Nitrided AISI 4140	53R_c†	37-42*	20
Cast Iron			
AGMA Grade 20	......	5	2.7
AGMA Grade 30	175 Bhn	8.5	4.6
AGMA Grade 40	200 Bhn	13	7
Nodular Iron			
ASTM Grade 60-40-18	Annealed	15	8
ASTM Grade 80-55-06		20	11
ASTM Grade 100-70-03	Normalized	26	14
ASTM Grade 120-90-02	Quenched & temp.	30	18.5

Table 7 – Safety Factors for Fatigue and Yield Strength

Reliability	Factor K_R
Fatigue	
High	1.50+
Fewer than 1 failure in 100	1.00
Fewer than 1 failure in 3	0.70
Yield	
High	3.00+
Normal	1.33

for gears with smooth profiles operating with adequate lubrication. Some "as-hobbed" or shaped gears, or those with rough-textured profiles, should use more conservative stresses. In this case, special attention should be given to the lubricant. Procedures for inducing favorable surface stresses for increased profile durability are not yet generally used.

Except for heavily loaded gears or those subjected to unusual environments, no substantial difference in allowable contact stress exists among the normal qualities of available commercial steels. Free-machining steels may be used to obtain improved machinability or a better surface finish.

Because pitting is a fatigue phenomenon, it displays a scatter which must be allowed for by a safety factor to ensure reliability. If this factor is not included in the basic design calculations, Table 5 can be used as a guide and the s_{ac} values adjusted accordingly. It should be remembered that "failure" does not necessarily mean an immediate failure under applied load, but rather shorter life than expected.

If one of the mating gear elements is considerably harder than the other, the allowable stress of the softer element can be increased under certain conditions. Normally, the gear ratio must be high – over 8:1 – and the gears large before any appreciable improvement is obtained. Typical of gears for which such a correction is normally made are those for large kilns, or for ball mills. The appropriate AGMA standards contain recommended values of the C_H factor used to rate gearsets having large differences in hardness.

Generally, temperature factor $C_T = 1$ when gears operate with oil or with gear-blank temperatures not exceeding 250F. In some instances, it is necessary to use $C_T > 1$ for carburized gears operating at oil temperatures above 180F. Tests have indicated a drop of several points R_c hardness for carburized steels subjected to 200F for 10,000 hr, as well as a 6 to 8% reduction in fatigue strength.

When gears are proportioned on the basis of allowable surface fatigue stress, surface yielding is seldom a problem. This is partially because the contact stress only increases as the square root of the transmitted load. Allowable overloads of 100% above the surface-fatigue rating are commonly specified. Greater amounts of overload are often successfully carried. However, repeated overloading can cause plastic flow, which ripples or grooves the profile or extrudes a "wire edge" at the tip of the tooth. This extruded material can affect lubrication. Excessive plastic flow of the profile can induce abrasive wear because of the rough surface texture developed.

Surface yielding does not cause immediate or catastrophic failure and the use of heavier viscosities or extreme-pressure lubricants along with reduced loading can alleviate a troublesome situation when it is encountered.

The effect of impact or brittle-fracture properties of gear materials on surface stresses need not be considered, except for the peak stresses developed by im-

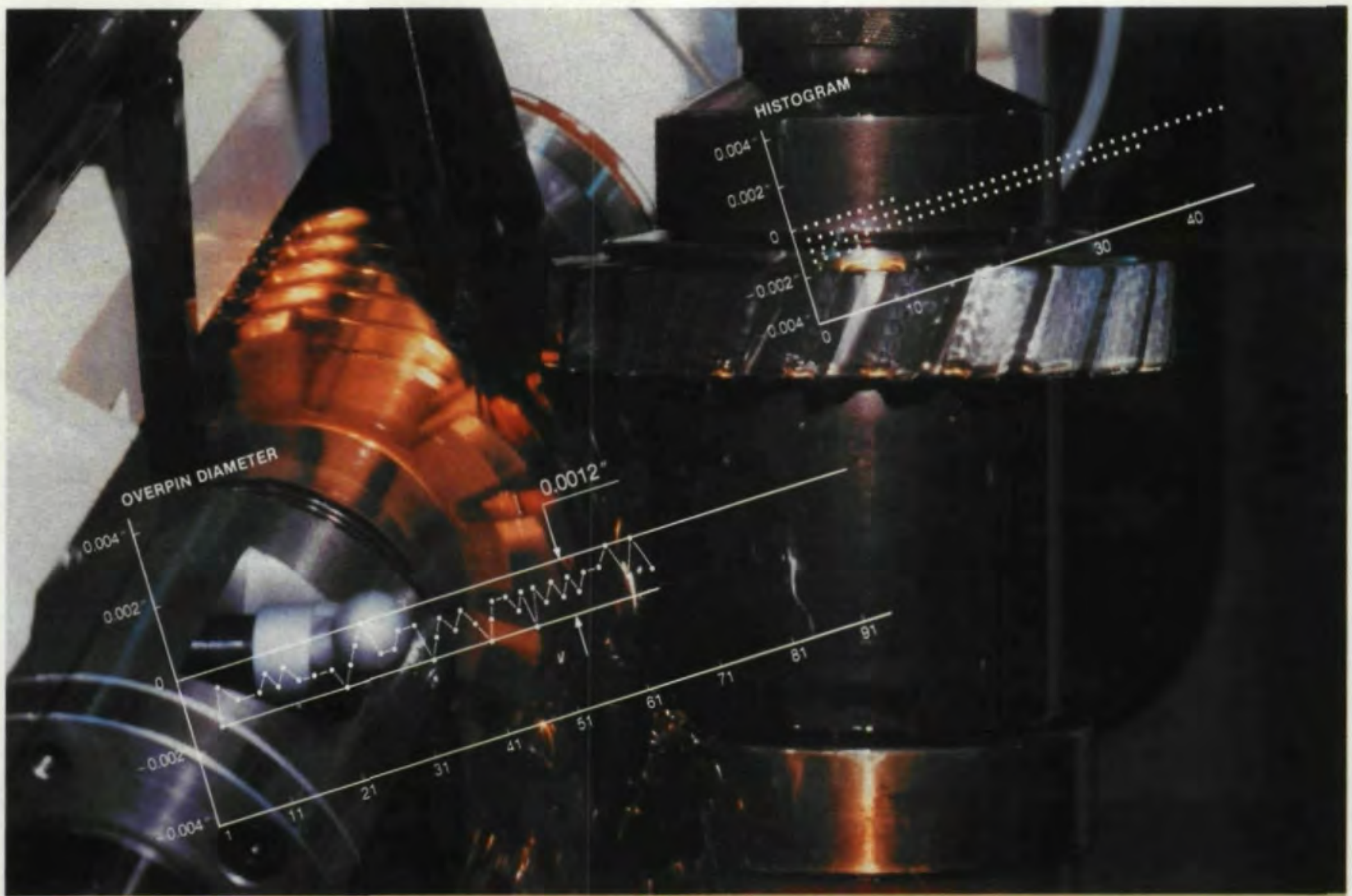

CAN YOU GET CONSISTENT OVERPIN DIAMETER OF 0.0012" FROM COLD START?

You can, with Mitsubishi's new GA-Series Gear Hobbers!

Here's the reason why you can get such a consistent accuracy over hours of continuous running. To maintain the thermal stability of the machine, the hydraulic oil is maintained to a constant temperature by a refrigerating unit and the unit is isolated from the machine. The 36" wide 3-runway bed and heavy duty ball screws also plays a big role in maintaining high accuracy.

Not only is the machine accurate but also can withstand heavy duty cuts due to the robust construction of the machine and an AC servo motor driven direct hob drive mechanism. A hydraulically controlled backlash eliminator on the indexing table permits "reverse hand conventional cutting" which gives 4 to 5 times more cutter life on your tools.

Another prominent feature of the machine is the conversational "MENU" programming. Just key in the gear and hob data and select the type of material you are going to cut. The computer of the CNC will do the rest for you. No calculation of cutter path or selection of cutting parameters.

Needless to say, with a full CNC machine, the changeover time can be reduced to a maximum of 90%.

These are only a part of what our GA-series can do for you. For more information, write to our Bensenville office below or call, area code 312-860-4220 NOW!

SPECIFICATIONS

	GA250NC	GA40CNC
Maximum part diameter	10"	16"
Maximum DP	4	4
Maximum radial travel	8.26"	10"
Maximum axial travel	10.6"	10.6"
Worktable diameter	8.45"	16.5"
Hob speed range	200~600rpm	200~600rpm
Hob drive motor	10hp	10hp

MITSUBISHI
HEAVY INDUSTRIES, LTD.
5-1, Marunouchi 2-chome, Chiyoda-ku, Tokyo, Japan
Cable Address: HISHIJU TOKYO

Mitsubishi Heavy Industries America, Inc.
873 Supreme Drive, Bensenville, IL 60106 Phone: (312) 860-4220

pulse or impact loading.

Tooth Strength

The tooth-strength rating formula – *AGMA 225.01, Dec. 1967, "Information Sheet for Strength of Spur, Helical, Herringbone and Bevel Gear Teeth"* – is

$$s_t = \underbrace{\left(\frac{W_t K_o}{K_v}\right)}_{\text{(Load)}} \underbrace{\left(\frac{P_d}{F}\right)}_{\text{(Size)}} \underbrace{\left(\frac{K_s K_m}{J}\right)}_{\text{(Stress dist.)}} \tag{3}$$

where

$$s_t \leqq s_{at} \underbrace{\left(\frac{K_L}{K_R K_T}\right)}_{\text{(Stress)}} \tag{4}$$

Again, allowable stress is the most important term in selecting a material.

The fatigue and yield resistance necessary to prevent the fracture of a gear tooth depend on more complex relationships between materials properties than those for profile durability. This is true primarily because the root-radius stress varies directly with the load. Fortunately, the root stress can be calculated fairly accurately by applying standard beam or plate theories.

Some allowable fatigue stresses s_{at} used with the AGMA formula are listed in Table 6.

Allowable stress or fatigue strength is normally determined for 10^7 cycles, with adjustments for shorter finite life made by using the K_L factor given in Fig. 2. Unlike C_L, K_L depends on fatigue notch-sensitivity, which is somewhat proportional to hardness; hence the necessity for several curves for various gear hardnesses.

Experience suggests that a clearly defined knee is not always present in the gear fatigue stress/cycle plot. This phenomenon might be an inherent property, as it is with non-ferrous materials. But it is more likely a result of wear or other service-developed changes which affect either the dynamic loading, load distribution, or stress system. For conservative design, sometimes, s_{at} is reduced by the K_L factor determined from curve B in Fig. 2.

Normally the stress at the root of the tooth varies from zero to the maximum working tensile stress. If a fully reversed stress is present, as it is with reversing loads or with idler gears, the allowable stress should be 70% of the values shown in Table 6.

The quality of the material has a pronounced effect on the strength of gear

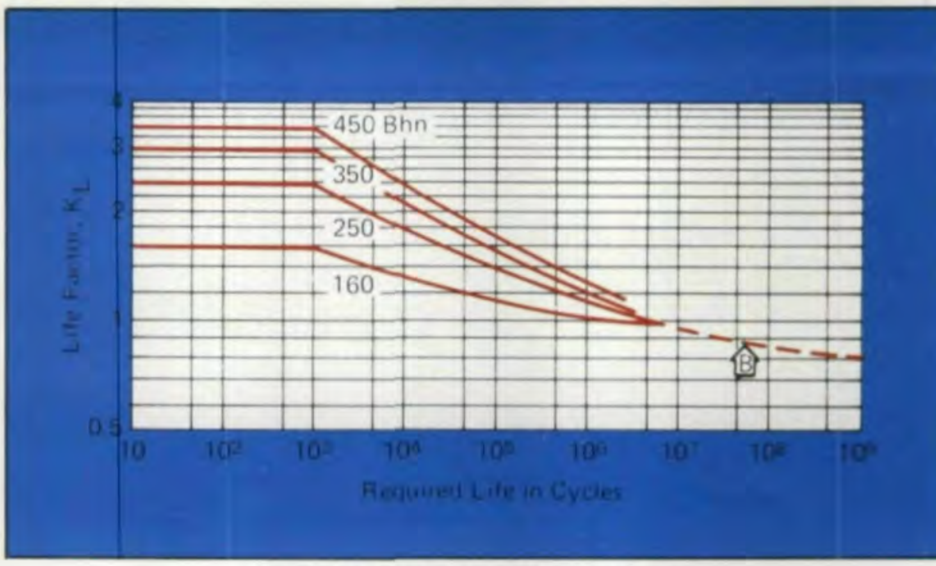

Fig. 2 – Life factor for strength rating of gears.

teeth, more so than in the case of pitting resistance. The values shown in Table 6 are for commercially available steels. In the absence of a clear understanding of the criteria for judging quality, the lower values should be used. These are suitable for steels with a cleanliness typical of resulphurized or leaded steels.

The upper values in Table 6 would require steels produced under good melting and pouring conditions. Cast steels require adequate directional and progressive solidification. Rolled and forged steels will probably require vacuum treatment, with special instructions to prevent excessive reduction during rolling or forging; this procedure will provide a desirable direction of fiber flow lines without excessive reduction in transverse properties. Finally, heat treatment should be under rigid supervision in accurately controlled furnaces, followed by careful hardness and metallographic inspection. For high-speed gears, or for drives requiring maximum reliability, additional inspection, for example magnetic and ultrasonic inspection, is a necessity.

Fatigue: The fatigue strength of a gear tooth is significantly affected by size, surface finish, and residual stresses at the root radii. Residual stresses in a favorable direction can be developed by metallurgical processing such as case carburizing or nitriding. Under certain circumstances, flame or induction hardening, which do not develop a uniform hardness pattern on the profile or in the root area, can induce significant unfavorable stress patterns. Mechanical processing, such as shot peening, to induce favorable root stresses is used successfully.

The fatigue strength of gear teeth follows a statistical pattern, so that a safety factor should be used. Some recommended factors are listed in Table 7.

It is important to remember that a tooth fracture, unlike profile pitting, is catastrophic and cannot be repaired or alleviated by reducing load or changing lubricant. Impact loads in geared systems are commonly two or more times the rated load. Because gears have backlash and are loosely coupled, both the electrical torque and inertial energy of an electric motor can be released simultaneously, so that peak torques of two to four times the nameplate rating are not uncommon. For this reason an adequate safety factor, K_R, and life factor, K_L, are important.

Yield: Loads which develop a root stress above the yield strength of the material cause the gear tooth to bend permanently. Since gear-tooth dimensions are held to 0.001 or less, only a slight permanent bend or distortion can affect the geometric dimensions sufficient to cause interference on high dynamic loads. This will quickly result in a fatigue fracture.

The allowable yield stress for steel recommended for use with the AGMA rating formula is shown in Fig. 3. The alloy composition, heat-treatment effectiveness, and section size affect the yield strength at any ultimate strength or hardness, so that more accurate yield-strength

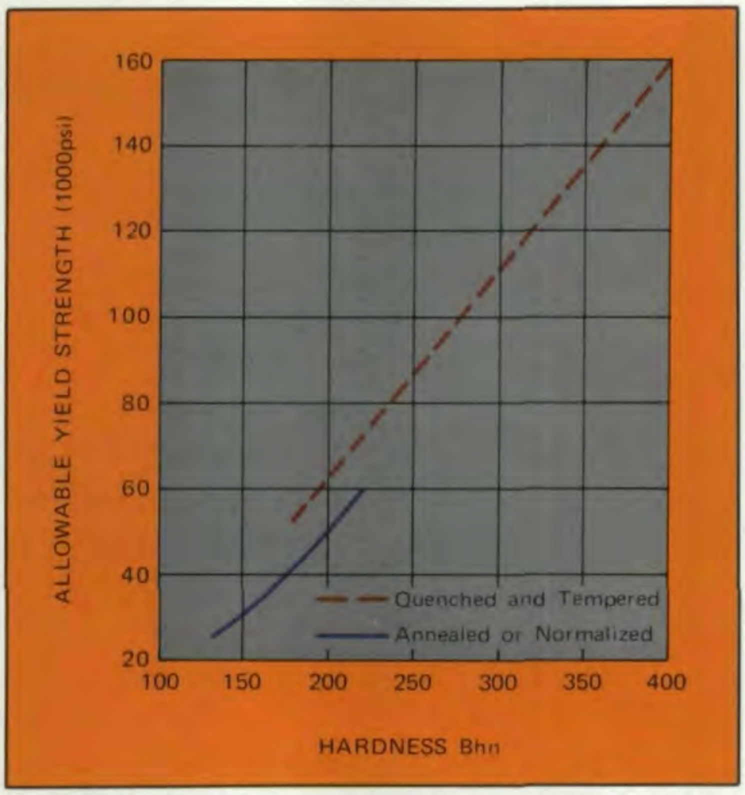

Fig. 3 – Allowable yield stress recommended for use with AGMA formulas.

data can be used if it is available.

As a general rule, when peak loads exceed 200% of the allowable endurance stress (100% overload), it is necessary to consider yield in both the design calculations and material selection. Table 7 lists appropriate safety factors for use when selecting materials for yield strength.

Operating temperatures can affect the allowable stress. According to AGMA Standards, when gears operate at oil or gear-blank temperatures not exceeding 250F temperature factor, generally $K_T = 1$. For case-carburized gears at temperatures above 160F, K_T may be found from

$$K_T = \frac{460 + T_F}{620} \quad (5)$$

where T_F = peak operating oil temperature, deg F.

Fatigue failure initiated by a bent tooth caused by loads above the yield strength is not uncommon and should not be disregarded even for surface-hardened gears. This is particularly true when the design is based on allowable fatigue stresses which have been increased by favorable induced surface stresses.

Impact: Although impact is not significant in evaluating a material for surface durability, it can be important in tooth-strength considerations.

The first step is to determine whether or not destructive impact can be developed in the gear system. Normally, if the time to develop the peak stress is a significant proportion of the natural period of vibration, the stress can be calculated from loads deduced from the oscillatory characteristics of the mass elastic system. The material must then be selected on the basis of yield strength or, if sufficient cycles are involved, fatigue strength.

In some specific applications – mostly determined by field experience – impact properties should be considered as a matter of course. One example is service at low temperatures, which are known to reduce impact strengths. Here steels containing nickel and those having fully quenched and tempered metallographic structures are desirable. Lower hardness and sometimes lower carbon content are beneficial, although these must be considered with an eye to the required size of gearing and costs. Obviously the direction of grain flow, transverse properties, and area reduction during forging must be controlled.

Brittle fractures of gear teeth occur only occasionally. Efforts to correlate material properties with brittle-fracture analysis have not yet produced results of value to the designer, although some progress is being made.

Wear

The wear in contacting teeth varies from an unmeasurable amount with fully hydrodynamic lubrication, through intermediate and boundary stages, to dry metal-to-metal contact. Hydrodynamic lubrication is present when the ratio of film thickness to surface finish exceeds approximately 1.4; boundary lubrication when the ratio is between 0.05 to 0.2; and dry lubrication when the ratio is less than 0.01. These are approximate guides based on tests with straight mineral oils.

Normally, wear is encountered only when surface finishes are rough, speeds are very low, or loads and velocities are high. There are four types of wear: adhesive, abrasive, corrosive, and fatigue.

Generally, when ferrous metals are used for gears, the wear rate decreases with increasing hardness. Under certain conditions, softer gears will polish to a fine surface finish and a good load distribution; this provides improved lubrication. In some cases, the profile will be worn to a non-involute shape; once this "wearing-in" has occurred, little wear will follow. If this beneficial wear does not occur, high hardness, obtained by quenching or by a surface-hardening source such as induction or flame hardening, carburizing, or some form of nitriding must be used.

It is not uncommon for changes to occur in the dedendum of heavily loaded gears, particularly at slow speeds. A concave surface is developed which soon stabilizes and in no way affects the load-carrying capability of the gears. This phenomenon is due to a number of reasons, one of them being the fact that the rolling and sliding are in opposite directions on the dedendum.

In some carburized and hardened gears a frosted appearance develops. This ultimately results in surface spalling, which in turn can initiate a tooth fracture. This frosting is probably due to microscopic pitting. Better surface finish

(continued on page 38)

CLASSIFIED

Rates: Classified Display—$100 per inch (minimum 3″) Type will be set to advertiser's layout or *Gear Technology* will set type at no extra charge. **Word Count:** 35 characters per line, 7 lines per inch.

Payment: Full payment must accompany classified ads. Mail copy to *Gear Technology*, P.O. Box 1426, Elk Grove Village, IL 60007. **Agency Commission:** No agency commission on classifieds.

Closing date: Ads must be received by the 25th of the month, two months prior to publication. **Acceptance:** Publisher reserves the right to accept or reject classified advertisements at his discretion.

Precision Products
by **Western**

SPLINE GAGES
MASTER GEARS
SPUR – HELICAL
VARIABLE SPLINE GAGES
SPLINE ARBORS
& SPLINE CHUCKS

WESTERN SPLINE GAGE INC.
P.O. Box 702, 285 James Street
Holland, MI 49423
616-399-4021 Telex 226305

CIRCLE A-16 ON READER REPLY CARD

SPIRAL BEVEL GEARS

Protype or production up to 34″
Breakdown work – fast turnaround
Complete machining, heat treat, lapping and testing
CALL US!

B&R MACHINING
PO Box 536
Sharon, TN 38255
1-800-238-0651

CIRCLE A-17 ON READER REPLY CARD

GEAR TOOTH GRINDING & HONING ONLY

Production Quantities
3/4″ P.D. to 27.5″ P.D.;
3.5 D.P. and 11″ Face

We have no turning, hobbing or shaping capability

ALLEGHENY GEAR CORP.
23 Dick Road
Depew, NY 14043
716-684-3811

CIRCLE A-18 ON READER REPLY CARD

HELP WANTED

MANUFACTURING MANAGER GEARS

Aircraft and precision parts manufacturer (gears, shafts, housings) seeks experienced manufacturing manager capable of running manufacturing operations of an eighty man job shop. Must have working knowledge of aircraft parts, quality requirements, tools, fixtures, processing and manufacturing. Exceptional opportunity for right individual.

Send resume to

ACR INDUSTRIES, INC.
29200 Calahan
Roseville, Michigan 48066

GEAR ENGINEER

Position open for applicants with extensive experience in air craft gear processing. Must have complete knowledge of gear manufacturing. Applicants with estimating experience preferred. Must be ambitious and have a desire to advance.

ACR INDUSTRIES, INC.
29200 Calahan
Roseville, Michigan 48066
(313) 773-0450

WANTED PROCESS ENGINEER

Inside showroom sales and administrative duties. Gear machines and all types of machine tools. Sales oriented, but sales experience not necessary.

Send resume to:

Dept. C
P.O. Box 1426
Elk Grove Village, IL 60007

All replies held in strictest confidence

FOR SALE – NEW PRODUCT

NEW

GEAR DEBURRING MACHINE

0″-72″ diameter

Deburrs both sides simultaneously. Can handle work between centers, fully universal and automatic.

Write:

Deburr
P.O. Box 118602
Cincinnati, Ohio 45211

CIRCLE A-21 ON READER REPLY CARD

MACHINED PLASTIC GEARS . . .
(continued from page 29)

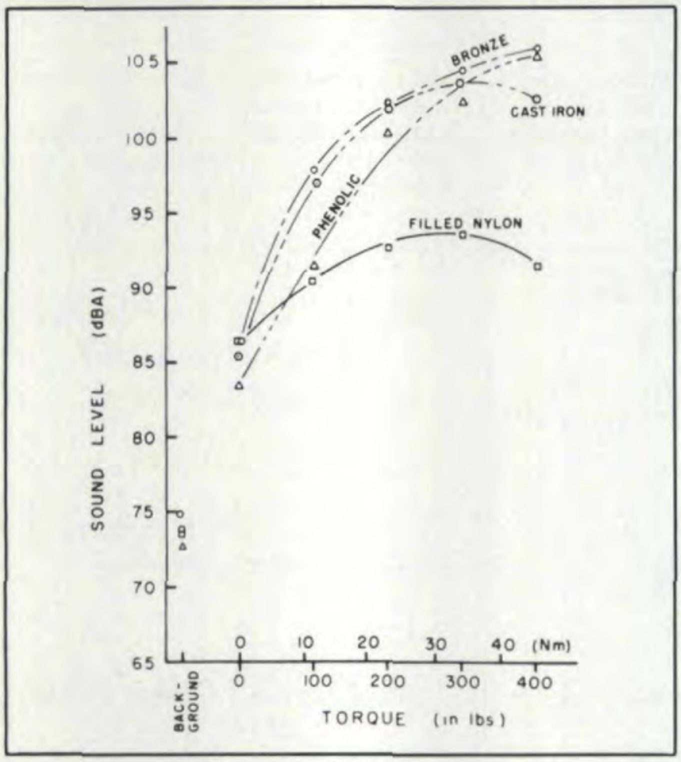

Fig. 5 – Sound Level Vs. Torque

bronze and cast iron test gear noise increased more than 10 dBA. The sound levels of phenolic and bronze gears progressed with increased load. The cast nylon test gear demonstrated its characteristics of noise dampening at all load level test points. A noise reduction of 8 to 14½ dBA was recorded at loads of 22.6, 33.9 and 45.2 N-m (200, 300 and 400 inch-lbs.) in comparison to the other three test gear materials. In actual use, noise reductions in excess of 10 dBA have been recorded in gear trains which incorporate cast nylon gears. Fig. 5 shows a slight dip in sound level at the highest test load of 45.2 N-m (400 inch-lbs.) for cast nylon and cast iron. This is probably due to the increased tooth contact ratio at the higher load. Cast iron is also considered to have some noise dampening qualities.

References

1. FICKEL, H., "Das Spanabhebende Bearbeiten der Kunststoffe," Carl Hanser, Mnchen, 1956.
2. DUDLEY, D. W., "Gear Handbook," McGraw-Hill, New York-Toronto-London, 1962.
3. KOBAYASHI, A., "Machining of Plastics," McGraw-Hill, 1967, New York.
4. The Polymer Corporation, "Nylon Gear Design and Fabrication Manual," BR-36D, 12/83.
5. COTTINGHAM, R.A. and WINNERLING, H.A., "An Advanced Low Noise Stock Feed Tube," Paper Noisexpo, Chicago, 1974.

This paper was previously presented at the 1984 technical meeting of the American Society of Mechanical Engineers.

E-3 ON READER REPLY CARD

TECHNICAL CALENDAR

Sept. 16-18 1985 — Gear Noise Course, Ohio State University

This course will cover general noise measurements and analysis, causes of gear noise, gear reduction techniques, dynamic modelling, signal analysis and gear boxes. For further information contact: Mr. Richard D. Frasher, Director, Continuing Education, College of Engineering, 2070 Neil Ave., Columbus, Ohio 43210, (614) 422-8143.

Oct. 14-16 1985 — American Gear Manufacturers Fall Technical Meeting, Fairmont Hotel, San Francisco, CA

For further information contact: AGMA Headquarters, 101 S. Peyton St., Alexander, VA 22314 (703) 684-0211.

Nov. 19-21 1985 — Society of Manufacturing Engineers Gear Processing and Manufacturing Clinic, Detroit, Michigan.

CALL FOR PAPERS: The Society of Manufacturing Engineers has issued a call for papers for this meeting. The meeting will also include vendor tabletop exhibits. For more information, contact Dianne Leverton at SME (313) 271-1500, ext. 394.

March 17-19 1986 — International Conference on Austempered Ductile Iron, Ann Arbor, Michigan

CALL FOR PAPERS: The organizing committee is seeking papers for this conference. Of particular interest are papers on the engineering properties of Austempered Ductile Iron, quality assurance techniques and experience, product tests, and process and product development case histories based on cost savings, cost avoidance and product improvement. Abstracts to be submitted by August 30, 1985 to: ADI, Gear Research Institute, P.O. Box 353, Naperville, IL 60566. For further Information contact: Dale Breen (312) 355-4200 or Jay F. Janowak (313) 392-7100.

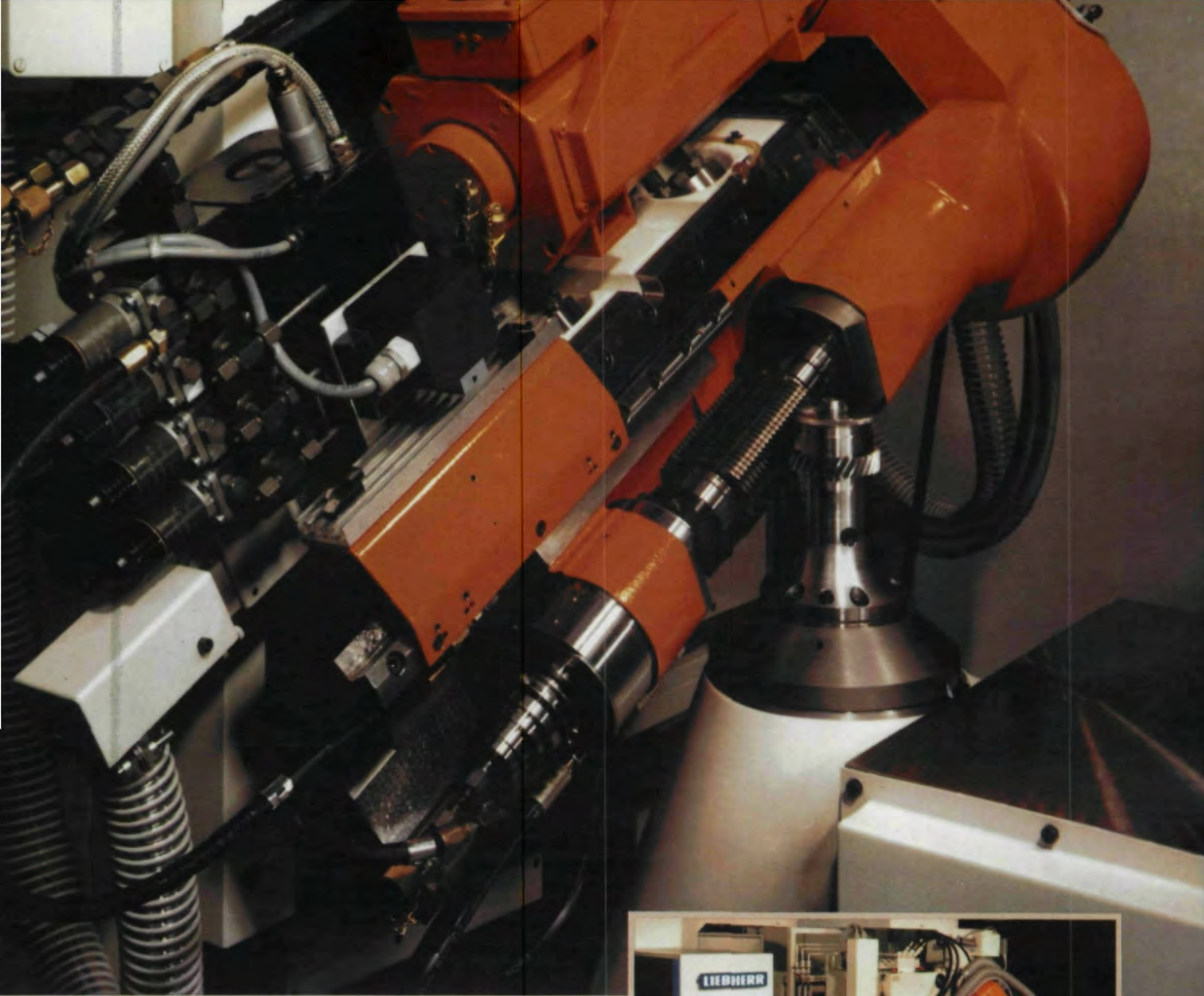


LIEBHERR